THESIS

COUPLED ANALYTICAL MODELING OF WATER LEVEL DYNAMICS AND ENERGY USE FOR OPERATIONAL WELL FIELDS IN THE DENVER BASIN AQUIFERS

Submitted by

Jennifer Anne Davis

Department of Geosciences

In partial fulfillment of the requirements

For the Degree of Master of Science

Colorado State University

Fort Collins, Colorado

Summer 2013

Master's Committee:

Advisor: Michael Ronayne
Co-Advisor: Thomas Sale

William Sanford
Domenico Bau

ABSTRACT

COUPLED ANALYTICAL MODELING OF WATER LEVEL DYNAMICS AND ENERGY USE FOR OPERATIONAL WELL FIELDS IN THE DENVER BASIN AQUIFERS

The South Metro Denver area in Colorado has been experiencing rapid growth in recent years and many municipalities in this region rely on the groundwater resources available in the Denver Basin as their chief water supply. As the population continues to increase, municipal water demands must be met with a sustainable approach. The Denver Basin aquifer system consists of four major aquifers that are composed of interbedded layers of sandstones, siltstones, and shales. The aquifers receive limited annual recharge and consequently the groundwater within them has the potential to be depleted. Declining water levels associated with groundwater depletion, interference between pumping wells, and fouling of wells is leading to losses in well productivity. Furthermore, declining water levels translates to higher electrical energy costs associated with water production.

Regional-scale numerical models developed for the Denver Basin aquifer system do not capture the local-scale drawdown about pumping wells, which is needed to effectively manage existing groundwater well fields. This research project utilizes production well data from the town of Castle Rock, Colorado to test the merits of using a Theis based approach to model water levels about production wells in the Denver and Arapahoe aquifers in Castle Rock. The model applies superposition of the Theis solution throughout both space and time to resolve the combined effects of pumping from multiple wells. This research demonstrated that the analytical method can be successfully applied as a predictor of continuous water levels at pumping wells. In addition, the analytical model provided a novel method for estimating aquifer properties using data from an operational well field, and it contributed a better understanding of the cross-well interferences that increase well drawdown. The model results were used to evaluate alternative pumping scenarios intended to reduce electrical energy costs associated with water production and increase sustainable yields from these aquifers. The alternative pumping scenarios achieved a net reduction in energy consumption ranging from 1.62% to 13.0% and led to a stronger conceptual understanding of how each aquifer responds to varying pumping conditions. This research demonstrates that the analytical solution modeling approach may be beneficial for application to many other projects involving groundwater supply management and optimization.

ACKNOWLEDGEMENTS

I would like to thank the Town of Castle Rock, Colorado Utilities Department for providing the data and financial support to make this research project possible.

I would like to show my great appreciation and respect for Dr. Michael Ronayne, who was willing to take me on as his graduate student advisee, giving me the opportunity to be a part of the Colorado State University community. His shared knowledge and experience has been immeasurably helpful and has contributed to my growth and success as both a student and a professional alike.

I would like to express my deep gratitude to Dr. Thomas Sale, who saw the potential in harnessing my passion for freshwater supply management and graciously offered me the opportunity to work on this project. This experience has had an enormous positive impact on me, both in my professional and personal life.

I would also like thank Dr. William Sanford and Dr. Domenico Bau for being on my committee and offering their time and support in reviewing my work for this project.

Additionally, I would like to thank my family and friends for their patience, support, and guidance throughout this process. Their time spent lending an ear or providing some much needed good humor at times was invaluable.

TABLE OF CONTENTS

LIST OF TABLES

LIST OF FIGURES

CHAPTER 1 – INTRODUCTION

1.1 Motivation

As population rises, demands for Earth's resources increase as well. The necessity for understanding the Earth's freshwater resources and limitations of these supplies is an increasing concern. Demands for groundwater, a finite resource, continue to increase while supply is limited. Developed areas where groundwater is depended on as a primary source for municipal supply have a heightened need to manage and maintain their groundwater system responsibly.

Effective groundwater management is particularly important in populated areas with arid or semi-arid climates, such as the southwest and mountain west regions of the United States. The Denver Basin aquifer system is an example of a groundwater reservoir that receives low amounts of recharge due to the dry climate and the presence of confining units that limit infiltration of meteoric water. The urgency for proper management of the finite groundwater resources provided in the system is widely recognized. Particularly, the South Metro Denver region of Colorado is an area affected by these water supply issues. Justifiably, this location has been the focus of previous studies regarding water supply management concerns [e.g., Robson, 1987; Paschke et al., 2011]. Groundwater models can provide predictions of water level fluctuations caused by pumping and the subsequent effects of pumping over an extended period of time. These models, commonly calculated numerically, provide an understanding of the hydrogeologic conditions and potential outcomes that increasing demands on the Denver Basin aquifers can create.

Municipalities throughout the South Metro Denver region rely heavily on groundwater available in the Denver Basin aquifer system for their freshwater supply [Paschke et al., 2011].

The town of Castle Rock relies solely on groundwater for municipal water supply. The town has been experiencing rapid growth, with a population increase from 20,224 in the year 2000 to over 50,000 in 2012 [Moore, 2012]. Increasing demands on the aquifers in the Denver Metropolitan area are a concern as water levels are reported to be declining [Pottorff, 2011]. Like other municipalities that rely on groundwater, Castle Rock has well fields consisting of multiple production wells. The cones of depression created when wells are pumped can interfere with each other and consequentially enhance the drawdown effects at a well. Declining water levels associated with groundwater production, interference between pumping wells, and fouling of wells contributes to losses in well productivity, which translates into a need for additional wells and higher energy costs associated with water production.

This research utilizes superposition of the Theis [1935] solution for modeling water level fluctuations. Additionally this research demonstrates a novel approach to estimate aquifer properties. The large spatial discretization (1 mile to ¼ mile) used in previous numerical groundwater models developed for Castle Rock does not adequately represent the observed drawdown and steep cones of depression occurring about individual wells [Sale, 2007; Sale et al., 2009]. An analytical solution model was therefore chosen because of its potential to capture the detail and depth of the steep drawdown profiles. The analytical approach avoids the grid discretization required by numerical models [Haitjema, 1995; Yeh and Chang, 2013], allowing for more accurate determination of water levels about individual wells. Analytical models have been successfully applied to well fields in a variety of previous studies [e.g., Bair et al., 1991; Ahlfeld and Laverty, 2011].

1.2 Research Objectives

The initial objective of this project was to develop and test the ability of superposition of the Theis solution to accurately predict production well water levels in the Denver and Arapahoe aquifers in Castle Rock, Colorado. The calibration process used to achieve the initial objective led to the realization that the model is useful as a tool to estimate the values of hydrogeologic properties such as transmissivity and storativity. After being successfully applied to predict water levels, the analytical model was coupled to a power equation to estimate energy consumption associated with pumping. The second objective of this research project was to evaluate alternative pumping techniques intended to reduce energy consumption and improve sustainability of the aquifers. Ultimately, the purpose of this work was to gain a better conceptual understanding of the actively pumped Denver Basin aquifers and provide insight to improving groundwater supply management.

1.3 Organization and Content

The remainder of this thesis is organized into four additional chapters. The study site's geology, hydrogeology, and available data are reviewed in Chapter 2. Explanation of analytical solutions and modeling methods used in this research are covered in Chapter 3. Chapter 4 reveals results of the modeling efforts and related discussions, followed by a summarization of conclusions in Chapter 5.

CHAPTER 2 – DESCRIPTION OF THE STUDY AREA AND SITE DATA

In Colorado, the 6,700 mi^2 Denver Basin aquifer system extends north to south from Greeley to Colorado Springs and from the Rocky Mountain Front Range east out to Limon [Figure 2.1; Robson & Banta, 1995]. Robson [1989] estimated that the amount of groundwater stored in the Denver Basin bedrock aquifers exceeds the amount of water in Lake Erie. However, the semi-arid environment of the Front Range low rates of recharge causes the groundwater within the Denver Basin to be a finite resource. Castle Rock, Colorado is situated along the western flank of the Denver Basin aquifer system and is one of many towns included in the Front Range urban corridor. Castle Rock is heavily reliant on groundwater from the Denver Basin aquifers for their municipal water supply [Town of Castle Rock, 2006]. With increasing population, a local scale analysis of water levels and well field performance is needed to support efficient groundwater extraction in this area.

2.1 Geologic Setting

Castle Rock, Colorado was named after the most dominant rock outcrop in the area, the Castle Rock Conglomerate. This unit, formed in the latest Eocene, is the youngest sedimentary rock preserved in the Denver Basin [Evanoff, 2007], and it overlies the primary bedrock aquifers [Figure 2.2]. The Denver Basin is an elongated, asymmetric, structural basin that extends from Colorado to eastern Wyoming, western Nebraska, and western Kansas. The basin is characterized by steeply dipping to overturned beds along the western edge, low-angle dipping beds along the eastern edge, and a synclinal hinge underlying the areas from Denver to Cheyenne [Robson, 1987]. Formation of the basin began during the Late Cretaceous with deposition of marine shales which comprise the Pierre shale. As ancient sea levels regressed, sands of the Fox

Hills Sandstone interbedded with the lagoon, swamp, and continental deposits of the Laramie Formation. Uplift and erosion of the Ancestral Rockies during the Laramide Orogeny (80 to 70 Ma) forced the Denver Basin to further subside and fill with the deposits that make up the Arapahoe and Denver Formations. Synorogenic fluvial deposits contributed to the formation of coalescing alluvial fans over the Denver Basin ending around 63.9 Ma. After a period of depositional quiescence and extensive erosion, additional fluvial sediments were deposited during the beginning in the Eocene [Cole et al., 2010].

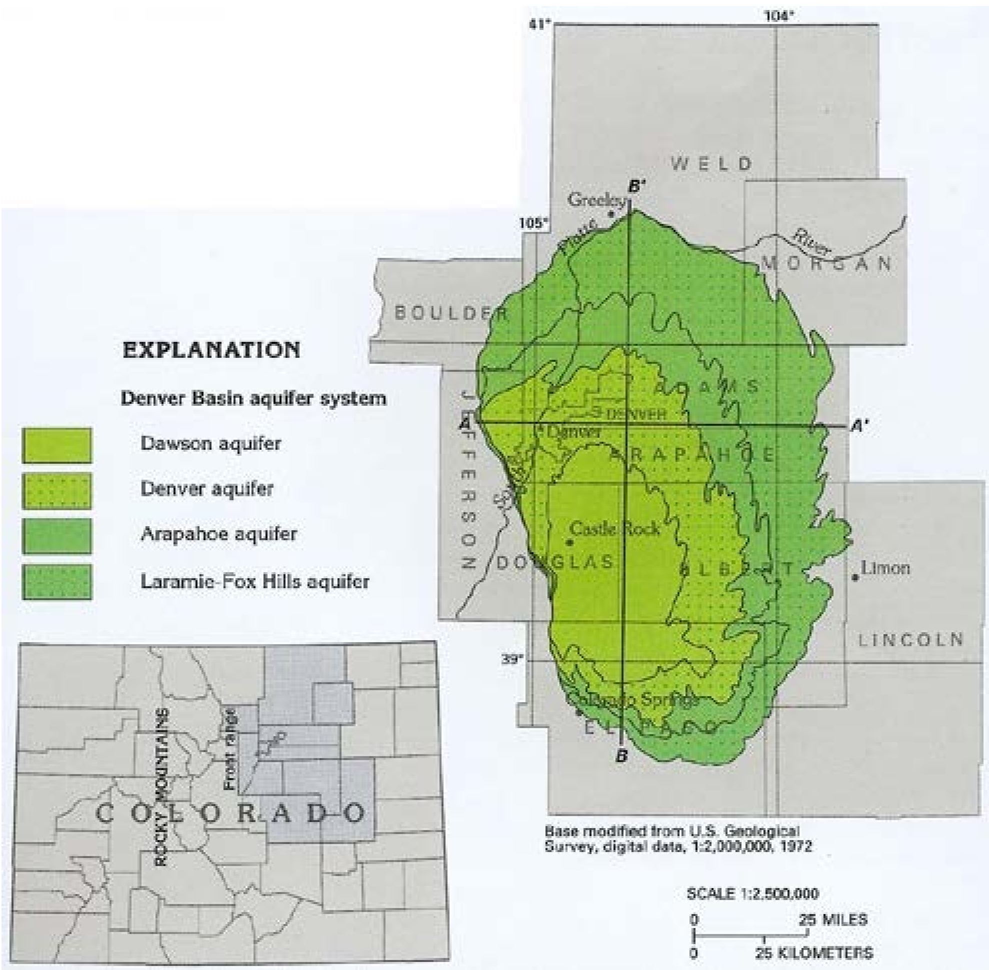

Figure 2.1: Location map for the Denver Basin aquifer system [Robson & Banta, 1995].

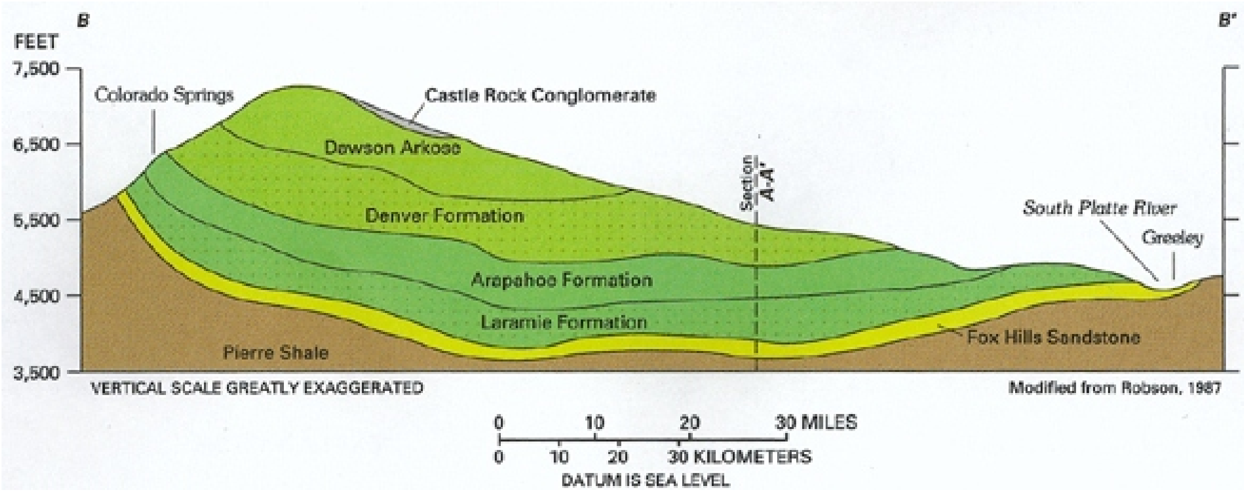

Figure 2.2: Cross sectional diagram of the Denver Basin aquifer system [Robson & Banta, 1995].

2.2 Hydrogeologic Description

Beneath the localized, unconfined aquifers present in the alluvium found along active stream channels, five water-bearing geologic formations make up the Denver Basin aquifer system. The five water-bearing sequences, Dawson Arkose Formation, Denver Formation, Arapahoe Formation, Laramie Formation, and Fox Hills Sandstone Formation, have a combined thickness of 3,200 feet in an area approximately 20 miles south of Castle Rock, where the thickness reaches its greatest value [Robson, 1987]. Due to the absence of a separating confining layer, past hydrogeologic studies of the Denver Basin have grouped the Laramie and Fox Hills Formations into a single aquifer unit [Robson, 1987; Paschke et al., 2011]. Thus there are four major aquifers. From most shallow to greatest depth, these are the Dawson, Denver, Arapahoe, and the Laramie-Fox Hills aquifers. The base of the Denver Basin aquifer system is marked by the Pierre Shale, which underlies the Fox Hills Sandstone and is over 5,000 feet thick [Robson, 1987]. Each of the aquifers are composed of varying fractions of interbedded sandstones, siltstones, and shales. In the vicinity of Castle Rock increasing fractions of sandstone are observed as one progress from the north-northeast to the south-southwest [Figure 2.3]. Although historically the aquifers have been overgeneralized as predominantly sandstone units, multiple studies have provided evidence that strong heterogeneity exists within the aquifers both laterally and vertically [Raynolds, 2002; Raynolds and Johnson, 2003; Woodard et al., 2002; Sale et al., 2009]. Sale et al. [2009] concluded that the structure of the Denver Basin aquifers in the vicinity of Castle Rock reflects an alluvial fan deposit associated with mass wasting off the Rockies during the Laramide orogeny. Furthermore, Sale et al. [2009] observes local discontinuity in stratigraphy between closely spaced wells.

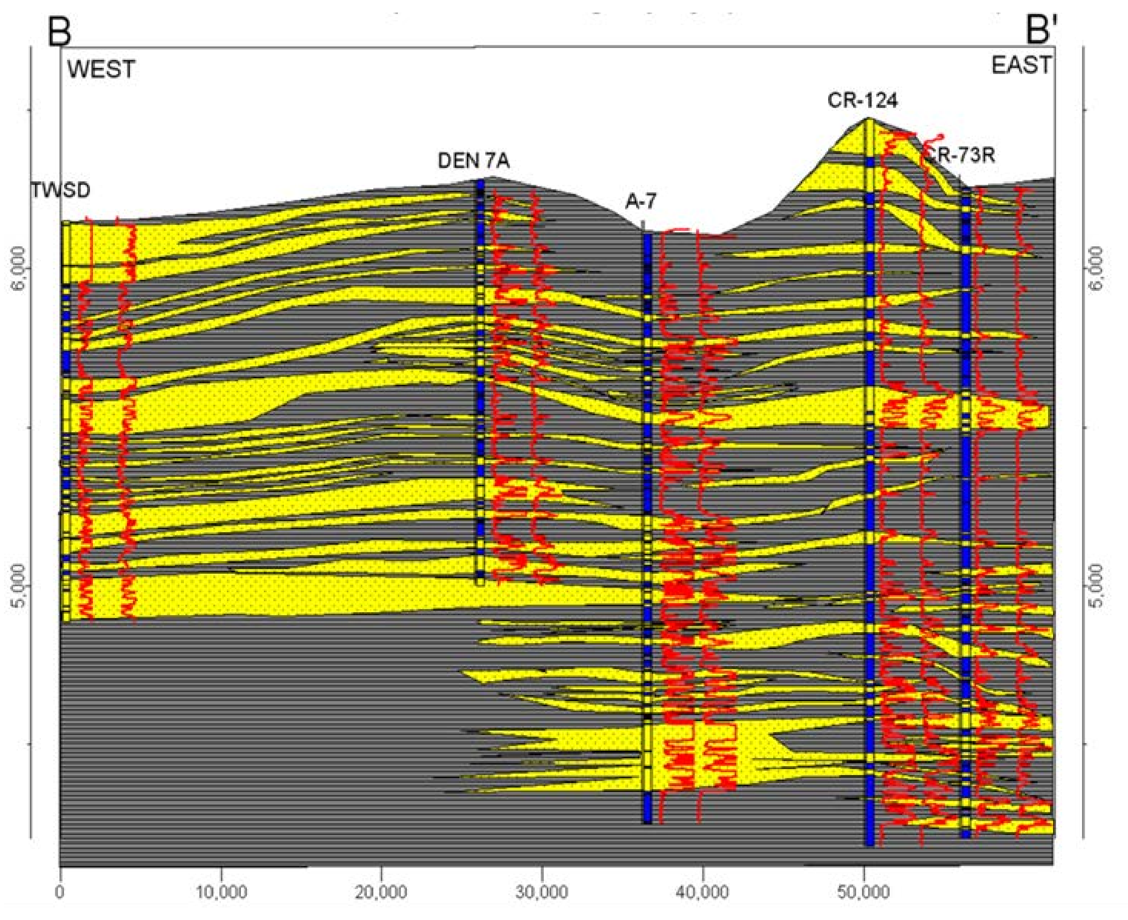

Figure 2.3: Stratigraphic cross sectional diagram depicting the complexity of structural heterogeneity within the Denver aquifer in the vicinity of Castle Rock, Colorado. Highlighted regions represent sandstone layers [Sale et al., 2009].

The unconfined aquifers overlaying the confined aquifers in the Denver Basin occur locally, primarily adjacent to active stream channels. These unconfined aquifers are present in saturated alluvial deposits composed of sands, gravels, and clays, found along streams in the South Platte and Arkansas River watersheds [Robson, 1987; Robson & Banta, 1995]. Near Castle Rock, the Plum Creek alluvium forms an unconfined aquifer with shallow groundwater that interacts with surface water in the creek. Pumping-test results yielded a median hydraulic conductivity value of 480 ft/day for the unconsolidated alluvial aquifers in the Denver Basin [Paschke et al., 2011]. In addition to the shallow alluvial deposits along modern channels, unconfined conditions also occur in the bedrock aquifers at and near outcrop areas [Robson & Banta, 1995].

The Dawson aquifer exists within the Dawson Arkose Formation and is the uppermost unit in the Denver Basin aquifer system. The Dawson is the least extensive of the bedrock aquifers in the Denver Basin system and covers roughly 1,200 square miles between Denver and Colorado Springs [Figure 2.1; Robson & Banta, 1995]. Consisting of conglomerates, sandstones, siltstones, and shales, the aquifer is divided into upper and lower units with a shale-rich confining layer between them. Sediments in the Upper Dawson are primarily coarse-grained arkosic sandstones interbedded with siltstones and shales and the Lower Dawson aquifer contains sediment grains of varying sizes, deposited as Laramide synorogenic alluvium [Robson, 1987; Robson & Banta, 1995; Paschke et al., 2011]. Thickness of the aquifer ranges from 200-900 feet with a saturated interval of 100-400 feet in most areas [Robson, 1987]. In the area of Castle Rock specifically, the thickness of the aquifer is 200-300 feet with 100-200 feet of saturated sandstone [Sale, 2007].

The Denver Formation contains the Denver aquifer. Larger than the Dawson, the Denver aquifer covers approximately 3,000 square miles, is 600 to 1,200 feet in thickness including confining layers, and underlies the city of Denver, Colorado [Robson & Banta, 1995; Paschke et al., 2011]. The Denver aquifer is composed of interbedded shales, claystones, siltstones, and sandstones containing volcanic ash, lignitic coal, and plant fossils. Vertebrate fossils mark the Cretaceous-Tertiary boundary found throughout the upper portion of the aquifer while alluvial fan deposits found along the western part of the basin diminish to the east [Robson, 1987; Robson & Banta, 1995; Paschke et al., 2011]. Although this aquifer contains usable quantities of water, the water-bearing layers of sandstone and siltstone are sporadic and poorly defined with the net thickness of saturated sandstone being 250-350 feet in the Castle Rock area [Robson & Banta, 1995; Sale, 2007].

The Arapahoe Formation, a 400-700 foot thick stratum of interbedded conglomerates, sandstones, siltstones, and shales [Robson, 1987], contains the 400-600 foot thick Arapahoe aquifer [Paschke et al., 2011]. The areal extent of this unit is around two-thirds that of the entire Denver Basin aquifer system and covers approximately 4,300 mi^2 [Robson & Banta, 1995]. Shale layers of the overlying Denver Formation mark the top of the Arapahoe aquifer while the shales, thin beds of sandstones and siltstones, and coals that make up the upper portion of the underlying Laramie Formation denote the base of the aquifer. Shale is also present as a delineating layer within the Arapahoe, dividing the aquifer into upper and lower portions. The upper portion is noted as having a higher concentration of shales while the lower portion has a greater percentage of sands. Alluvial fan deposits present in the Denver Formation are also found in the Arapahoe; however the deposits in the Arapahoe are generally coarser-grained and found in thicker sequences [Robson, 1987; Robson & Banta, 1995; Paschke et al., 2011].

Douglas County and El Paso County have the most transmissive of these fan deposits, providing a major source of potable water for their municipal supply. The Arapahoe aquifer is the most permeable bedrock aquifer in the basin [Paschke et al., 2011]. In the vicinity of Castle Rock, this unit has a saturated thickness of 250-350 feet [Sale, 2007]

The lowermost, oldest, and most extensive of the aquifers in the Denver Basin is the Laramie-Fox Hills. This aquifer underlies the entire basin, and therefore has an areal extent of nearly 7,000 mi^2 [Robson and Banta, 1995]. Sandstones from the lower portion of the Laramie Formation along with the Fox Hills Sandstone comprise this aquifer. The confining unit that divides the Laramie-Fox Hills from the overlying Arapahoe aquifer consists of the shale, coal, and small amounts of siltstones and sandstones present in the upper Laramie Formation [Robson, 1987; Paschke et al., 2011]. The western flank of this impermeable layer reaches a thickness of 700 feet and thins out in a wedge shape to the eastern flank where thickness is as little as 100 feet [Paschke et al., 2011]. The sediments in the Laramie-Fox Hills aquifer are mostly fine- to very fine-grained sandstones and siltstones interbedded with shales, with the base of the aquifer established by the Pierre Shale. The limits of this aquifer represent the extent of the Denver Basin aquifer system and similarly the greatest depth in this aquifer, reaching 2,200-2,300 feet below ground surface, signifies the deepest part of the system [Paschke et al., 2011]. Throughout the entire aquifer, thicknesses range from 0 feet at the boundaries to 300 feet at maximum depth [Robson, 1987]. In the area of Castle Rock this aquifer's thickness ranges from 200-300 feet [Sale, 2007].

2.3 Available Pumping and Water Level Data

Castle Rock's four primary well fields, interchangeably referred to as "pumping centers", are shown in Figure 2.4. Data from the Meadows Pumping Center and the Castle Oaks Pumping Center were used for analysis in this study. Table 2.1 lists the wells utilized for each well field. Modeling of the Meadows Pumping Center was based on flow rate and water level data collected between June 2nd, 2007 and March 21st, 2011. For the Castle Oaks Pumping Center, the modeling analysis period extended from June 2nd, 2007 to May 22nd, 2012.

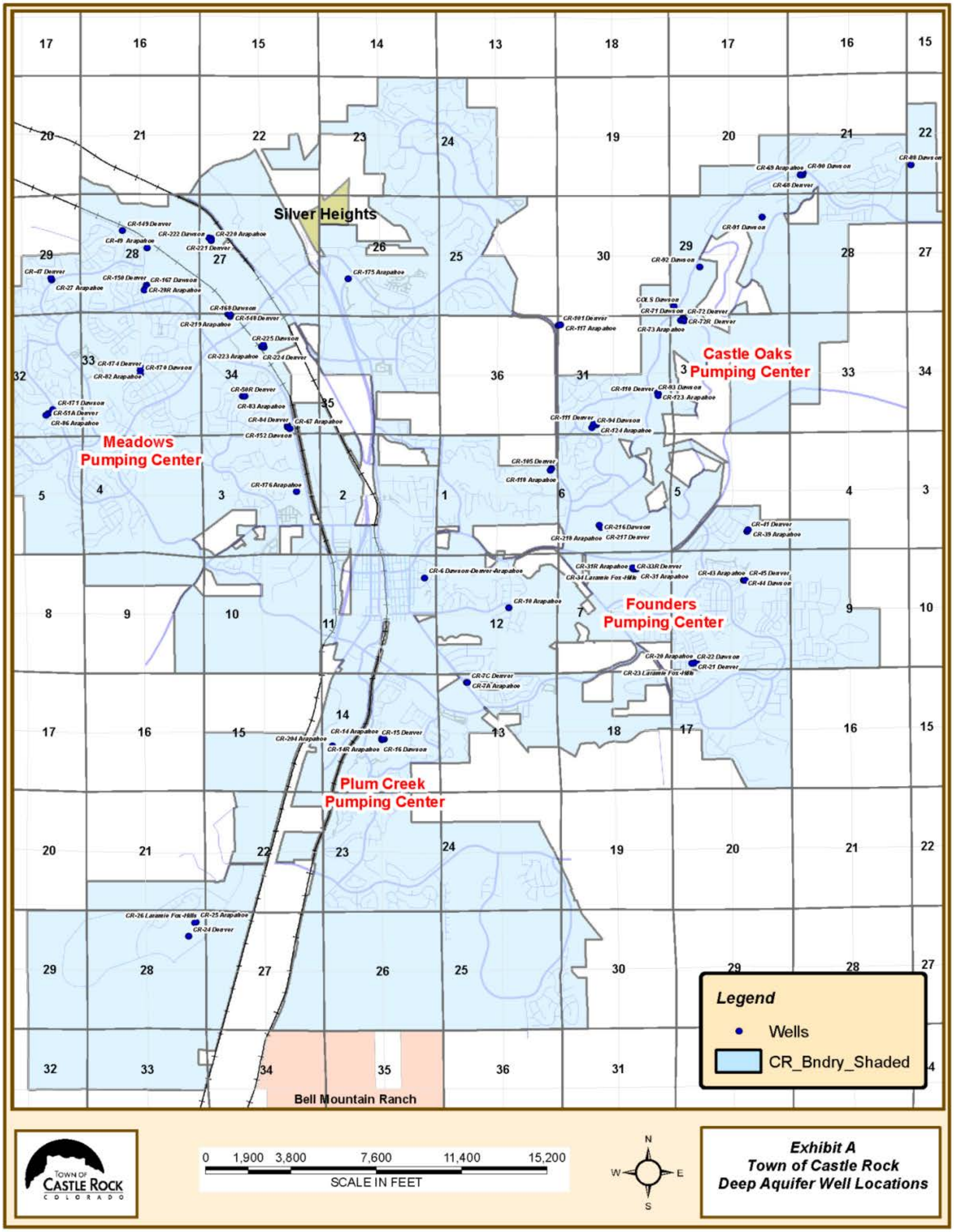

Figure 2.4: Map showing Castle Rock well locations within each pumping center. Provided by the Castle Rock Utilities Department.

Water level data available for use in this research were collected by pressure sensors equipped in operational municipal water supply wells (see Table 2.1 for sensor depths). The measured water levels along with flow rates, which are gaged at each pumping well, were provided by the Town of Castle Rock Utilities Department. Figure 2.5 shows an example water level hydrograph, along with the measured pumping rates, for municipal well CR221 in the Meadows Pumping Center.

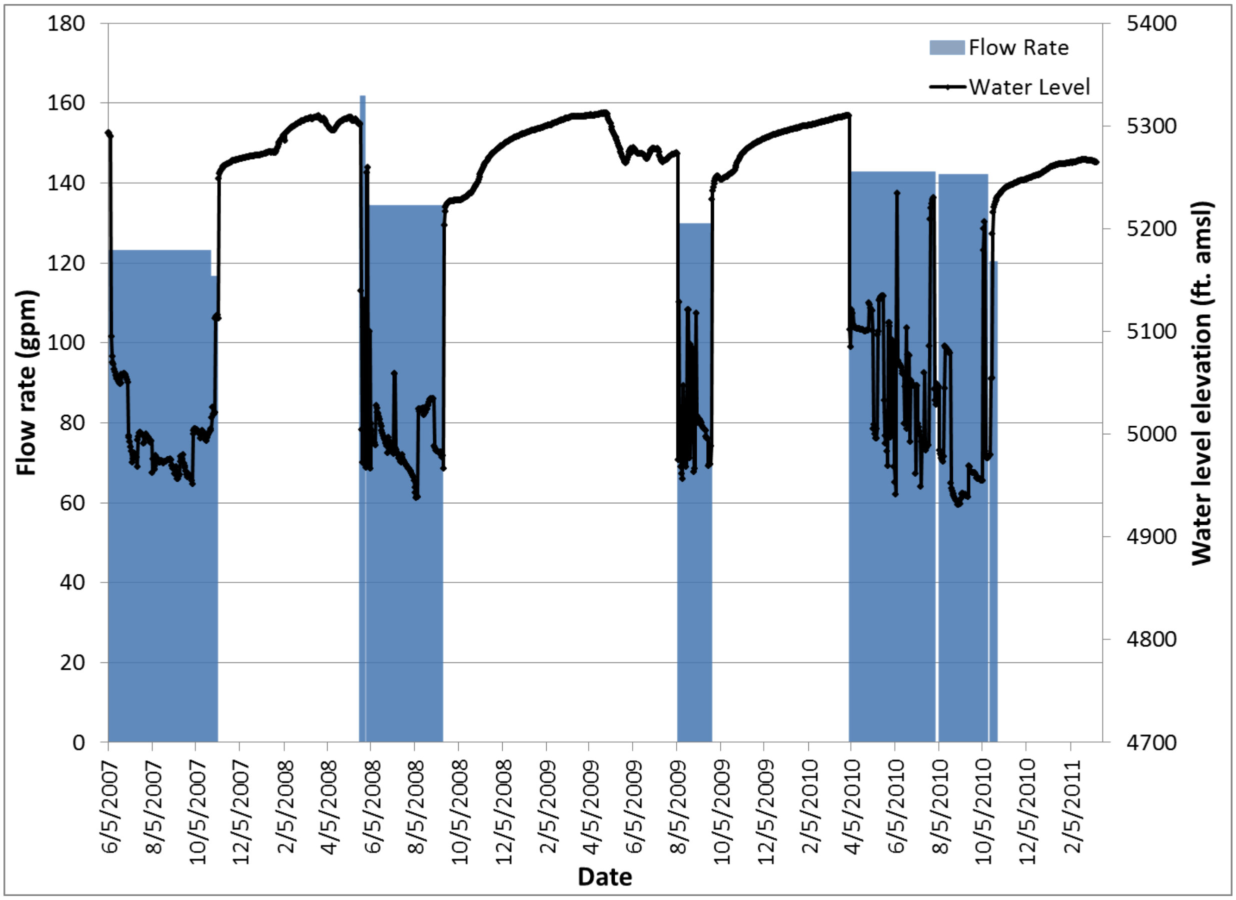

Figure 2.5: Water level hydrograph with associated pumping rates for well CR221, based on historical data.

Table 2.1: Production well data

Pumping Center	Aquifer	Well Name	Well Head Elevation (ft. amsl)	Transducer Probe Depth (ft)	Pumping Rate Range* (gpm)
Meadows	Denver	CR148	6115	1279	166 – 345
		CR149	6034	1100	194 – 244
		CR150	6132	1175	134 – 282
		CR174	6179	1116	76 – 208
		CR221	6026	1162	116 – 162
		CR47	6110	1145	121 – 202
		CR50R	6182	1380	153 – 275
		CR51A	6264	1156	0
	Arapahoe	CR86	6265	1690	117 – 245
		CR83	6186	1766	111 – 345
		CR82	6184	1710	143 – 303
		CR49	6054	1516	53 – 317
		CR28R	6136	1712	299 – 696
		CR27	6111	1562	68 – 98
		CR223	6103	1718	273 – 341
		CR219	6120	1708	307 – 613
Castle Oaks	Denver	CR105	6600	1725	208 – 336
		CR110	6350	1395	309 – 590
		CR111	6482	1585	313 – 536
	Arapahoe	CR118	6609	2265	340 – 567
		CR123	6349	2037	205 – 336
		CR124	6476	2150	227 – 531

*Values represent the range of pumping rates during the historical modeling period (2007- 2011/Meadows, -2012/Castle Oaks).

CHAPTER 3 – METHODS

Mathematical models are a standard means for examining a dynamic physical system and making predictions. However, it is important to note that all models are based on assumptions and simplifications. Consequently, a model's accuracy is limited to the current level of knowledge and understanding of the system it represents. Many approaches to modeling groundwater have been undertaken, each providing a platform for successive modeling efforts. Several past studies of Denver Basin groundwater have involved the application of numerical models. For example, previous numerical models for the Denver Basin aquifer system have been constructed for the area surrounding Castle Rock [Sale, 2007]. The level of detail needed for each modeling effort depends on the objectives of the modeling, and it is important to keep this in mind when interpreting model outputs. For instance, the intent of a model constructed to assess the entire Denver Basin aquifer system may be to determine tributary versus nontributary groundwater and the effects that groundwater extraction may have on the surface waters. Alternatively, models developed on a more detailed, local-scale analysis may be more useful to assess local groundwater supplies for the greatly increasing populations in the South Metro Denver regions. Discretization used in numerical models requires the model domain to be expressed as gridded cells, and the representative output is an approximation of a governing flow equation. In numerical models, source/sink terms like pumping are applied over an entire grid cell. As a result, the simulated drawdown at a production well is underpredicted when using the numerical approach. This is a disadvantage of standard numerical models when applied to aquifers with active production wells, particularly if there is a need to calculate hydraulic head near the well.

This research project required a mathematical modeling technique to accurately calculate water levels at production wells within active pumping centers. An analytical solution method based on superposition of the Theis [1935] equation was applied for this purpose. To assess energy use associated with pumping wells, the analytical solution was coupled to a power equation that quantifies energy demand for a given pumping rate and water level.

3.1 Application of the Theis Superposition Model

Superposition of the Theis equation was used in this study to model water levels at pumping wells. The Theis equation is as follows:

$$s(r,t) = \frac{Q}{4\pi T} W(u) \tag{3.1}$$

where, *s* = drawdown [L] at a particular radial distance *r* from the pumped well and time *t* since the start of pumping, *Q* = pumping rate [L^3/T], *T* = transmissivity [L^2/T], and *W(u)*, the well function can be expressed as the infinite series:

$$W(u) = -0.577216 - lnu + u - \frac{u^2}{2*2!} + \frac{u^3}{3*3!} - \frac{u^4}{4*4!} + \cdots \tag{3.2}$$

with *u* being defined as:

$$u = \frac{r^2 S}{4Tt} \tag{3.3}$$

where *S* is the storativity of the aquifer.

In a multiple well system, like the well fields considered in this study, aquifer drawdown is influenced by more than one pumping well. Applying superposition of the Theis equation, the drawdown at any point in the aquifer can be calculated as the sum of the drawdowns created by each well individually. Therefore, the principle of superposition of solutions can be applied to the Theis [1935] equation. For a well field with n wells, associated pumping rates of Q_1, Q_2,…, Q_n, and radial distances from each well r_1, r_2,…, r_n, the following equation is used [Freeze & Cherry, 1970]:

$$s = \frac{Q_1}{4\pi T} W(u_1) + \frac{Q_2}{4\pi T} W(u_2) + \cdots + \frac{Q_n}{4\pi T} W(u_n) \tag{3.4}$$

$$u_i = \frac{r_i^2 S}{4T t_i} \quad i = 1, 2, \ldots, n \tag{3.5}$$

with t_i defined as time from the start of pumping for well with Q_i.

Assumptions used in the development of the Theis equation include the following: the aquifer is homogeneous, isotropic, and under confined conditions with a uniform thickness; the aquifer has an infinite areal extent; the well fully penetrates the entire thickness of the aquifer; Darcy's law is valid and groundwater has constant properties (density and viscosity); the potentiometric surface is horizontal prior to pumping and not changing with time; all changes in the potentiometric surface are due to pumping; no recharge takes place to the aquifer above the cone of depression. In a natural system one or more of these assumptions are commonly violated, however the solution often still yields a reasonable approximation of drawdown [Domenico & Schwartz, 1990].

The model applies superposition of the Theis solution throughout both space and time by summing drawdown across multiple wells in a well field while additionally summing drawdown over the course of a given amount of time, respectively. Minor adjustments to well locations were made such that drawdown could be calculated about each pumped well. Well locations were moved to a distance of 0.5 ft. from the given well coordinates to avoid calculating drawdown directly at a well. As an additional part of evaluating the solution, the analytical solution accounts for individual well loss values which can affect water levels in wells and commonly occurs in wells over time if no rehabilitation has taken place. Consideration of the well loss is necessary since this research is focused on water level fluctuations at pumped wells. The well loss is determined as:

$$s_w = CQ^2 \tag{3.6}$$

where s_w = well loss (drawdown that is attributed to turbulent flow around the well screen and casing) and Q = pumping rate [Domenico & Schwartz, 1990]. Rearranging the above equation yields the following expression for the well loss constant (C):

$$C = \frac{s_w}{Q^2} \tag{3.7}$$

Drawdown at a pumping well is calculated as the aquifer drawdown (actual formation drawdown at the outer edge of the well gravel pack) plus the drawdown due to well losses. The analytical model used in this study allows for the determination of drawdown without the need for initial static water levels, which may not be available for an active well field. Programming code that implements the analytical model is provided in Appendix A.

To obtain the necessary parameters for water level modeling using the Theis equation, raw data provided for this study required a process of filtering, organizing, and re-formatting in order to obtain model input values. Daily water levels were acquired by extracting the water level fluctuation values for each well at 12 a.m. on each day and converting into potentiometric surface elevation values in feet above sea level. To determine pumping times and associated flow rates, pumping sequences were established and average flow rates over the pumped periods were used. Pumping sequences were considered for any time period where continuous pumping reached or exceeded 13 hours. Similarly, for a well to be considered in a non-pumping period, the flow rate must have been at or near zero for 13 hours or longer. This simplification was necessary to keep the data used for model inputs at a computationally reasonable amount. Drawdown values were calculated and summed over the entire modeled period in two-day time steps.

3.1.1 Calibration Process

Data used for the model calibration consisted of more than three years of hourly water level and pumping rate data collected from operational well fields in Castle Rock (see Section 2.3 for a description of the data). Well locations and pumping times with associated flow rates were input as known values. The values for transmissivity, storativity, natural slope of the potentiometric surface, and individual well loss constants were applied as variables. Plots of model-calculated water levels against historical daily water levels were used to iteratively find a visual best-fit between the two sets of values. Calibrated models were developed for both the Denver and Arapahoe aquifers in each of the two well fields analyzed in this study. Figure 3.1 depicts a flow chart illustrating the calibration process. Upon completion of the calibration, potentiometric surface plots were produced using a computational grid with 50-meter resolution.

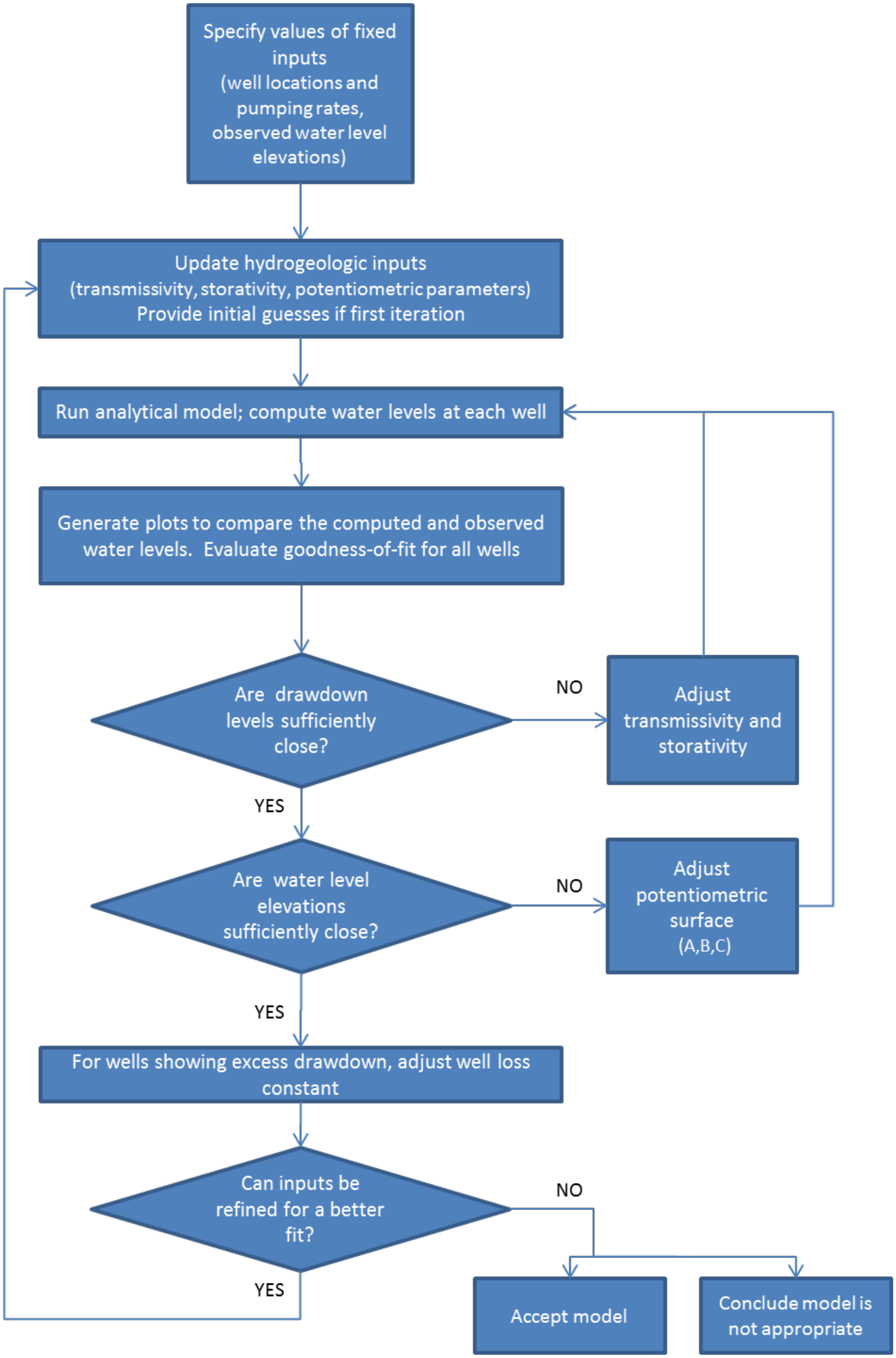

Figure 3.1: Flow chart illustrating the decision process used for model calibrations.

3.2 Modeling of Power and Energy Use

The success of the analytical solution model in predicting water levels led to the use of a power equation to assess energy consumption associated with operation of the Castle Rock pumping centers. The purpose of this modeling effort was to provide a basis for exploring alternative pumping scenarios intended to reduce energy costs associated with pumping.

3.2.1 Power Equation

The following power equation was employed in the model:

$$Power = \frac{Q * \rho * g * TDH}{pump\ efficiency} \tag{3.8}$$

where Q = pumping rate [L^3/T] , ρ = standard density of water [M/L^3], g = standard gravitational acceleration constant [L/T^2] , *TDH* = total dynamic head [L]. This form follows the basic equation for pump break horsepower (BHP) as defined by Sterrett [2007].

$$BHP = \frac{gpm * TDH\ (ft)}{3{,}960\ (a\ constant) * pump\ efficiency\ (as\ a\ decimal)} \tag{3.9}$$

A constant pump efficiency value of 0.8 was used in this model. Although the actual pump efficiencies may differ for the wells modeled, the purpose of the energy model was to determine if the alternative pumping scenarios could improve energy efficiency compared to historical pumping methods. Therefore interpretation of the modeled energy use is not affected as long as a constant pump efficiency value was used. Total dynamic head values were determined by subtracting water elevations at the wells, calculated using the Theis superposition model, from a static elevation representative of Castle Rock's water storage reservoir. A time increment of 10 days was used for calculation and summation of power values. To eliminate seasonal bias in the calculations, a 1000-day time period from February 22nd, 2008 to November 18th, 2010 was used. Power values calculated using this method were converted into units of energy using time step lengths in the model. Cumulative energy consumption based on historical pumping schedules was calculated for each well individually and for each aquifer in both the Meadows and Castle Oaks well fields. Programming code for the power and energy model is provided in Appendix A.

3.2.2 Alternative Pumping Scenarios

Total dynamic head holds a direct relationship to power (Eqn. 3.8). Consequently, reducing total dynamic head at any given well can reduce the power used by that well. This relationship inspired the fundamental concept used to create the designs for alternative pumping scenarios. Cross-well interferences can effectively increase total dynamic head values at wells. Conceptually, these well interferences could be reduced or eliminated by dispersing the order of wells to be pumped in a sequence that maximizes radial distance of actively pumping wells. Examples of the dispersed pumping assignments used for modeling are shown in Figures 3.2 and 3.3.

Seven pumping scenarios were created to implement varying combinations of the following primary design factors: dispersed pumping sequences, time limits for both pumping and recovery of wells, and alternative flow rates for wells. Table 3.1 summarizes the design factors used for each scenario. The pumping assignments illustrated in Figures 3.2 and 3.3

correspond to Scenarios 1, 2, 3, 3b, and 6. The primary constraint for each of the alternative pumping scenarios was the need to accrue a volume of water equal to or greater than the volume of water generated from historical pumping methods for each 10 day time step. Also, it was necessary to develop scenarios that did not store water in excess of Castle Rocks's reservoir storage capacity, which is approximately 7 million gallons. For consistency, power and energy consumption was modeled for each alternative pumping scenario in the same manner as the historical pumping data. Energy consumption values for each alternative pumping scenario were compared to the estimated historical energy use to determine if power and energy costs could be reduced.

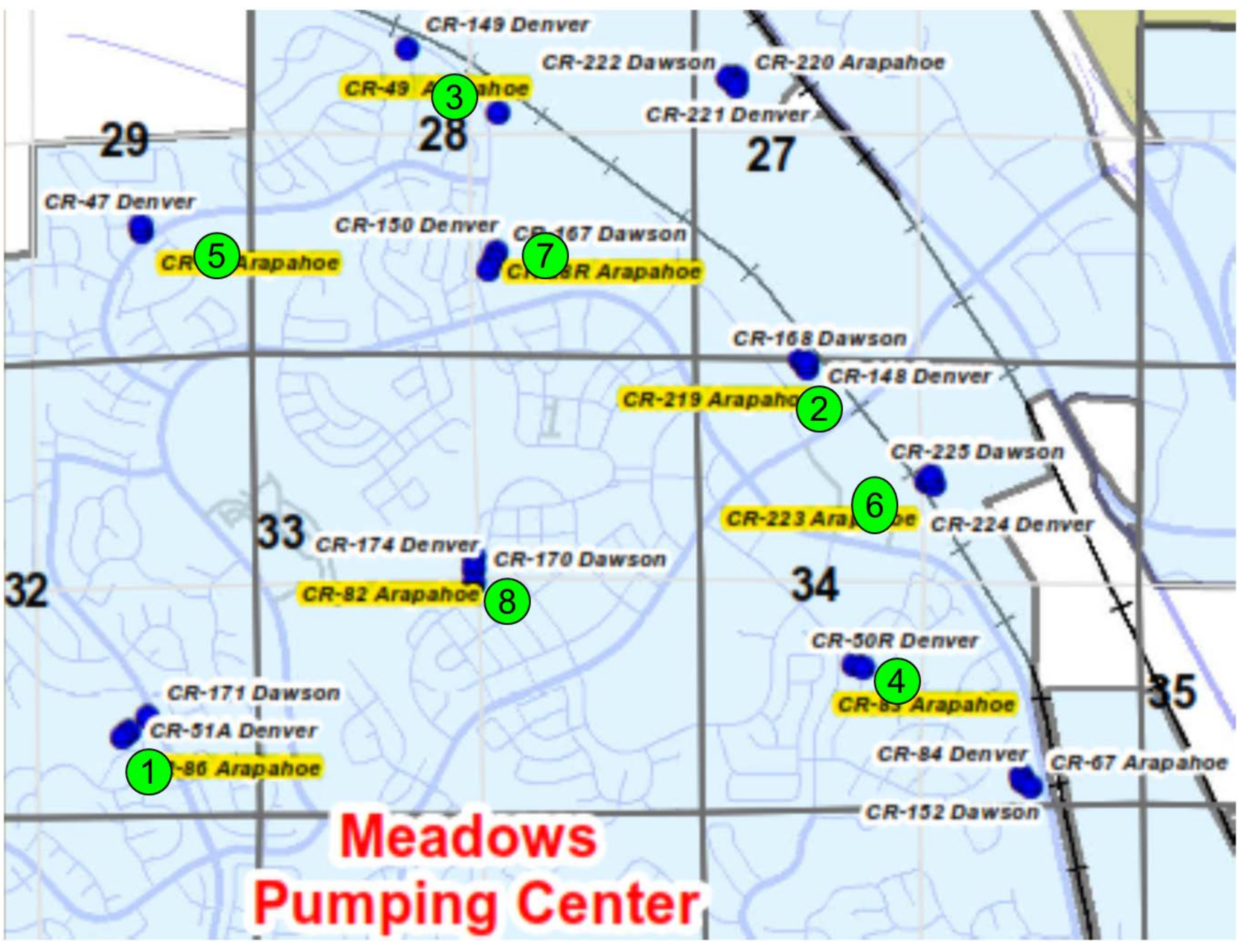

Figure 3.2: Example of dispersed pumping for the Arapahoe aquifer, Meadows Pumping Center. Circled numbers 1 through 8 represent order of pumping assigned to that well.

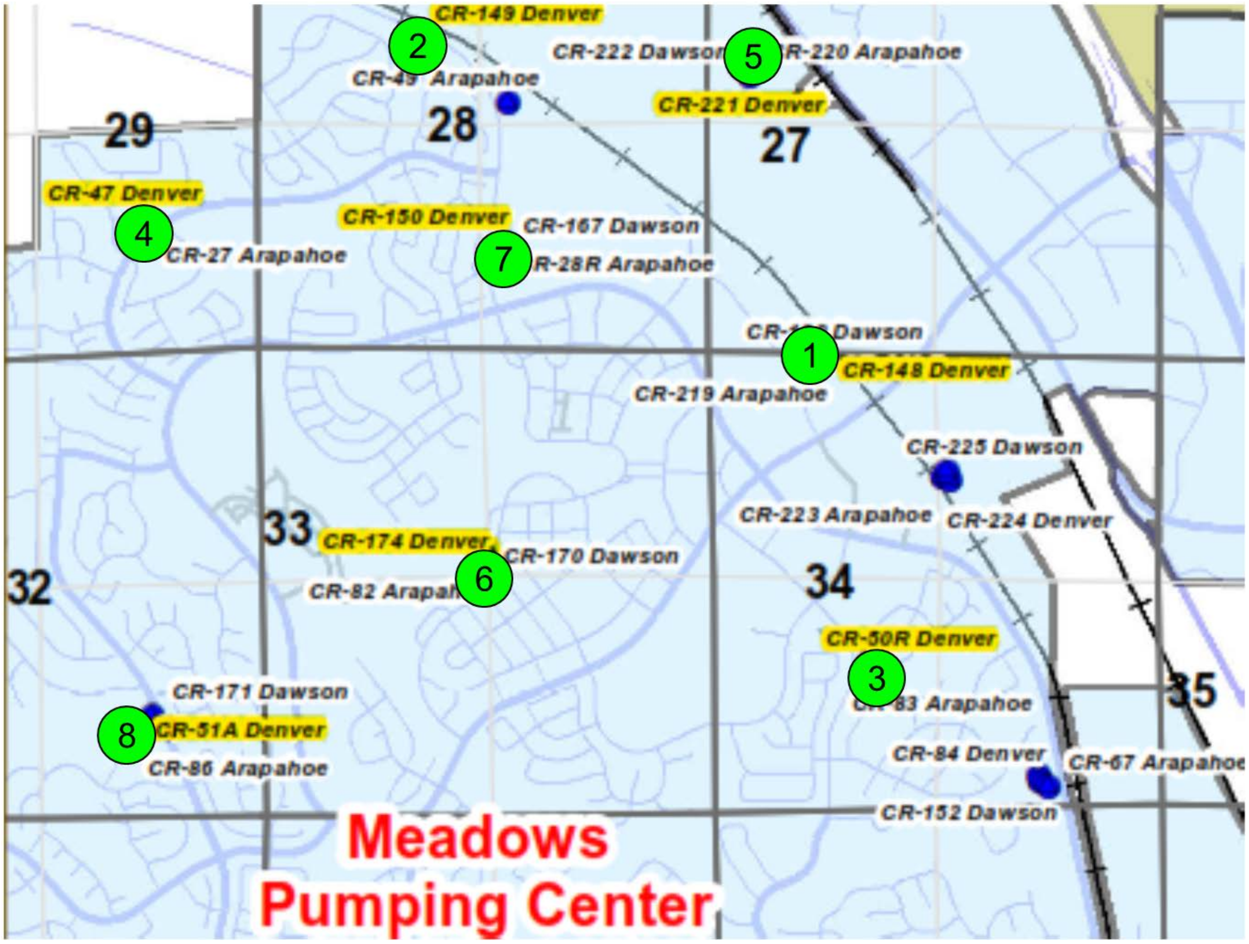

Figure 3.3: Example of dispersed pumping for the Denver aquifer, Meadows Pumping Center. Circled numbers 1 through 8 represent order of pumping assigned to that well.

Table 3.1: Summary of design factors used in developing each alternative pumping scenario

	Denver				Volume Demand Met	Arapahoe			
	Dispersed Pumping	Time Limit Pumping (days)	Minimum Recovery Time (days)	Flow Rates*		Dispersed Pumping	Time Limit Pumping (days)	Minimum Recovery Time (days)	Flow Rates*
Scenario #1	YES	100	100	Average historical	Both aquifers	YES	100	100	Average historical
Scenario #2	YES	60	60	Average historical	Per individual aquifer	YES	100	100	Average historical
Scenario #3	YES	60	120	Average historical	Both aquifers	YES	100	NONE	Average historical
Scenario #3b	YES	60	30 - 40	Average historical	Both aquifers	YES	100	NONE	Average historical
Scenario #4	NO, pump all wells	NONE	NONE	1/3 max. historical	Both aquifers	YES	100	NONE	Average historical
Scenario #5	NO, pump all wells	60	30	1/3 max. historical	Both aquifers	YES	100	NONE	Average historical
Scenario #6	YES	60	120	1/3 max. historical	Both aquifers	YES	100	NONE	Average historical

*Flow rates relative to the base case model.

CHAPTER 4 – RESULTS AND DISCUSSION

A primary objective of this research was to evaluate the ability of the Theis based model to predict water level fluctuations as well as energy consumption due to pumping. In achieving this primary objective, the model additionally proved its usefulness as a means to estimate aquifer characteristics, explore the potential for power and energy reduction through alternative pumping designs, and ultimately serve as a quantitative tool for groundwater supply management and optimization.

4.1 Analytical Modeling of Water Levels

The motivation for developing a groundwater model which applies an analytical solution method, implementing superposition of the Theis equation, was primarily to achieve a high level of detail for water levels at pumping wells while keeping computation time at a minimum. The complexity of the aquifer structure, high in heterogeneity, raises the issue as to whether the Theis solution can be applied despite violations of the Theis assumptions. The research expectations were met, with the models providing an accurate prediction of water levels despite any violations of assumptions made.

4.1.1 Model Calibration Results

Aquifer transmissivity, storativity, and natural slope of the potentiometric surface served as calibration parameters in addition to well loss constants. The model is designed to independently analyze each aquifer within a well field. Four analytical models were created for the following: Arapahoe aquifer-Meadows Pumping Center, Denver aquifer-Meadows Pumping Center, Arapahoe aquifer-Castle Oaks Pumping Center, and Denver aquifer-Castle Oaks

Pumping Center. A summary of the calibration results is provided in Table 4.1. The model-calibrated transmissivities are within ranges obtained from previous studies (Figure 4.1). The transmissivity values for the Arapahoe aquifer are further supported by stratigraphic cross sections developed from geophysical well log data [Sale et al., 2010]. These cross sections (see example in Figure 2.3) indicate that the transmissive layers within the aquifers are more abundant in the southwest area of Castle Rock and lessen to the northeast, a product of alluvial fan deposits from the Rocky Mountain Front Range thinning out towards the eastern plains. Although model results are consistent with this observed trend in transmissivity for the Arapahoe aquifer, the results for the Denver aquifer show a higher transmissivity in the Castle Oaks Pumping Center, which is to the east of the Meadows Pumping Center. Heterogeneity within the aquifer coupled with the local scale of the modeled area could be the reason for this result.

Example plots comparing modeled and observed historical water level elevations are provided in Figures 4.2 and 4.3. The model accurately predicted the timing of drawdown and recovery events. Additionally, the model provided a close approximation of the drawdown magnitude for each well. Comparison plots for all 22 wells are shown in Appendices B and C. These results show that the analytical model was able to produce the detail necessary to capture the localized, steep cones of depression that occur at pumped wells in the area.

Table 4.1: Summary of aquifer properties and well loss constants developed from model calibration process

Pumping Center	Aquifer	Transmissivity (gal/day*ft)	Transmissivity (ft^2/day)	Storativity	Potentiometric Slope (Ax+By+C)*	Well	Well Loss Constant (day^2/ft^5)**
Meadows	Denver	1000	134	0.0005	A= -0.00512 B= -0.011985 C= 185484.2 ft	CR148	$1x10^{-9}$
						CR149	$1 x10^{-8}$
						CR150	$1 x10^{-9}$
						CR174	$1 x10^{-9}$
						CR221	$1 x10^{-7}$
						CR47	$6 x10^{-10}$
						CR50R	$4 x10^{-10}$
						CR51A	0
	Arapahoe	4000	535	0.00005	A= -0.005 B= -0.012 C= 184961 ft	CR86	$2 x10^{-8}$
						CR83	$4 x10^{-8}$
						CR82	0
						CR49	$2 x10^{-8}$
						CR28R	0
						CR27	$1 x10^{-8}$
						CR223	$1 x10^{-8}$
						CR219	0
Castle Oaks	Denver	1800	241	0.0001	A= -0.0055 B= -0.01198 C= 186418.5 ft	CR105	$1.5 x10^{-7}$
						CR110	$9 x10^{-9}$
						CR111	$1 x10^{-10}$
	Arapahoe	2200	294	0.0007	A= -0.0056 B= -0.01198 C= 185818.5 ft	CR118	$1 x10^{-10}$
						CR123	$2 x10^{-8}$
						CR124	$2 x10^{-8}$

*x and y correspond to well locations

**Units derived from Domenico & Schwartz [1990]

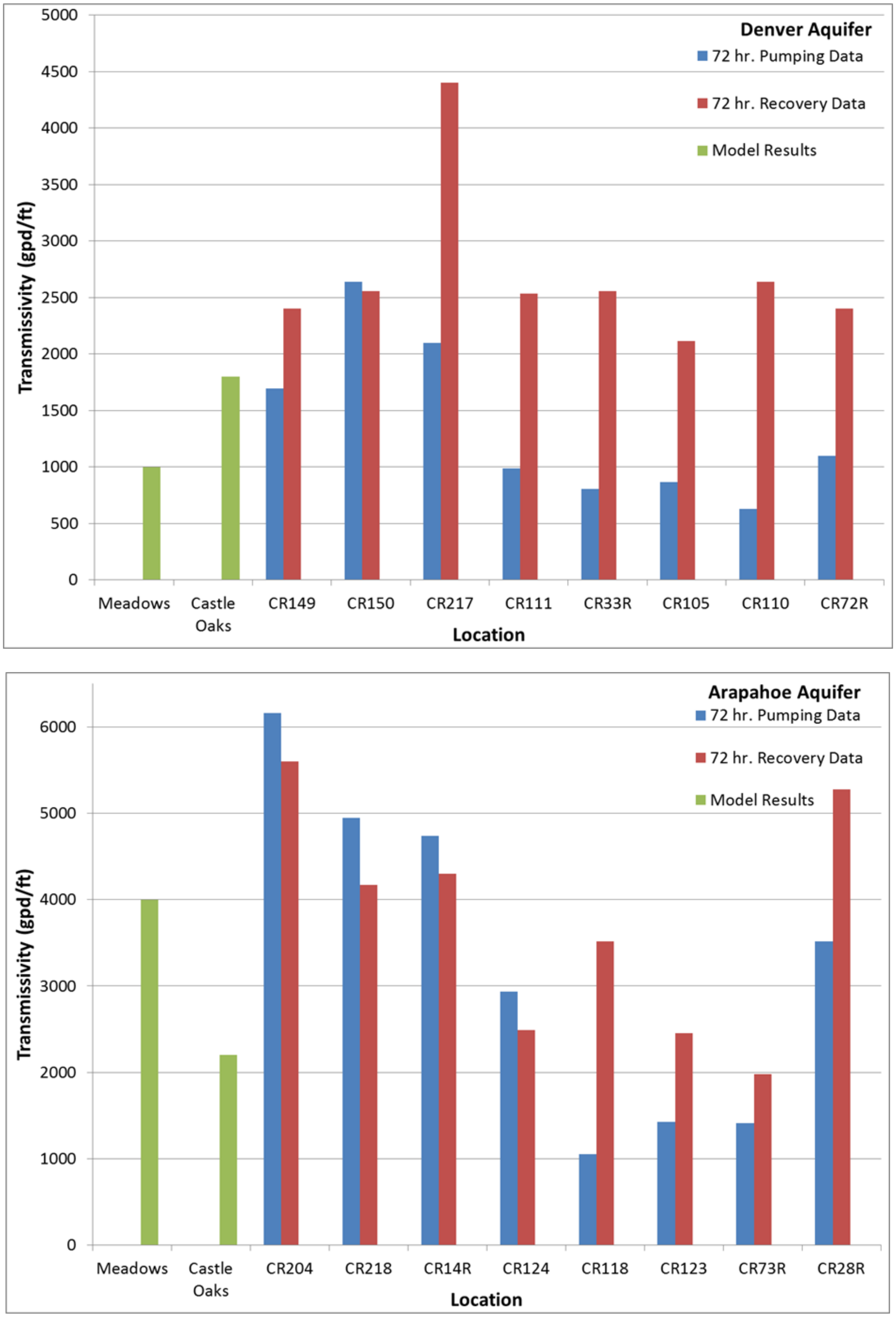

Figure 4.1: Comparison of model-calibrated transmissivities to previous estimates from single-well tests in the vicinity of Castle Rock, Colorado. (a) Denver aquifer. (b) Arapahoe aquifer. Single-well tests were conducted by Hemenway Groundwater Engineering.

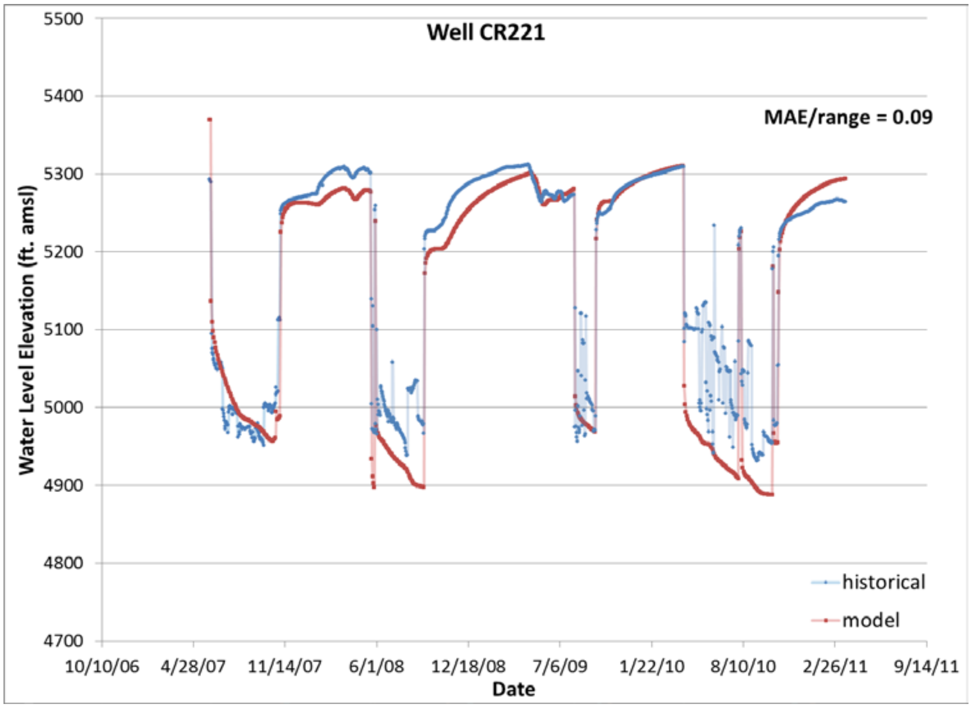

Figure 4.2: Modeled versus observed water levels for well CR221 in the Denver aquifer/Meadows well field.

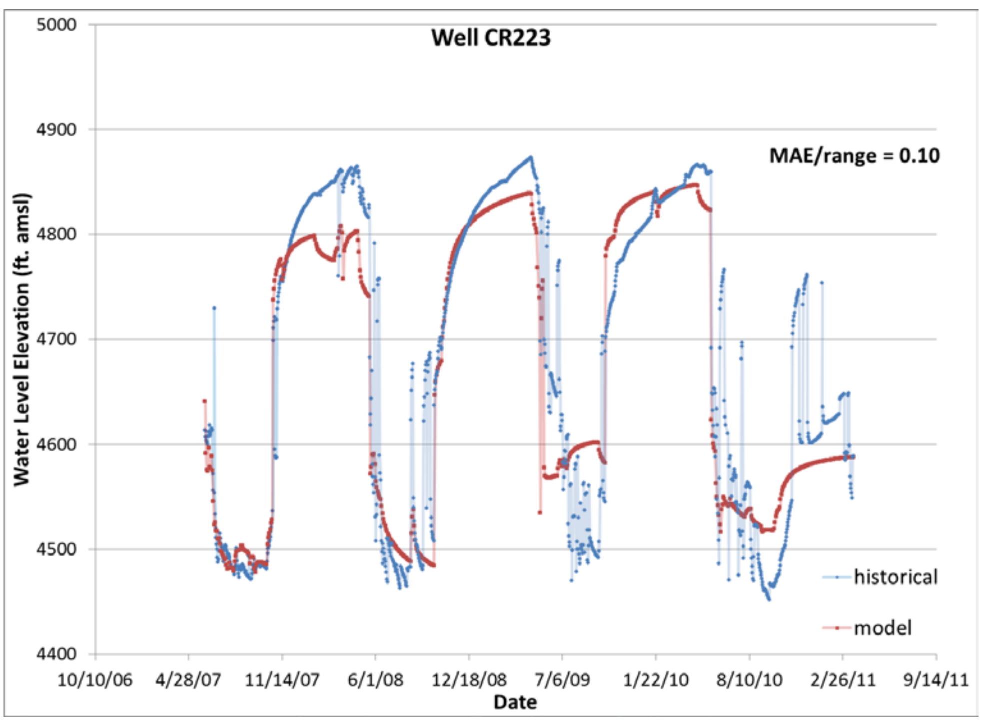

Figure 4.3: Modeled versus observed water levels for well CR223 in the Arapahoe aquifer/Meadows well field.

4.1.2 Quantitative Assessment of the Model Calibration

The analytical models were calibrated using a visual best-fit to measured water levels, as described in Section 3.1.1. The goodness-of-fit was subsequently quantified by calculating the mean absolute error (MAE) for each production well. The MAE was normalized by the observed range in measured water levels at each well (i.e., the minimum water level subtracted from the maximum water level). For all wells, the MAE/range values were between 0.06 and 0.31, averaging 0.14 (Appendix B). This means that the size of the residual (difference between modeled and observed water level) is, on average, approximately 1/7th of the total range in observed water levels at a given well.

It is important to note that in infrequent cases, periods of unrealistic data were not considered for the model analysis. Data was determined to be unrealistic and therefore unusable in instances where historical water levels were shown to be rising above ground surface, dropping to sea level, or when water levels showed no fluctuations despite multiple pumping sequences occurring. It is not uncommon for data collection devices to periodically malfunction or be disturbed for well maintenance, therefore these periods of unrealistic water levels were treated as gaps in usable data.

4.2 Power and Energy Use Calculations

A power and energy model was developed using historical data for both the Meadows and Castle Oaks well fields. Energy consumption was estimated for each individual well and also as an entire well field assessment. Well CR223 in the Denver aquifer/Meadows well field and well CR221 in the Arapahoe aquifer/Meadows well field are again considered as examples. The power and energy use for these wells is shown in Figures 4.4 and 4.5. The model uses drawdown profiles to predict timing and magnitude of the power requirement and associated cumulative energy consumption. It is important to note that the modeled power and energy values did not take into account other sources for power/energy use, such as power needed for start-up of pumps. A base model using historical water level and flow rate data was developed initially. This base model was then used as a means for comparison to the alternative pumping scenarios that were designed. The power and energy model was not calibrated against observed historical electrical energy consumption values because its sole purpose was to provide a way to evaluate a relative comparison with the alternative pumping scenarios.

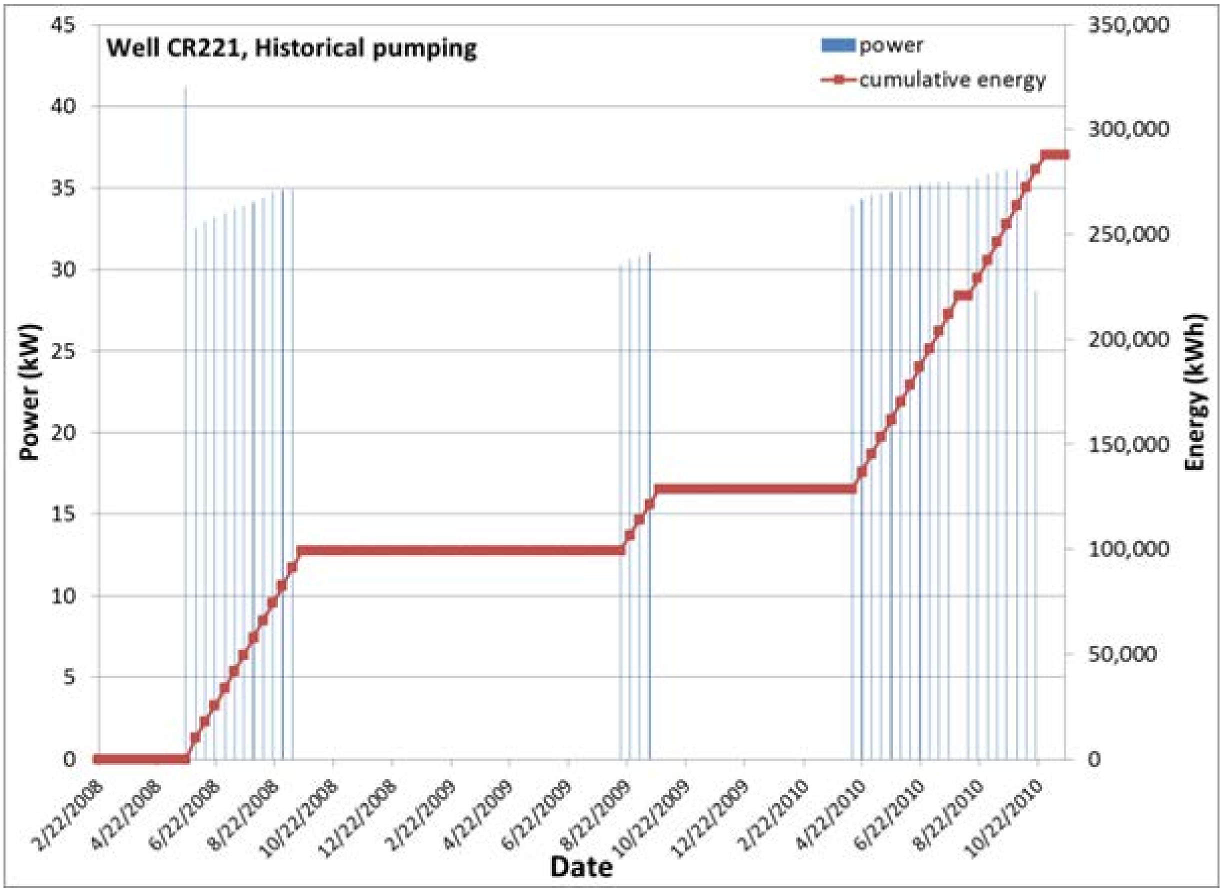

Figure 4.4: Modeled power and energy use for well CR221 in the Denver aquifer/Meadows well field, based on historical pumping techniques.

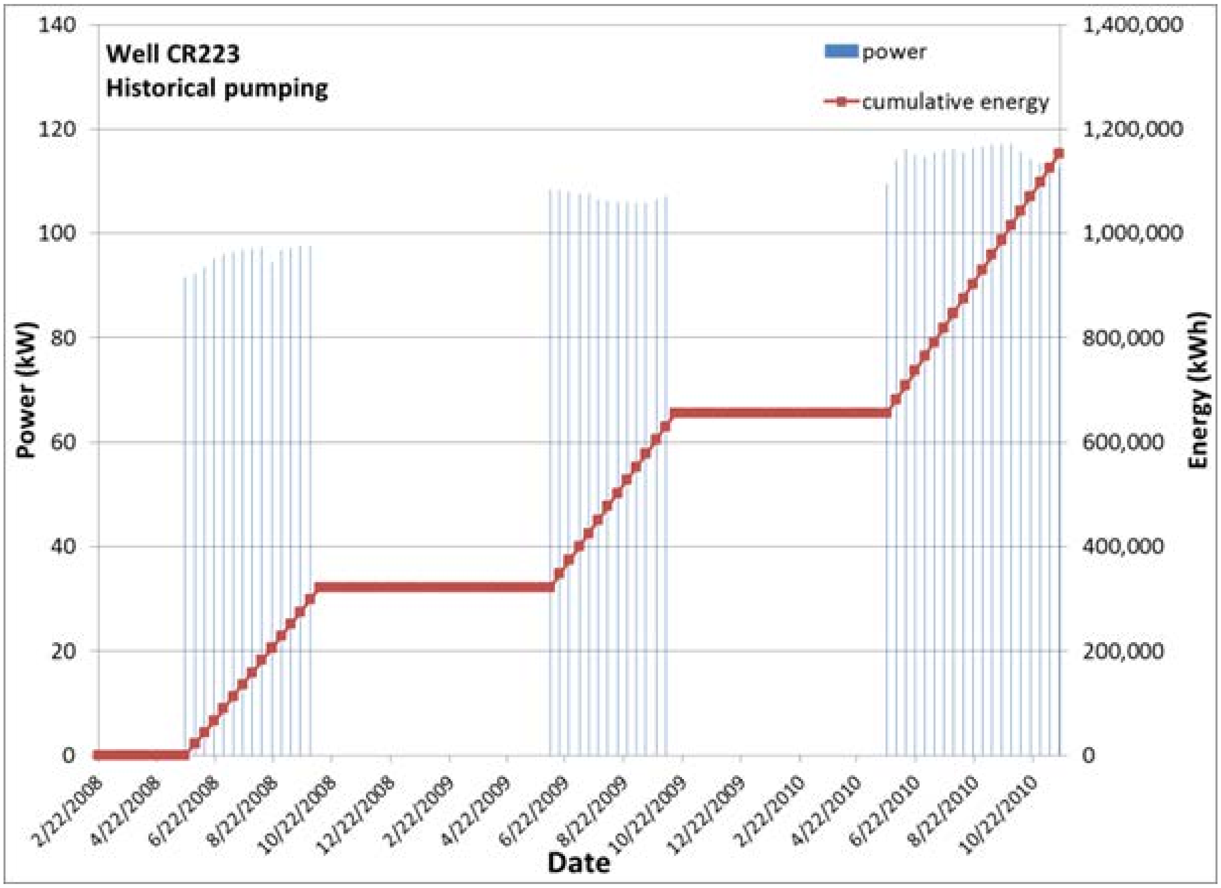

Figure 4.5: Modeled power and energy use for well CR223 in the Arapahoe aquifer/Meadows well field, based on historical pumping techniques.

4.2.1 Alternative Pumping Scenarios

The objective of the alternative pumping scenarios was to identify pumping schemes that reduce total energy use at Castle Rock well fields. The motivating concept was that drawdown at a given well could be lessened by developing a pumping strategy that would reduce cross-well interferences. Since the variable parameters of total dynamic head (TDH) and flow rate are directly related to power, these were focused on as a means of reducing power, and ultimately energy consumption as well. Application of the dispersed pumping technique is intended to lower TDH by maximizing radial distances between actively pumping wells and reducing cross-well interferences, when possible. However, this technique cannot be applied during peak seasons since all wells must be active to meet demands. Reducing flow rates restricts the severity of drawdown depths, consequently reducing TDH. Another means of reducing TDH was attempted by lessening the length of time allowed for pumping and additionally allowing a longer recovery period between pumping sequences. Similar to reducing flow rates, enforcing time constraints on pumping resulted in less severe drawdown depths.

A net reduction in energy was achieved in all seven alternative pumping scenarios that were developed. Table 4.2 provides a summary of the total energy consumption based on historical data as well as energy consumption comparisons for each alternative pumping scenario. Each pumping scenario produced a slightly different volume of water. Therefore, the energy consumption (kWh) was normalized by the total volume of water (gal) produced for each scenario. Scenario #4 provided the greatest reduction in energy consumption (13.0%) compared to historical pumping techniques. This scenario involved application of the customized dispersed pumping schedule for the Arapahoe aquifer and reduced flow rates for the Denver aquifer wells. Because the volume of water needed to meet demand is furnished through production from both aquifers, this allows for one aquifer to be stressed while the other aquifer recovers, when necessary. In the Denver aquifer scenario #4 produced energy consumption values that were greater than historical, yet still accomplished a favorable net energy reduction because of the remarkably lower energy consumption values achieved in the Arapahoe aquifer. Although it did not achieve the largest net energy reduction, scenario #5 (9.65% reduction from historical pumping techniques) produced energy consumption values that were notably less than historical in both the Denver and Arapahoe aquifers, simultaneously. The same techniques were applied to the Arapahoe aquifer in scenario #5 as those in scenario #4, using the customized dispersed pumping technique. But in scenario #5 the use of time constraints on pumping and recovery of wells in addition to reduced flow rates was applied to the Denver aquifer wells. This approach achieved a greater reduction in energy consumption in the Denver aquifer as compared to scenario #4. In the Arapahoe aquifer however, despite the reduction in energy from historical, scenario #5 produced higher energy consumption than did scenario #4 which led to a lesser net energy reduction than scenario #4. Under current practices, water demands are met cumulatively from both aquifers and therefore scenario #4 provides the best suggestion for alternative pumping techniques. But understanding each aquifer's response to pumping is beneficial as well; if demand methods were to change, scenario #5 provides the clarity to reduce energy in each aquifer individually. Reducing energy consumption not only translates into lower electrical costs associated with water production, it places less demand on the municipal electrical supply facility and reduced carbon emissions as well.

Table 4.2: Energy consumption for alternative pumping scenarios

	Denver Aquifer (kWh)	Arapahoe Aquifer (kWh)	Both Aquifers (kWh)	% Net Reduction in Energy from Historical	Cumulative Water Produced (gal)	Normalized Energy per Volume (kWh/gal)
Historical	1,160,663	4,002,287	5,162,950	NA	999,080,309	0.005168
Scenario #1	1,592,310	3,254,488	4,846,798	6.14	999,907,200	0.004847
Scenario #2	1,097,906	3,830,139	4,928,045	4.55	999,374,400	0.004850
Scenario #3	1,434,423	3,444,893	4,879,316	5.49	997,675,200	0.004891
Scenario #3b	2,756,780	1,826,543	4,583,323	11.23	998,870,400	0.004589
Scenario #4	1,610,470	2,879,569	4,490,039	13.03	995,527,872	0.004510
Scenario #5	1,113,747	3,551,199	4,664,946	9.65	995,035,104	0.004688
Scenario #6	585,761	4,493,571	5,079,332	1.62	994,605,312	0.005107

4.2.2 Analysis of the Response to Pumping in each Aquifer

Throughout the process of developing alternative pumping scenarios, a recurring pattern was observed in particular parameters promoting energy reduction more so within one aquifer over the other. For example, the dispersed pumping technique had a much more dramatic effect on reducing TDH and therefore energy consumption in the Arapahoe aquifer than it did in the Denver aquifer. Conversely, lowering flow rates or reducing the length of time allowed for pumping while increasing the recovery time for wells was most effective in the Denver aquifer. This evaluation enhances the conceptual understanding of the aquifers' response to pumping. The interpretation is that the Denver aquifer, with a lower transmissivity than the Arapahoe aquifer, will form more localized and steep cones of depression around the pumped wells and therefore cross-well interferences have less influence on drawdown depths compared to the Arapahoe aquifer. The primary objective to reduce energy consumption associated with pumping within the Denver aquifer is to focus on lessening the severity of drawdown, achieved through time constraints on pumping and/or lowering flow rates. The cones of depression that form in the Arapahoe aquifer will be more shallow and have a broader extent. Therefore, cross-well interferences have a stronger effect on enhancing drawdown levels, making the dispersed pumping technique highly favorable. By simply applying a combination of dispersed pumping in the Arapahoe aquifer along with time and flow rate restrictions in the Denver aquifer, long-term energy consumption can be significantly reduced. Figures 4.6 through 4.9 provide cross-sectional diagrams of modeled potentiometric surfaces for both the Denver and Arapahoe aquifers in the Meadows Pumping Center on September 9th, 2008. Figures 4.6 and 4.8 illustrate the deep cones of depression associated with historical pumping techniques. Figures 4.7 and 4.9 provide a visualization of how TDH can be reduced at the pumped wells by following the pumping techniques used in alternative pumping scenario #5 (see Table 3.1 for alternative pumping scenario design factors).

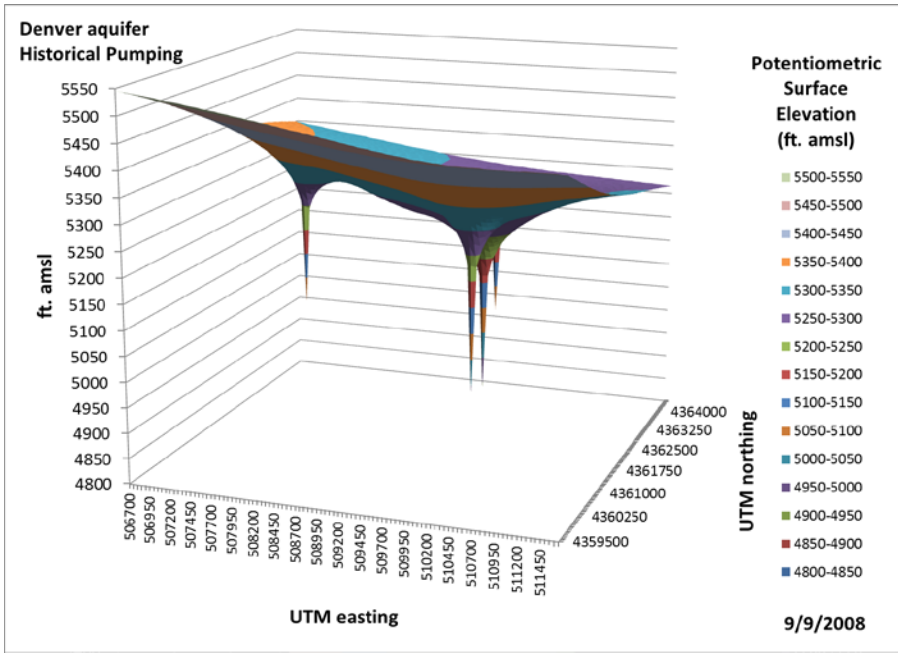

Figure 4.6: Modeled potentiometric surface on Sept 9, 2008 based on historical pumping techniques for the Denver aquifer, Meadows Pumping Center.

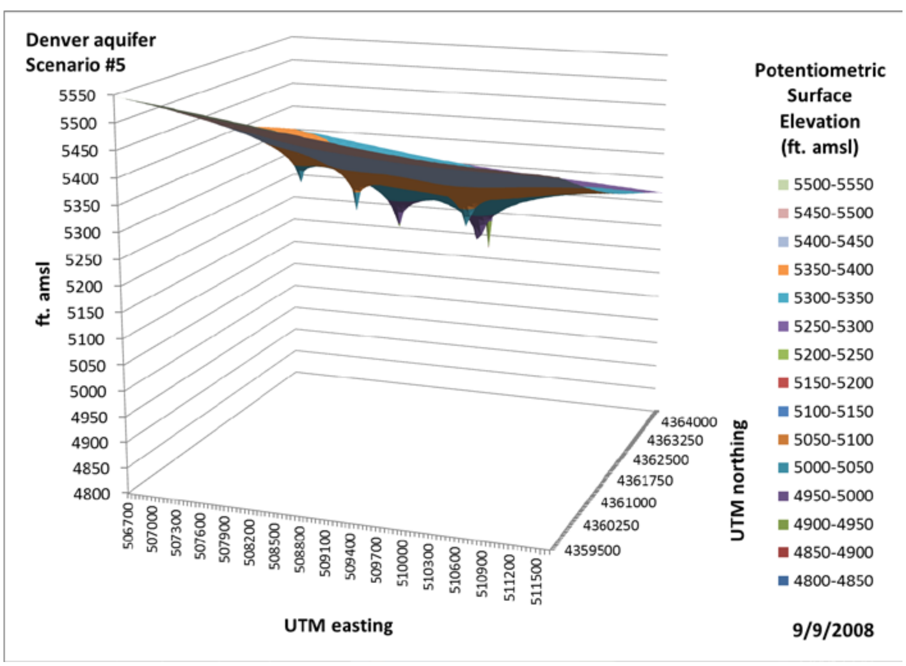

Figure 4.7: Modeled potentiometric surface on Sept 9, 2008 based on alternative pumping scenario #5 techniques for the Denver aquifer, Meadows Pumping Center.

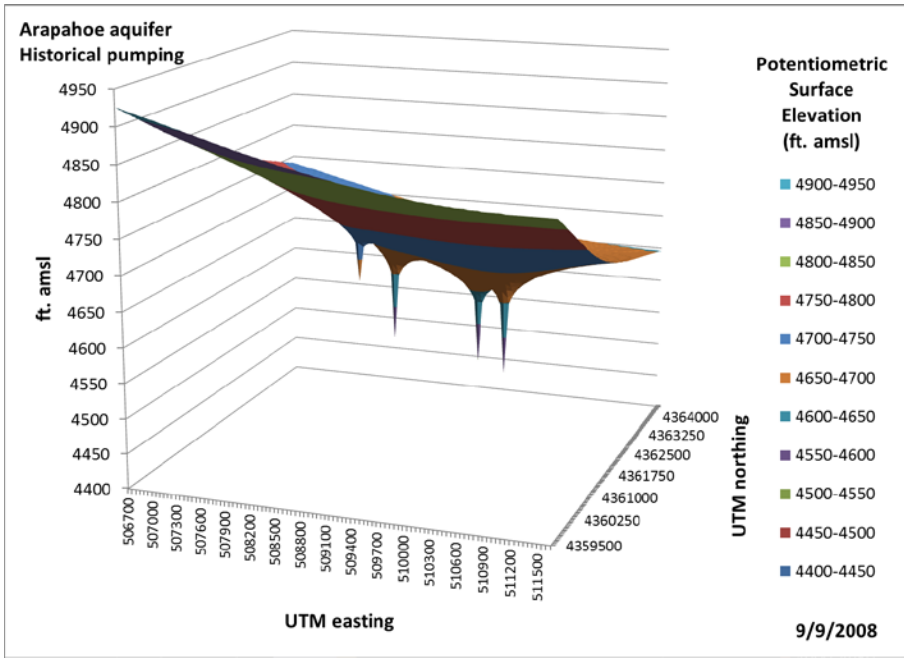

Figure 4.8: Modeled potentiometric surface on Sept 9, 2008 based on historical pumping techniques for the Arapahoe aquifer, Meadows Pumping Center.

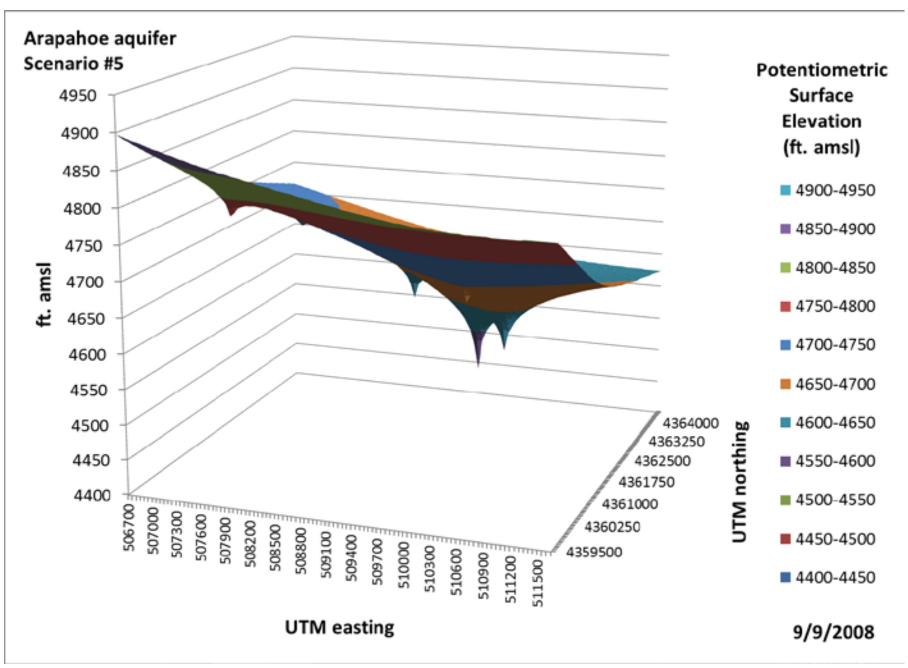

Figure 4.9: Modeled potentiometric surface on Sept 9, 2008 based on alternative pumping scenario #5 techniques for the Arapahoe aquifer, Meadows Pumping Center.

CHAPTER 5 – CONCLUSIONS

5.1 Summary of Study

Increasing demands on groundwater resources requires continual efforts to improve our understanding and management of these finite reserves. The analytical modeling technique employed in this research provided a suitable and valuable local-scale assessment of groundwater resources in the Denver Basin aquifer system. The objectives of this project were to accurately replicate historical water levels at pumping wells within the study site area, provide a means of estimating effective hydraulic properties (transmissivity and storativity) in a heterogeneous aquifer system with active pumping, and offer a tool for determining strategies to reduce energy consumption in a water supply well field. The efforts of this research have yielded positive results, lending confidence that the analytical solution models utilized in this study have the potential to be a strong contribution to the field of groundwater modeling and groundwater supply management.

5.2 Other Potential Applications and Future Research

For this research, analytical models were designed specifically for municipal water supply well fields. However, the applications of this modeling approach extend beyond the scope of municipalities. Many other groundwater supply assessments conducted within actively pumped aquifers could benefit from the methodology used in this research. Freshwater supplies are demanded not only for human consumption but for industrial purposes as well. Notably, the analytical models exhibit significant potential for assessing the benefits of aquifer storage and recovery (ASR) scenarios, which could contribute to energy reductions and aquifer sustainability. The existing modeling code would require only limited modification for new applications, thereby contributing to the efficiency of future projects.

With slight improvements the models have the feasibility to be a groundwater modeling tool that would be welcomed by the research community, especially if they were re-worked to run on a more automated level. The current modeling process is predominantly manual. For example, historical data are input into the model manually, and the calibration is achieved through an iterative, visual best fit. The optimization of energy consumption through alternative pumping scenarios in particular were manually designed. Developing a more automated modeling process would greatly enhance efficiency, improve optimizations, reduce the potential for errors, and make the model more broadly applicable for both research and practical problems.

REFERENCES

Ahlfeld, D.P., Laverty, M.M., 2011, Analytical solutions for minimization of energy use for groundwater pumping, *Water Resources Research*, Vol. 47, W06508.

Bair, E.S., Springer, A.E., Roadcap, G.S., 1991, Delineation of traveltime-related capture areas of wells using analytical flow models and particle-tracking analysis, *Ground Water*, Vol. 29(3), 387-397.

Cole, J.C., Trexler, J.H. Jr., Cashman, P.H., Miller, I.M., Shroba, R.R., Cosca, M.A., Workman, J.B., 2010, Beyond Colorado's Front Range- A new look at Laramide basin subsidence, sedimentation, and deformation in north-central Colorado. The Geological Society of America Field Guide 18.

Domenico, P.A., and Schwartz, F.W., 1990, Physical and Chemical Hydrogeology. John Wiley & Sons, Inc.

Evanoff, E., 2007, The Castle Rock Conglomerate. Geological Society of America Abstracts with Programs, Vol. 39, No. 6, p. 26.

Freeze, R.A., and Cherry, J.A., 1979, Groundwater. Prentice Hall, Englewood Cliffs, NJ.

Haitjema, H.M., 1995, Analytic element modeling of ground water flow. Academic Press, San Diego, CA.

Moore, R., 2012, March 1. Castle Rock population estimate tops 50,000, *ourCastleRocknews.com*. Available on the World Wide Web URL: http://www.ourcoloradonews.com/castlerock/news/ Retrieved 4/16/2013.

Paschke, S.S., Banta, E.R., Litke, D.W., 2011, Groundwater Availability of the Denver Basin Aquifer System, Colorado. U.S. Department of the Interior, U.S. Geological Survey Professional Paper 1770.

Pottorff, E.T., 2011, Ground Water Levels in the Denver Basin Bedrock Aquifers. Colorado Division of Water Resources, Department of Natural Resources.

PTC (2011), Mathcad Engineering Software v. 15.0: Parametric Technology Corporation, Needham, MA.

Raynolds, R.G., 2002, Upper Cretaceous and Tertiary stratigraphy of the Denver Basin, Colorado. *Rocky Mountain Geology*, Vol. 37(2), p. 111-134.

Raynolds, R.G., Johnson, K.R., 2003, Synopsis of the stratigraphy and paleontology of the uppermost Cretaceous and lower Tertiary strata in the Denver Basin, Colorado. *Rocky Mountain Geology*, Vol. 38(1), p. 171-181.

Robson, S.G., 1987, Bedrock Aquifers in the Denver Basin, Colorado- A Quantitative Water-Resources Appraisal. U.S. Geological Survey Professional Paper 1257.

Robson, S.G., 1989, Alluvial and Bedrock Aquifers of the Denver Basin-Eastern Colorado's Dual Ground-Water Resource. United States Geological Survey Water-Supply Paper 2302.

Robson, S.G. and Banta, E.R., 1995, Ground Water Atlas of the United States, "Arizona, Colorado, New Mexico, Utah, HA730=C". Available on World Wide Web, URL: USGS HA730-C: http://pubs.usgs.gov/ha/ha730/ch_c/C-text6.html Retrieved 4/16/2013.

Sale, T. 2007, Sustainability of Groundwater Production from the Denver Basin Aquifers in the Vicinity of Castle Rock, Colorado. Report generated for the Town of Castle Rock, Colorado.

Sale, T., Bailey, A., Maurer, A., 2010, 2010 Studies Supporting Sustainable Use of the Denver Basin Aquifers in the Vicinity of Castle Rock. Colorado State University Report. Project Report for the Town of Castle Rock, October 13, 2010.

Sale, T., Eldiery, A., Bailey, A., 2009, Compilation and Preliminary Analysis of Hydrogeologic Data from the Denver Basin Aquifers in the Vicinity of Castle Rock, Colorado. Colorado State University Report Project Report for the Town of Castle Rock, April 27, 2009.

Sterrett, R.J., 2007, Groundwater and Wells. Johnson Screens, a Weatherford Company.

Theis, C.V., 1935, The relation between the lowering of the piezometric surface and the rate and duration of discharge of a well using ground-water storage. *Transactions of the American Geophysical Union*, Vol. 16.

Town of Castle Rock, 2006, Water Resources Strategic Master Plan, January 2006.

Woodard, L.L., Sanford, W., Raynolds, R.G., 2002, Stratigraphic variability of specific yield within bedrock aquifers of the Denver Basin, Colorado. *Rocky Mountain Geology*, Vol. 37, No. 2, p. 229.

Yeh, H.D., Chang, Y.C., 2013, Recent advances in modeling of well hydraulics. *Advances in Water Resources*, Vol. 51, 27-51.

APPENDIX A – Modeling Code

This appendix contains programming code used for the water level modeling, generation of potentiometric surfaces, and power/energy calculations. Program code was developed by T. Sale at Colorado State University using PTC Mathcad Engineering Software.

APPENDIX A

Well Function

Subroutine for obtaining W(u) as a function of u

$$W(u) := \left| \begin{array}{l} X \leftarrow \int_u^{\infty} \frac{e^{-x}}{x}\,dx \quad \text{if } u > 0.01 \\ X \leftarrow -0.5772 - \ln(u) \quad \text{otherwise} \\ X \end{array} \right.$$

Theis Equation

$$s = \frac{Q}{4\pi \cdot T} W\left(\frac{r^2 S}{4 \cdot T \cdot t}\right)$$

Drawdown Calculation

$$s(No, N_{Wells}, t) := \left| \begin{array}{l} s \leftarrow 0 \cdot ft \\ \text{for } j \in 1 .. N_{Wells} \\ \quad \text{for } i \in 1 .. N_{steps} \\ \quad\quad \text{if } t > W_{Time_{i,j}} \\ \quad\quad\quad \left| \begin{array}{l} s \leftarrow s + \frac{W_{Q_{i,j}}}{4 \cdot \pi \cdot T} \cdot W\left[\frac{(r_{No,j})^2 \cdot S}{4 \cdot T \cdot (t - W_{Time_{i,j}})}\right] \quad \text{if } t \le W_{Time_{i+1,j}} \\ s \leftarrow s + \frac{W_{Q_{i,j}}}{4 \cdot \pi \cdot T} \cdot \left[W\left[\frac{(r_{No,j})^2 \cdot S}{4 \cdot T \cdot (t - W_{Time_{i,j}})}\right] - W\left[\frac{(r_{No,j})^2 \cdot S}{4 \cdot T \cdot (t - W_{Time_{i+1,j}})}\right]\right] \quad \text{otherwise} \end{array} \right. \\ s \end{array} \right.$$

Drawdown accounting for well losses:

$$sx(No, N_{Wells}, t) := \left| \begin{array}{l} s \leftarrow 0 \cdot ft \\ \text{for } j \in 1..N_{Wells} \\ \quad \text{for } i \in 1..N_{steps} \\ \quad\quad \text{if } t > W_{Time_{i,j}} \\ \quad\quad\quad \left| \begin{array}{l} s \leftarrow s + \dfrac{W_{Q_{i,j}}}{4 \cdot \pi \cdot T} \cdot W\left[\dfrac{(r_{No,j})^2 \cdot S}{4 \cdot T \cdot \left(t - W_{Time_{i,j}}\right)}\right] \text{ if } t \le W_{Time_{i+1,j}} \\ s \leftarrow s + \dfrac{W_{Q_{i,j}}}{4 \cdot \pi \cdot T} \cdot \left[W\left[\dfrac{(r_{No,j})^2 \cdot S}{4 \cdot T \cdot \left(t - W_{Time_{i,j}}\right)}\right] - W\left[\dfrac{(r_{No,j})^2 \cdot S}{4 \cdot T \cdot \left(t - W_{Time_{i+1,j}}\right)}\right]\right] \text{ otherwise} \end{array} \right. \\ \text{for } i \in 1..N_{steps} - 1 \\ \quad Q_{well} \leftarrow W_{Q_{i,No}} \text{ if } t < W_{Time_{i+1,No}} \wedge t > W_{Time_{i,No}} \\ s \leftarrow s + C_{No} \cdot Q_{well}{}^2 \end{array} \right.$$

Potentiometric Surfaces:

$$WTElev := \left| \begin{array}{l} \text{for } i \in 1..300 \\ \quad \text{for } j \in 1..200 \\ \quad\quad \left| \begin{array}{l} xx \leftarrow 506700 \cdot ft + i \cdot 100 \cdot ft \\ yy \leftarrow 4359500 \cdot ft + j \cdot 100 \cdot ft \\ WTElev_{i,j} \leftarrow A \cdot xx + B \cdot yy + Ref \end{array} \right. \\ WTElev \end{array} \right.$$

$$PumpElev(N_{Wells}, t) := \left| \begin{array}{l} \text{for } t \in 1..100 \\ \quad \text{for } s \in 1..100 \\ \quad\quad \left| \begin{array}{l} x \leftarrow 506700 \cdot m + t \cdot 50 \cdot m \\ y \leftarrow 4359500 \cdot m + s \cdot 50 \cdot m \\ WTElev \leftarrow A \cdot x + B \cdot y + Ref \\ ss \leftarrow xxxxx(x, y, N_{wells}, 39300 \cdot day) \\ PumpElev_{t,s} \leftarrow WTElev - ss \end{array} \right. \\ PumpElev \end{array} \right.$$

$$xxxxx(x, y, N_{Wells}, t) := \left| \begin{array}{l} s \leftarrow 0 \cdot ft \\ \text{for } j \in 1..N_{Wells} \\ \quad \text{for } i \in 1..N_{steps} \\ \quad\quad \text{if } t > W_{Time_{i,j}} \\ \quad\quad\quad \left| \begin{array}{l} s \leftarrow s + \dfrac{W_{Q_{i,j}}}{4 \cdot \pi \cdot T} \cdot W\left[\dfrac{\left[\sqrt{(x - X_j)^2 + (y - Y_j + 0.5 \cdot ft)^2}\right]^2 \cdot S}{4 \cdot T \cdot \left(t - W_{Time_{i,j}}\right)}\right] \text{ if } t \le W_{Time_{i+1,j}} \\ s \leftarrow s + \dfrac{W_{Q_{i,j}}}{4 \cdot \pi \cdot T} \cdot \left[W\left[\dfrac{\left[\sqrt{(x - X_j)^2 + (y - Y_j + 0.5 \cdot ft)^2}\right]^2 \cdot S}{4 \cdot T \cdot \left(t - W_{Time_{i,j}}\right)}\right] - W\left[\dfrac{\left[\sqrt{(x - X_j)^2 + (y - Y_j + 0.5 \cdot ft)^2}\right]^2 \cdot S}{4 \cdot T \cdot \left(t - W_{Time_{i+1,j}}\right)}\right]\right] \text{ otherwise} \end{array} \right. \\ s \end{array} \right.$$

Power Equation:

$$QQ(No, N_{steps}, t) := \left| \begin{array}{l} j \leftarrow No \\ \text{for } i \in 1..N_{steps} \\ \quad Q \leftarrow W_{Q_{i,j}} \ \text{ if } \ t \geq W_{Time_{i,j}} \wedge t < W_{Time_{i+1,j}} \\ Q \end{array} \right.$$

$$Reservoir := 6000 \cdot ft$$

$$Power(No, N_{Wells}, t, N_{steps}, Eff) := \frac{QQ(No, N_{steps}, t) \cdot 1 \frac{gm}{cm^3} \cdot g \cdot [Reservoir - (Static(No) - sx(No, N_{Wells}, t))]}{Eff}$$

Energy Calculation:

$$ttt(t_i, NN, \Delta t) := \left| \begin{array}{l} t_1 \leftarrow t_i \\ \text{for } i \in 1..NN \\ \quad t_{i+1} \leftarrow t_i + \Delta t \\ t \end{array} \right.$$

$$Energy_{Well}(No, N_{Wells}, N_{steps}, Eff) := \left| \begin{array}{l} Sum_1 \leftarrow 0 \cdot kW \cdot hr \\ \text{for } i \in 1..100 \\ \quad \left| \begin{array}{l} ZZZ \leftarrow Power(No, N_{Wells}, t_i, N_{steps}, Eff) \cdot 10 \cdot day \\ Sum_{i+1} \leftarrow Sum_i + ZZZ \end{array} \right. \\ Sum \end{array} \right.$$

APPENDIX B – Comparison of modeled and observed water levels

Appendix B contains plots of modeled and observed historical water level elevations versus time for all 22 wells considered during model development and calibration. MAE/range values obtained from subsequent statistical analysis for each well are provided with plots.

APPENDIX B

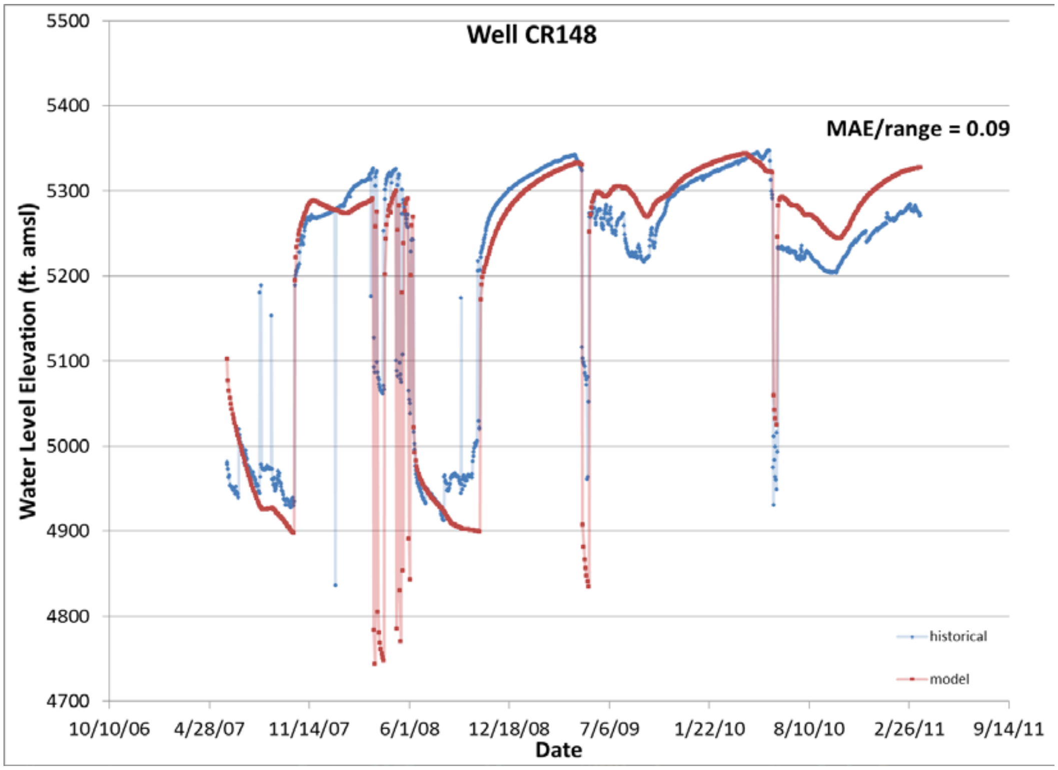
Well CR148
MAE/range = 0.09
Water Level Elevation (ft. amsl)
5500
5400
5300
5200
5100
5000
4900
4800
4700
10/10/06
4/28/07
11/14/07
6/1/08
12/18/08
7/6/09
1/22/10
8/10/10
2/26/11
9/14/11
Date
historical
model

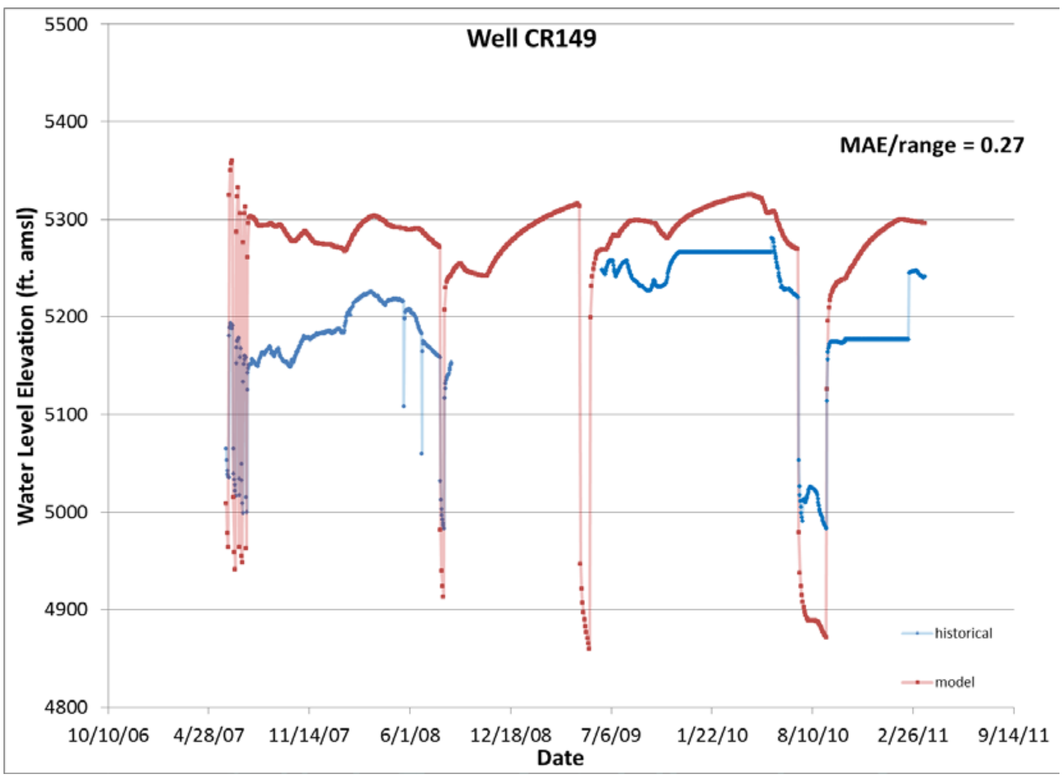
Well CR149
MAE/range = 0.27
Water Level Elevation (ft. amsl)
5500
5400
5300
5200
5100
5000
4900
4800
10/10/06
4/28/07
11/14/07
6/1/08
12/18/08
7/6/09
1/22/10
8/10/10
2/26/11
9/14/11
Date
historical
model

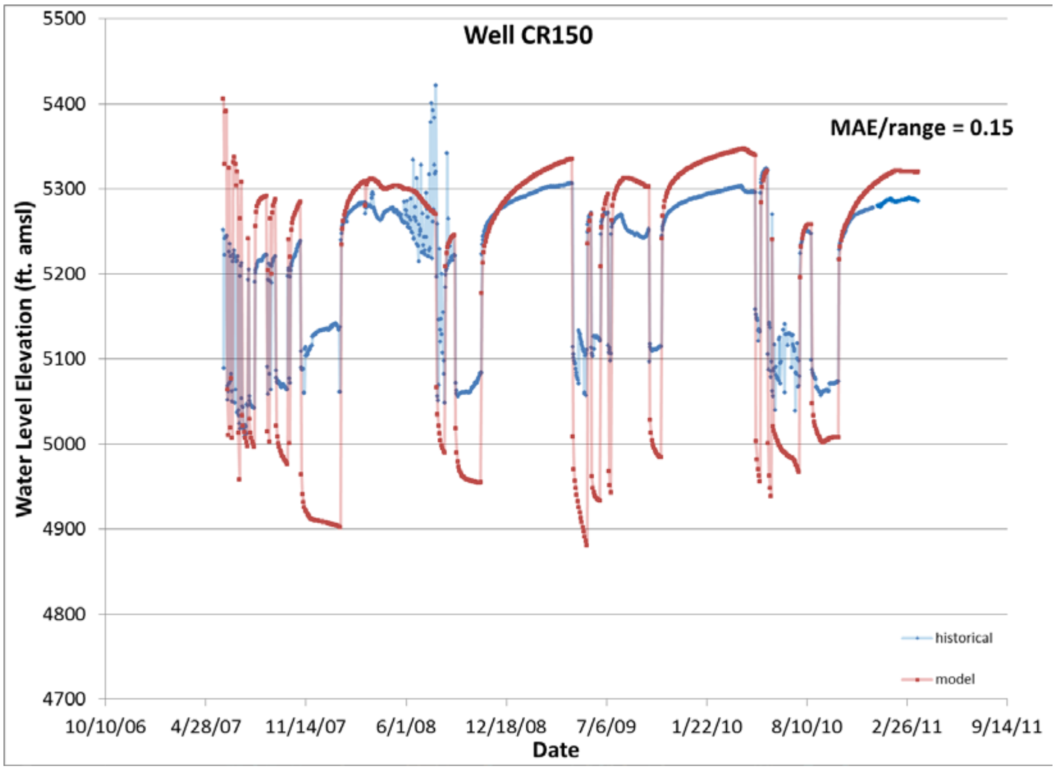
Well CR150
MAE/range = 0.15
Water Level Elevation (ft. amsl)
5500
5400
5300
5200
5100
5000
4900
4800
4700
10/10/06
4/28/07
11/14/07
6/1/08
12/18/08
7/6/09
1/22/10
8/10/10
2/26/11
9/14/11
Date
historical
model

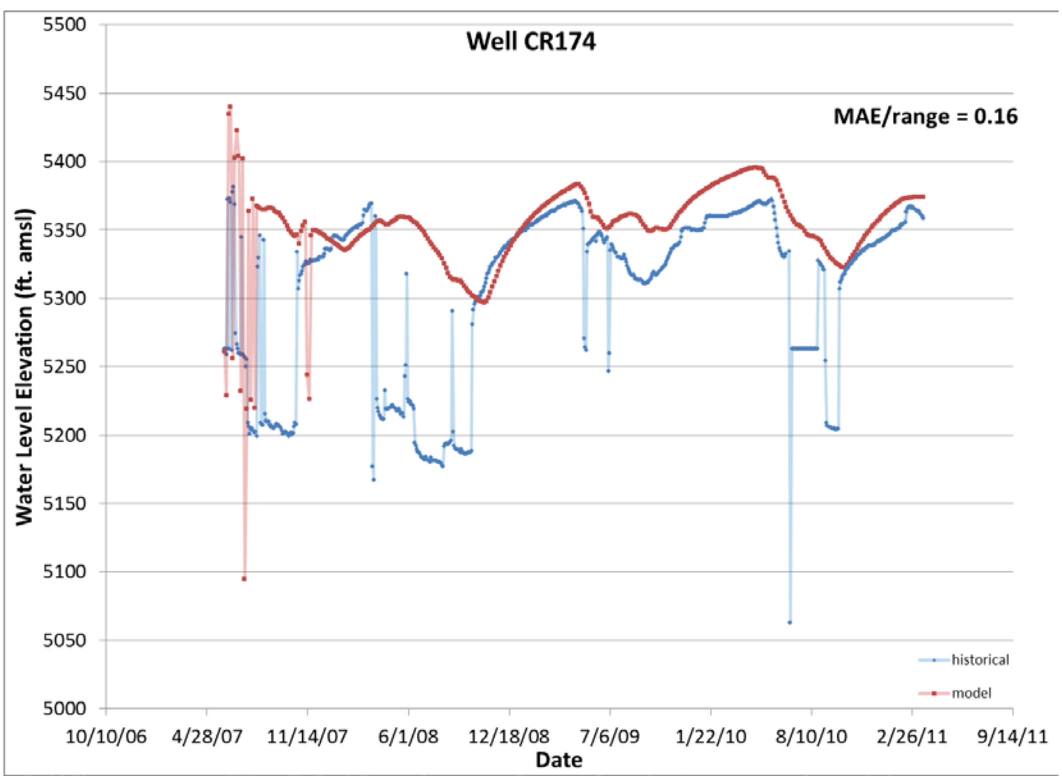
Well CR174
MAE/range = 0.16
Water Level Elevation (ft. amsl)
5500
5450
5400
5350
5300
5250
5200
5150
5100
5050
5000
10/10/06
4/28/07
11/14/07
6/1/08
12/18/08
7/6/09
1/22/10
8/10/10
2/26/11
9/14/11
Date
historical
model

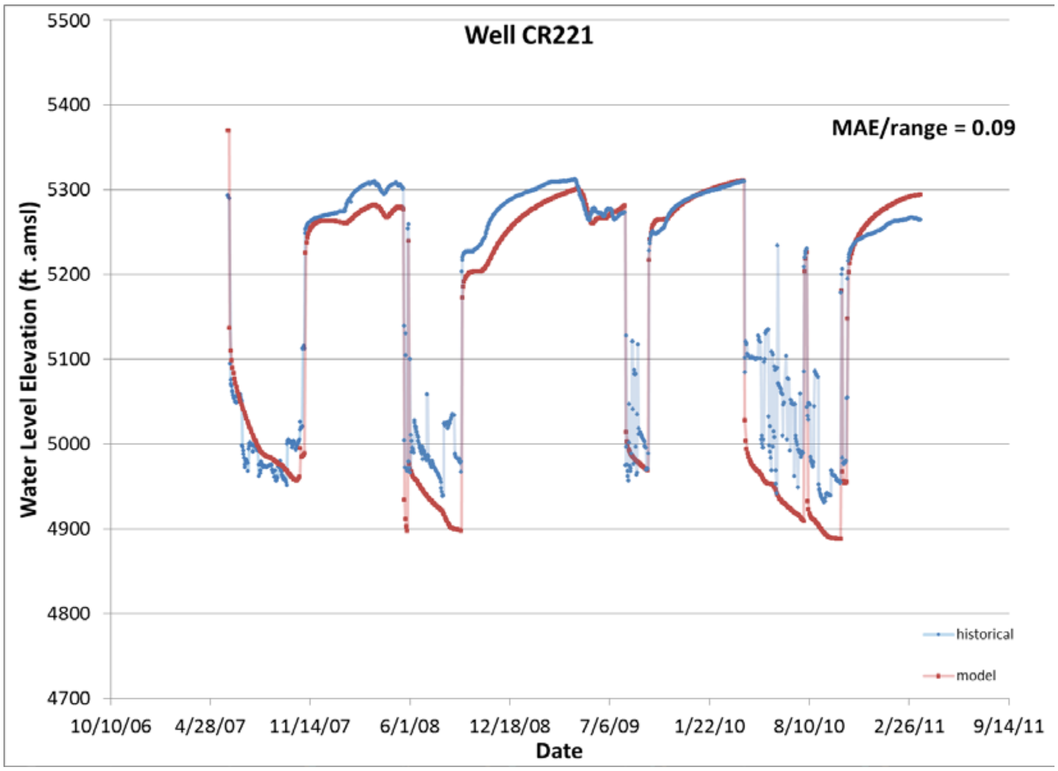
Well CR221
MAE/range = 0.09
Water Level Elevation (ft. amsl)
5500
5400
5300
5200
5100
5000
4900
4800
4700
10/10/06
4/28/07
11/14/07
6/1/08
12/18/08
7/6/09
1/22/10
8/10/10
2/26/11
9/14/11
Date
historical
model

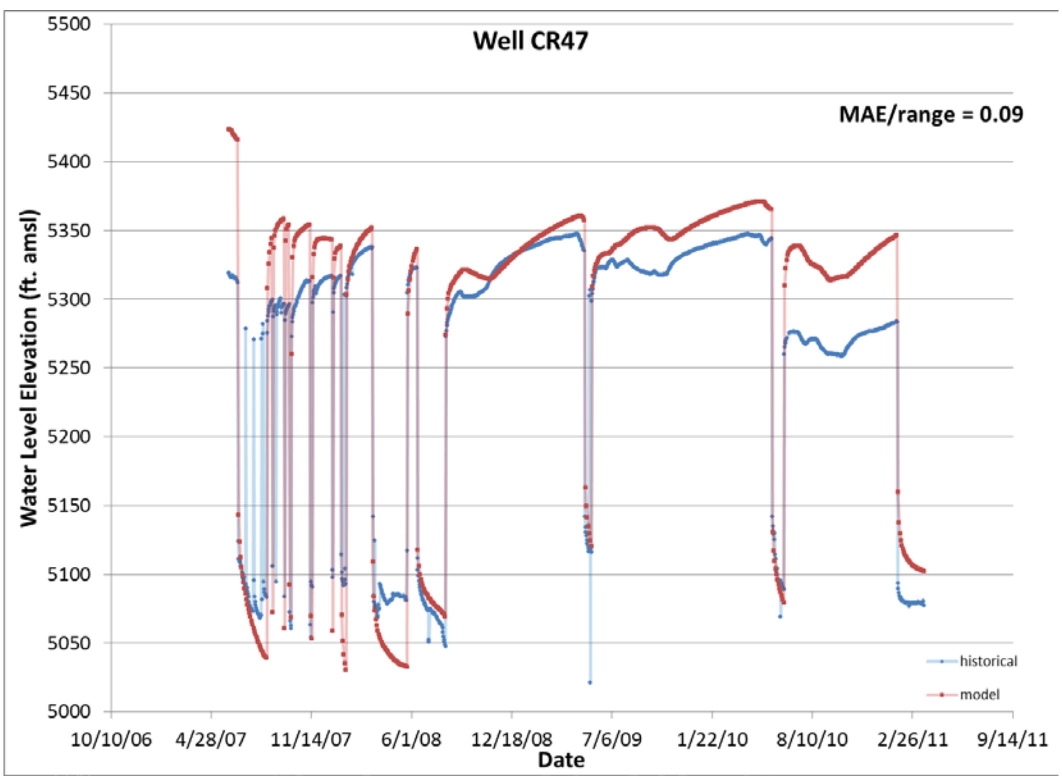
Well CR47
MAE/range = 0.09
Water Level Elevation (ft. amsl)
5500
5450
5400
5350
5300
5250
5200
5150
5100
5050
5000
10/10/06
4/28/07
11/14/07
6/1/08
12/18/08
7/6/09
1/22/10
8/10/10
2/26/11
9/14/11
Date
historical
model

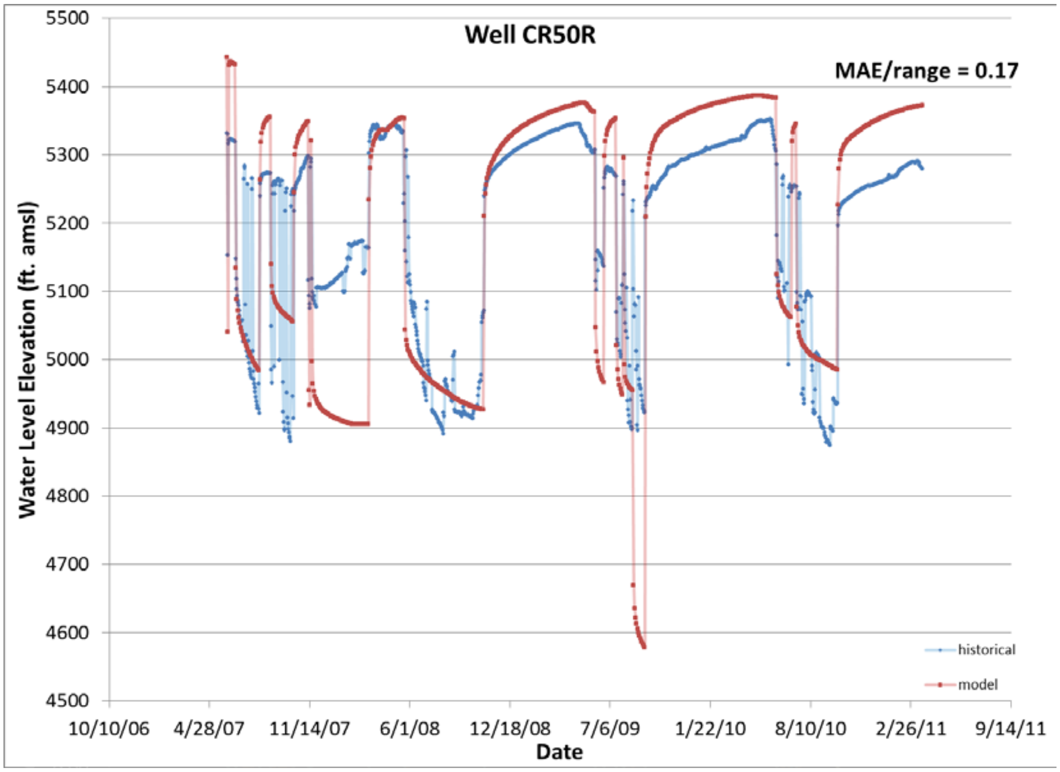

Well CR50R
MAE/range = 0.17
Water Level Elevation (ft. amsl)
5500
5400
5300
5200
5100
5000
4900
4800
4700
4600
4500
10/10/06
4/28/07
11/14/07
6/1/08
12/18/08
7/6/09
1/22/10
8/10/10
2/26/11
9/14/11
Date
historical
model

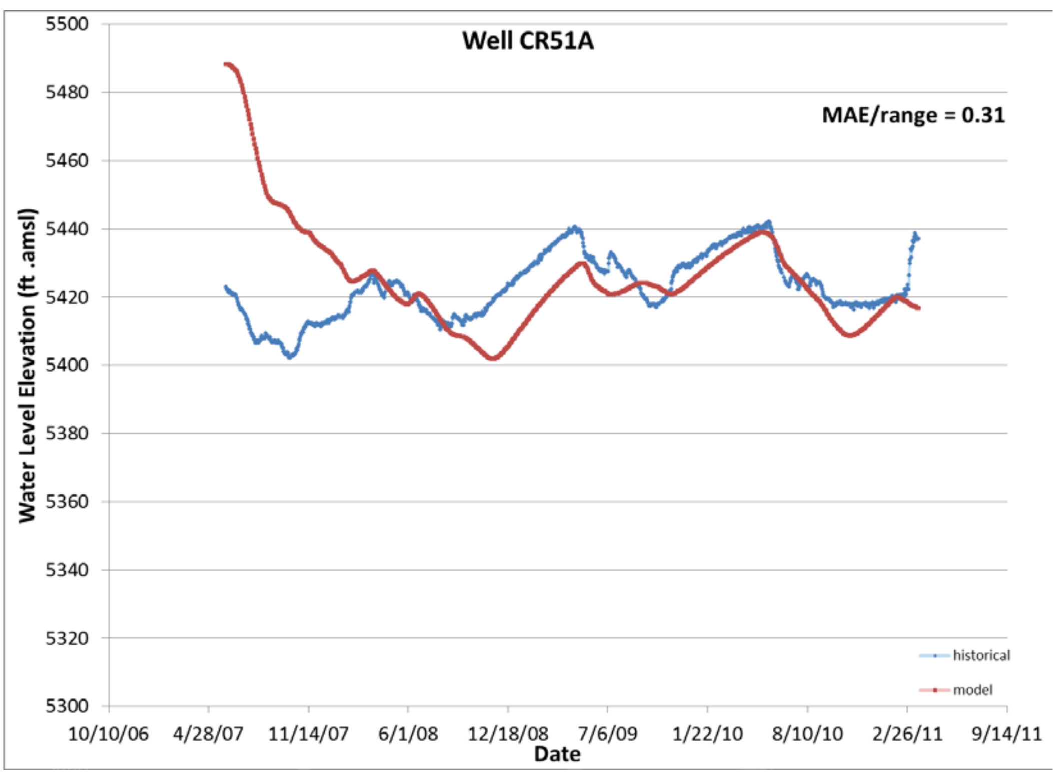

Well CR51A
MAE/range = 0.31
Water Level Elevation (ft .amsl)
5500
5480
5460
5440
5420
5400
5380
5360
5340
5320
5300
10/10/06
4/28/07
11/14/07
6/1/08
12/18/08
7/6/09
1/22/10
8/10/10
2/26/11
9/14/11
Date
historical
model

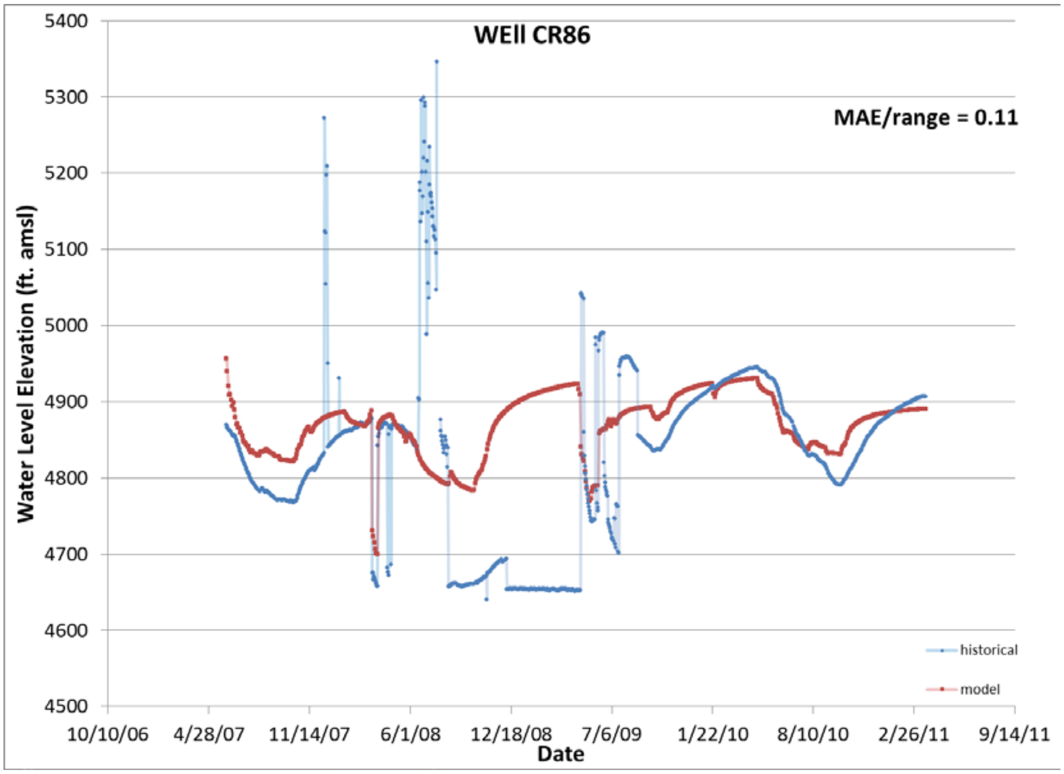
WEll CR86
MAE/range = 0.11
Water Level Elevation (ft. amsl)
5400
5300
5200
5100
5000
4900
4800
4700
4600
4500
10/10/06
4/28/07
11/14/07
6/1/08
12/18/08
7/6/09
1/22/10
8/10/10
2/26/11
9/14/11
Date
historical
model

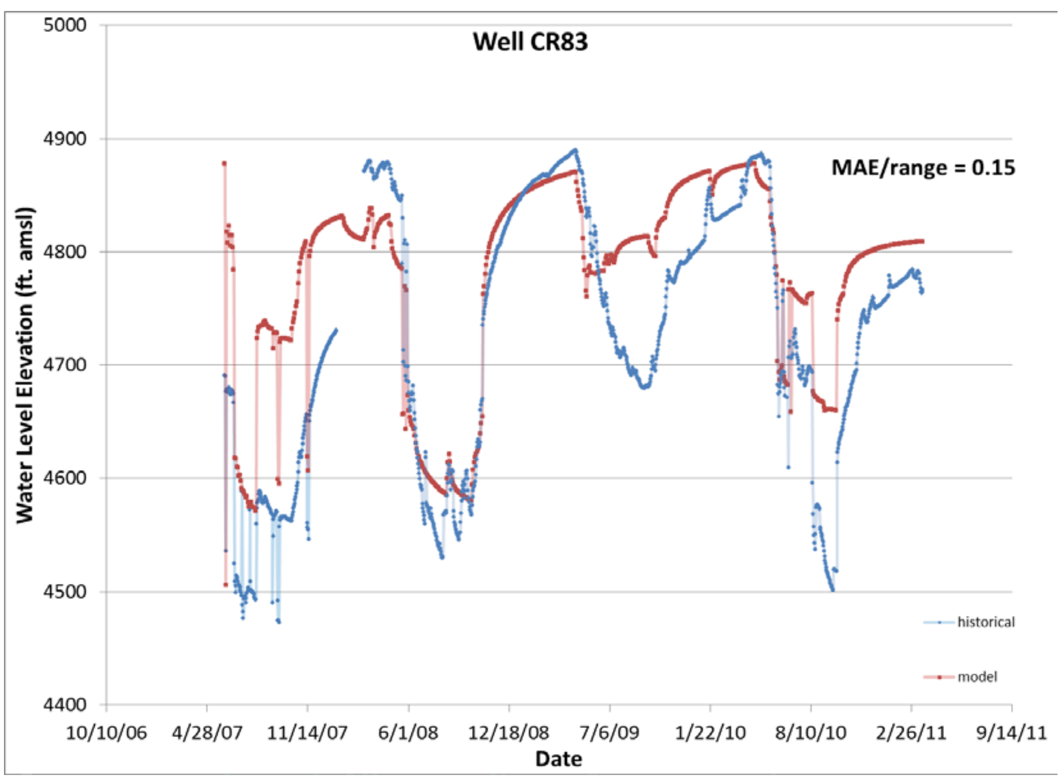
Well CR83
MAE/range = 0.15
Water Level Elevation (ft. amsl)
5000
4900
4800
4700
4600
4500
4400
10/10/06
4/28/07
11/14/07
6/1/08
12/18/08
7/6/09
1/22/10
8/10/10
2/26/11
9/14/11
Date
historical
model

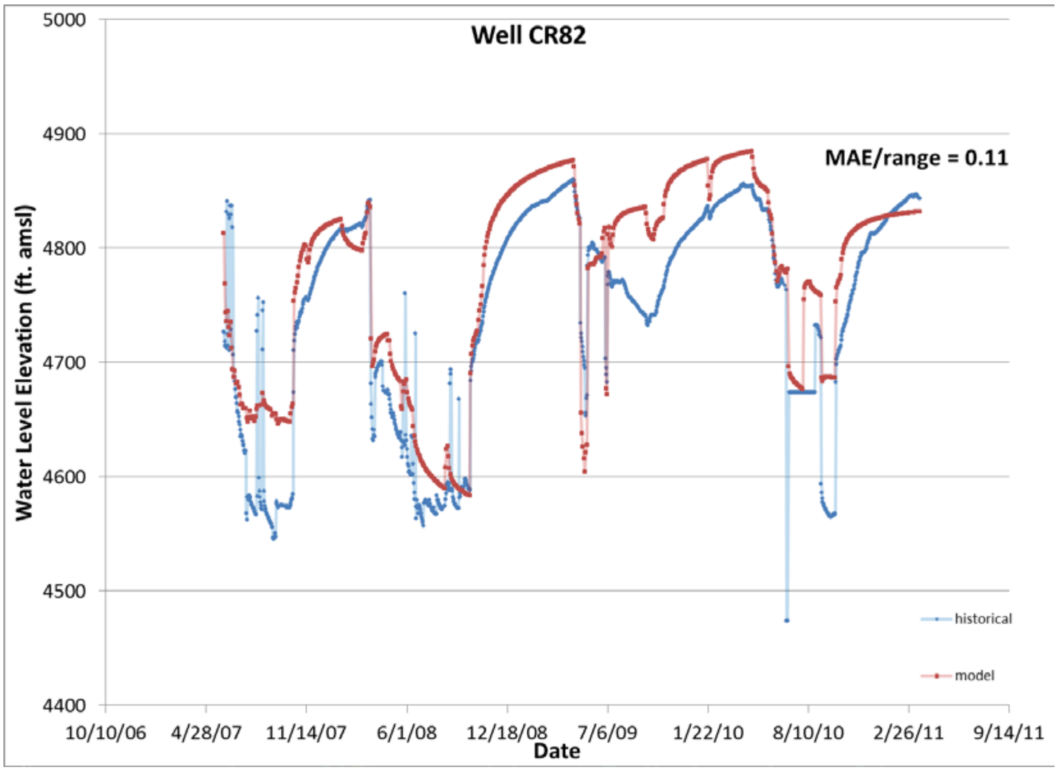
Well CR82
MAE/range = 0.11
Water Level Elevation (ft. amsl)
5000
4900
4800
4700
4600
4500
4400
10/10/06
4/28/07
11/14/07
6/1/08
12/18/08
7/6/09
1/22/10
8/10/10
2/26/11
9/14/11
Date
historical
model

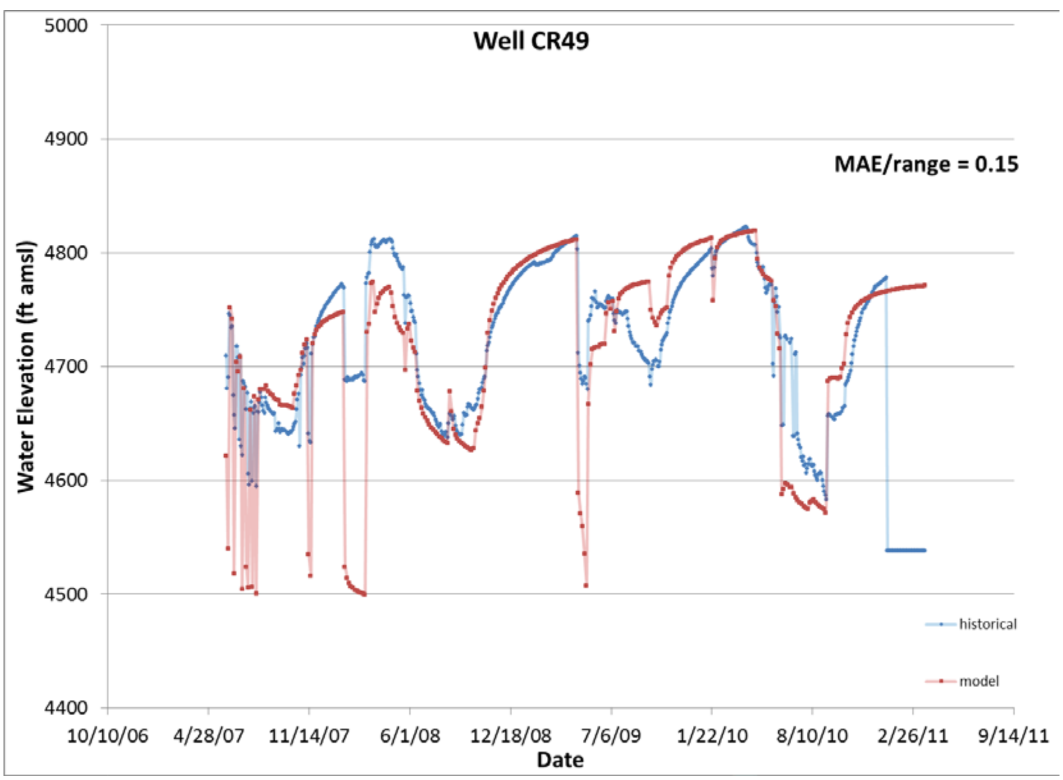
Well CR49
MAE/range = 0.15
Water Elevation (ft amsl)
5000
4900
4800
4700
4600
4500
4400
10/10/06
4/28/07
11/14/07
6/1/08
12/18/08
7/6/09
1/22/10
8/10/10
2/26/11
9/14/11
Date
historical
model

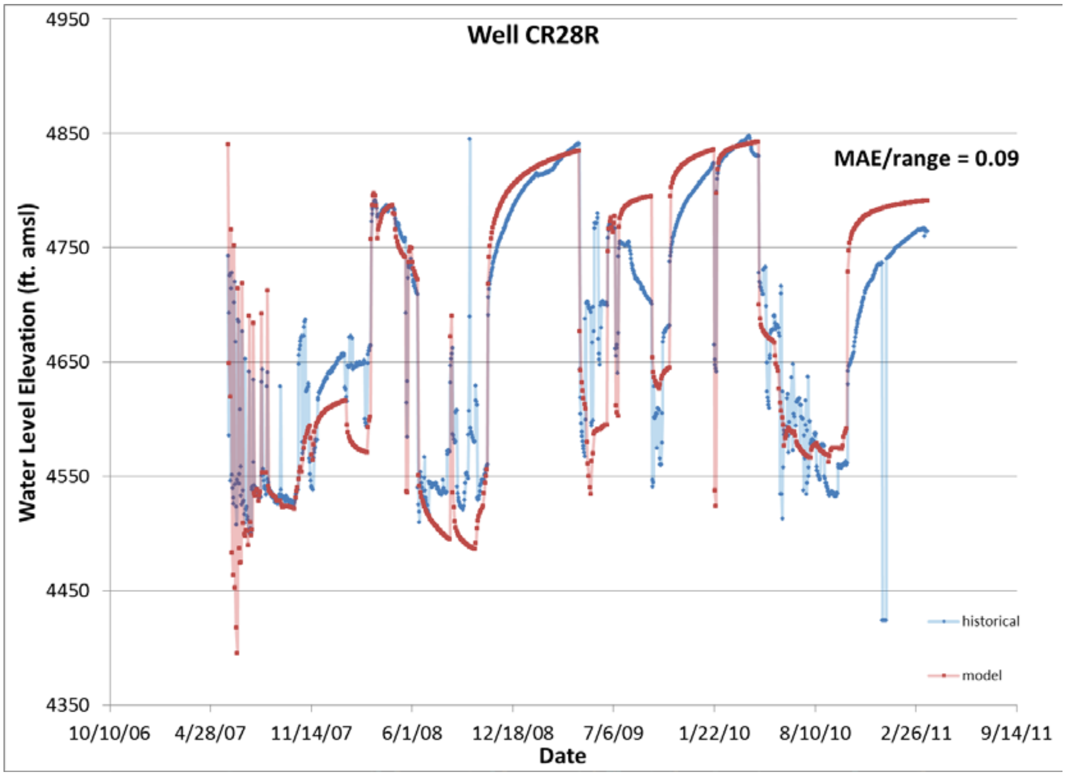
Well CR28R
MAE/range = 0.09
Water Level Elevation (ft. amsl)
4950
4850
4750
4650
4550
4450
4350
10/10/06
4/28/07
11/14/07
6/1/08
12/18/08
7/6/09
1/22/10
8/10/10
2/26/11
9/14/11
Date
historical
model

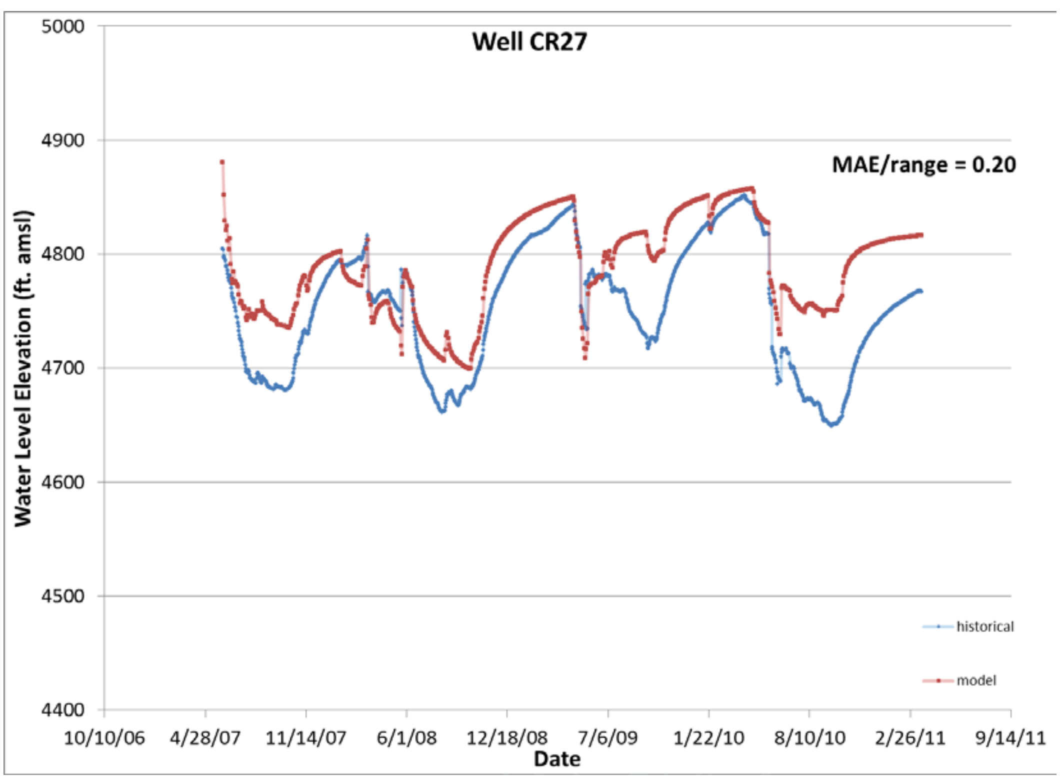
Well CR27
MAE/range = 0.20
Water Level Elevation (ft. amsl)
5000
4900
4800
4700
4600
4500
4400
10/10/06
4/28/07
11/14/07
6/1/08
12/18/08
7/6/09
1/22/10
8/10/10
2/26/11
9/14/11
Date
historical
model

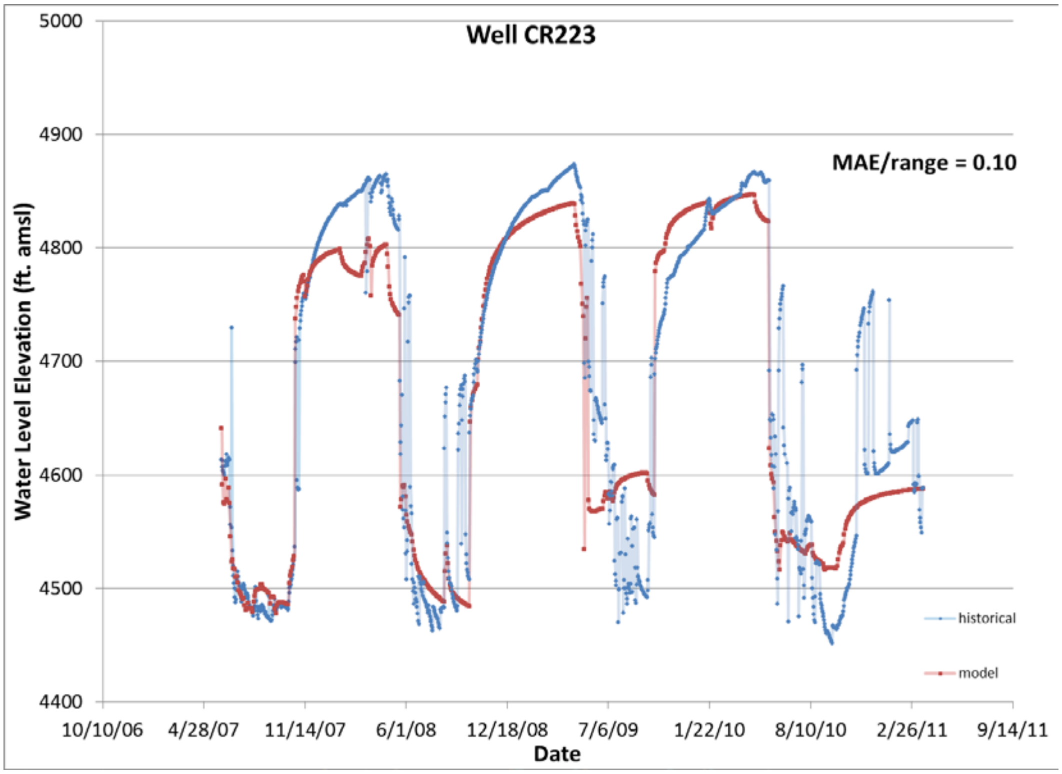
Well CR223
MAE/range = 0.10
Water Level Elevation (ft. amsl)
5000
4900
4800
4700
4600
4500
4400
10/10/06
4/28/07
11/14/07
6/1/08
12/18/08
7/6/09
1/22/10
8/10/10
2/26/11
9/14/11
Date
historical
model

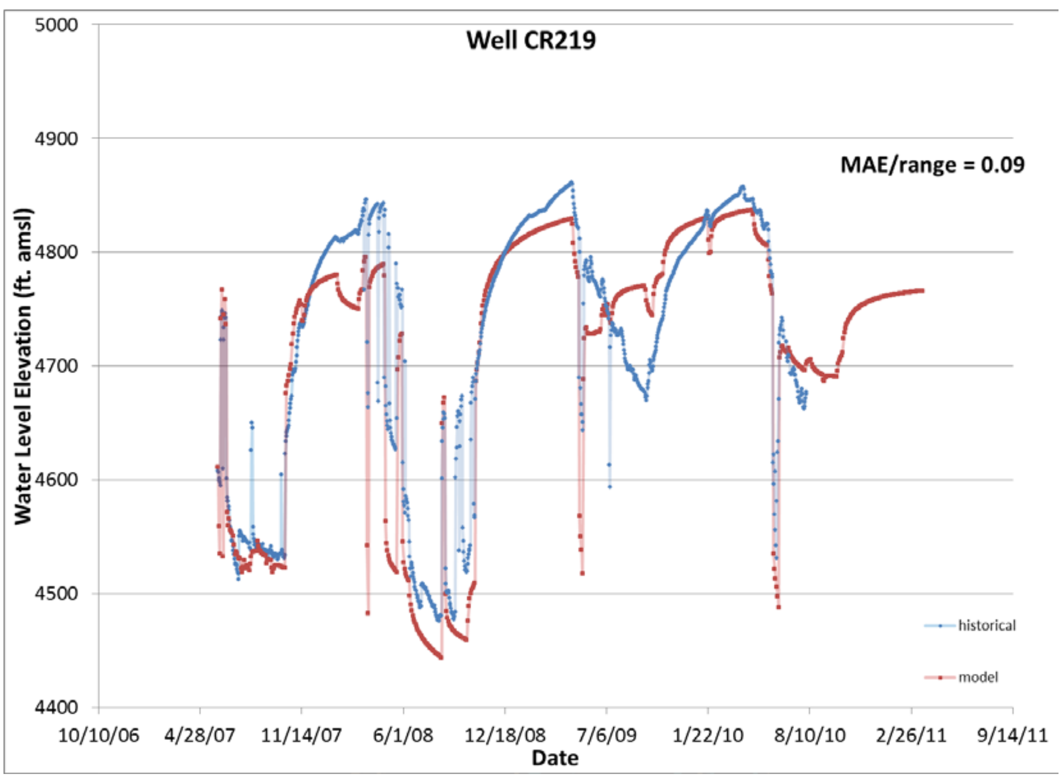
Well CR219
MAE/range = 0.09
Water Level Elevation (ft. amsl)
5000
4900
4800
4700
4600
4500
4400
10/10/06
4/28/07
11/14/07
6/1/08
12/18/08
7/6/09
1/22/10
8/10/10
2/26/11
9/14/11
Date
historical
model

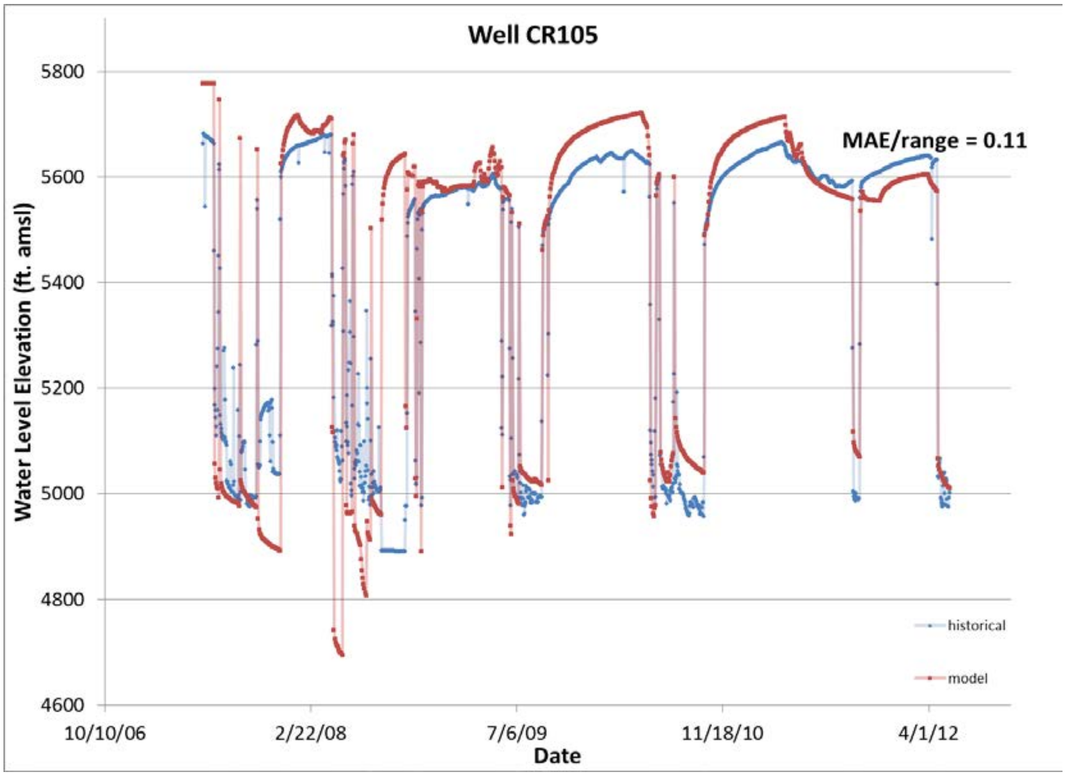
Well CR105
MAE/range = 0.11
Water Level Elevation (ft. amsl)
5800
5600
5400
5200
5000
4800
4600
10/10/06
2/22/08
7/6/09
11/18/10
4/1/12
Date
historical
model

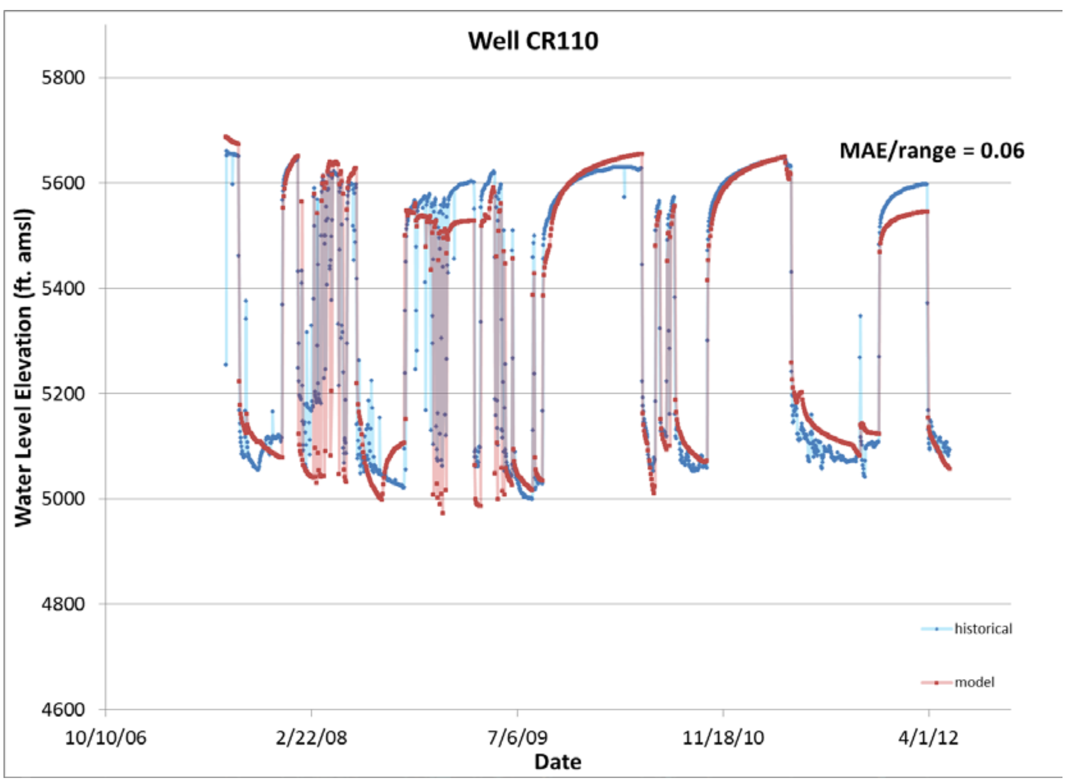
Well CR110
MAE/range = 0.06
Water Level Elevation (ft. amsl)
5800
5600
5400
5200
5000
4800
4600
10/10/06
2/22/08
7/6/09
11/18/10
4/1/12
Date
historical
model

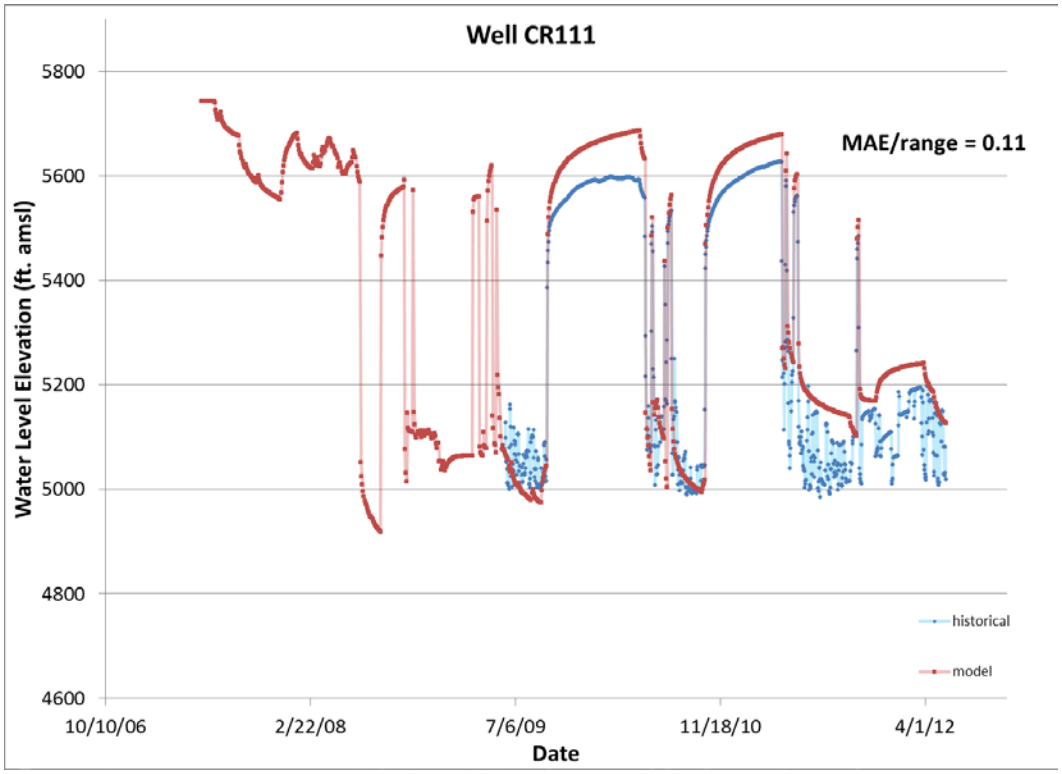
Well CR111
MAE/range = 0.11
Water Level Elevation (ft. amsl)
5800
5600
5400
5200
5000
4800
4600
10/10/06
2/22/08
7/6/09
11/18/10
4/1/12
Date
historical
model

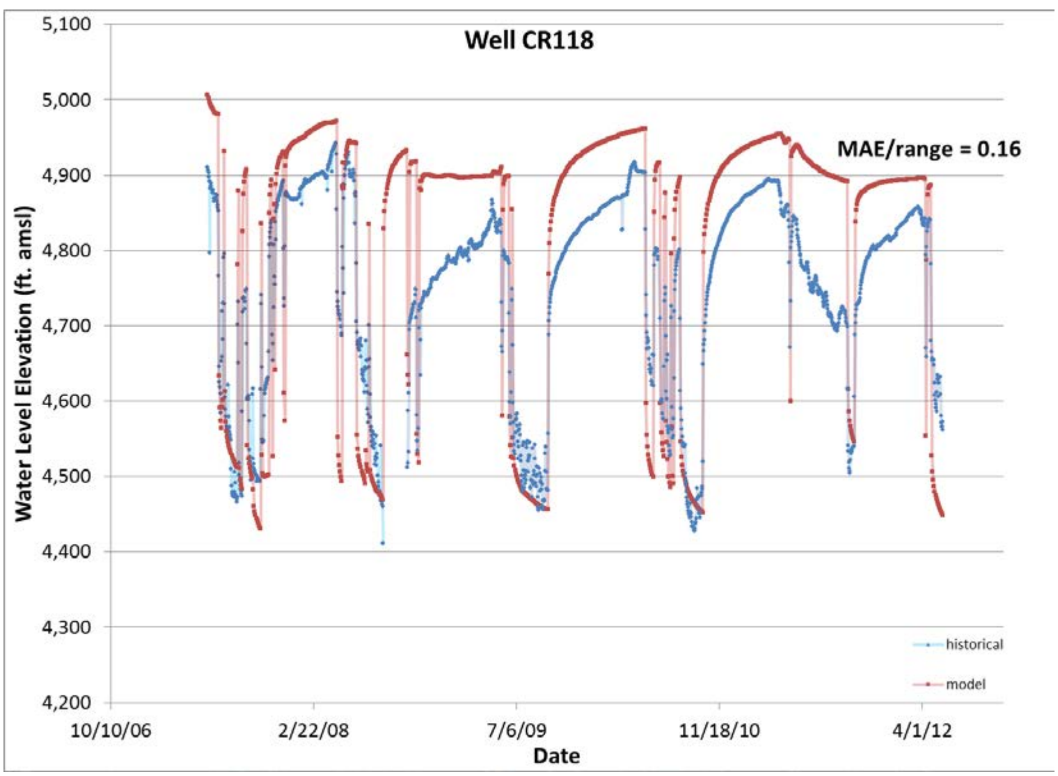
Well CR118
MAE/range = 0.16
Water Level Elevation (ft. amsl)
5,100
5,000
4,900
4,800
4,700
4,600
4,500
4,400
4,300
4,200
10/10/06
2/22/08
7/6/09
11/18/10
4/1/12
Date
historical
model

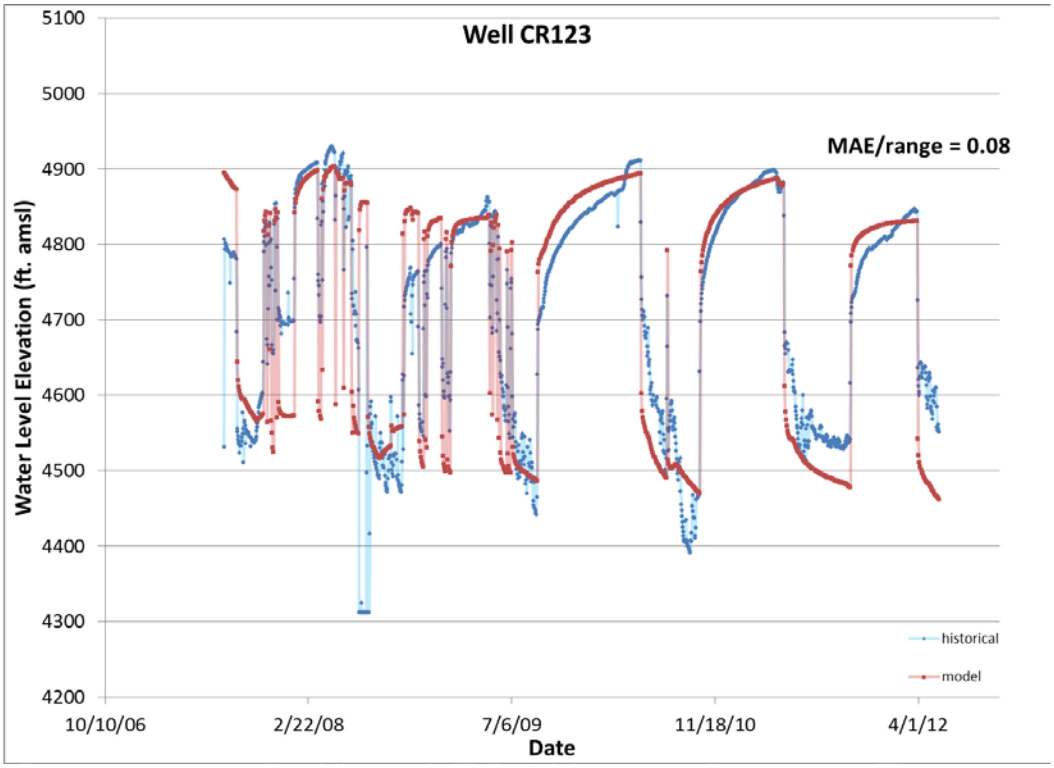
Well CR123
MAE/range = 0.08
5100
5000
4900
4800
4700
4600
4500
4400
4300
4200
Water Level Elevation (ft. amsl)
10/10/06
2/22/08
7/6/09
11/18/10
4/1/12
Date
historical
model

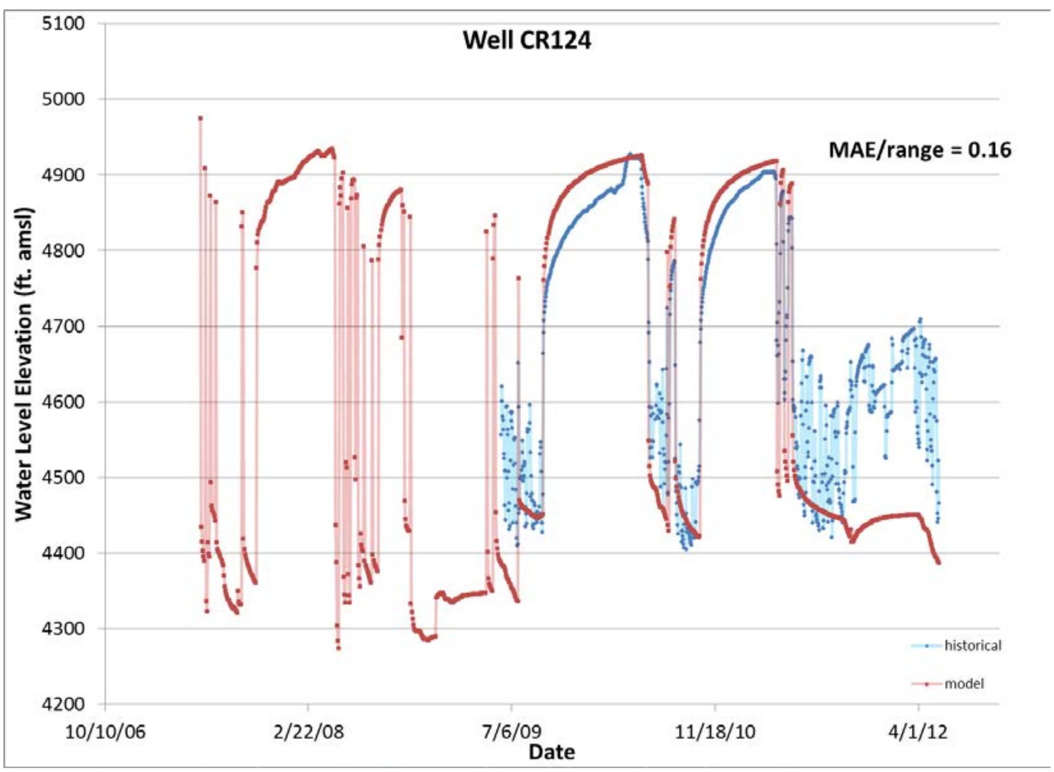
Well CR124
MAE/range = 0.16
5100
5000
4900
4800
4700
4600
4500
4400
4300
4200
Water Level Elevation (ft. amsl)
10/10/06
2/22/08
7/6/09
11/18/10
4/1/12
Date
historical
model

APPENDIX C – Comparison of modeled and observed water levels, scatter plots

Appendix C contains scatter plots of modeled versus observed historical water level elevations for all 22 wells considered during model development and calibration.

APPENDIX C

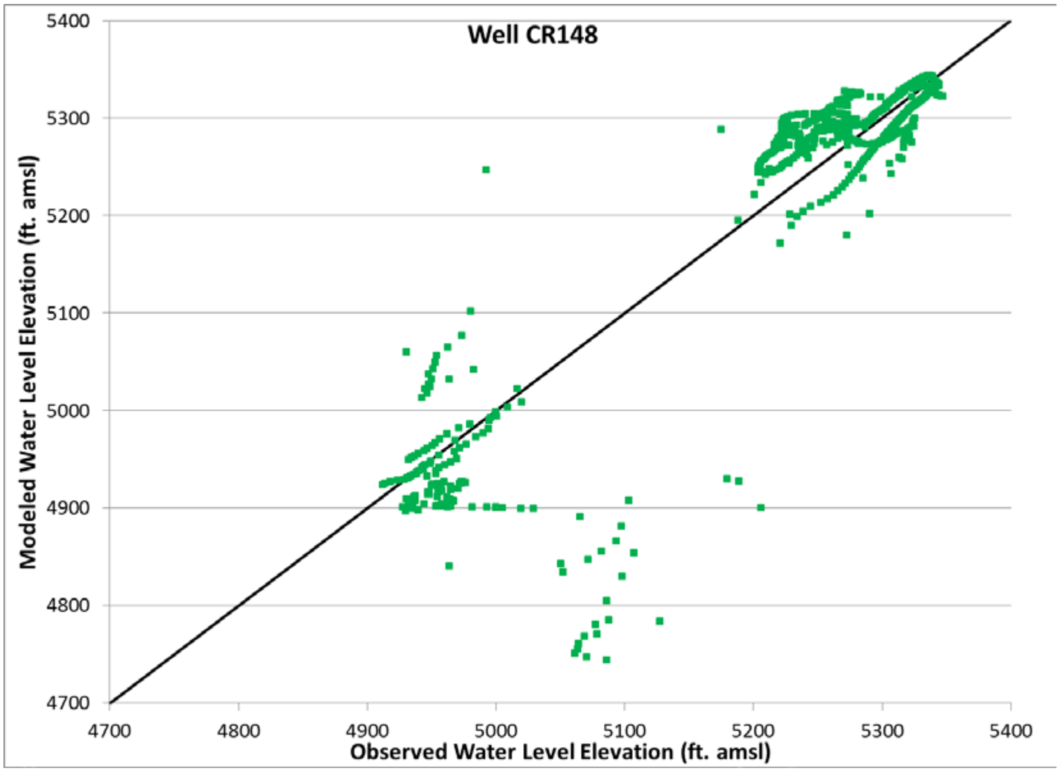

Well CR148
Modeled Water Level Elevation (ft. amsl)
Observed Water Level Elevation (ft. amsl)
5400
5300
5200
5100
5000
4900
4800
4700
4700
4800
4900
5000
5100
5200
5300
5400

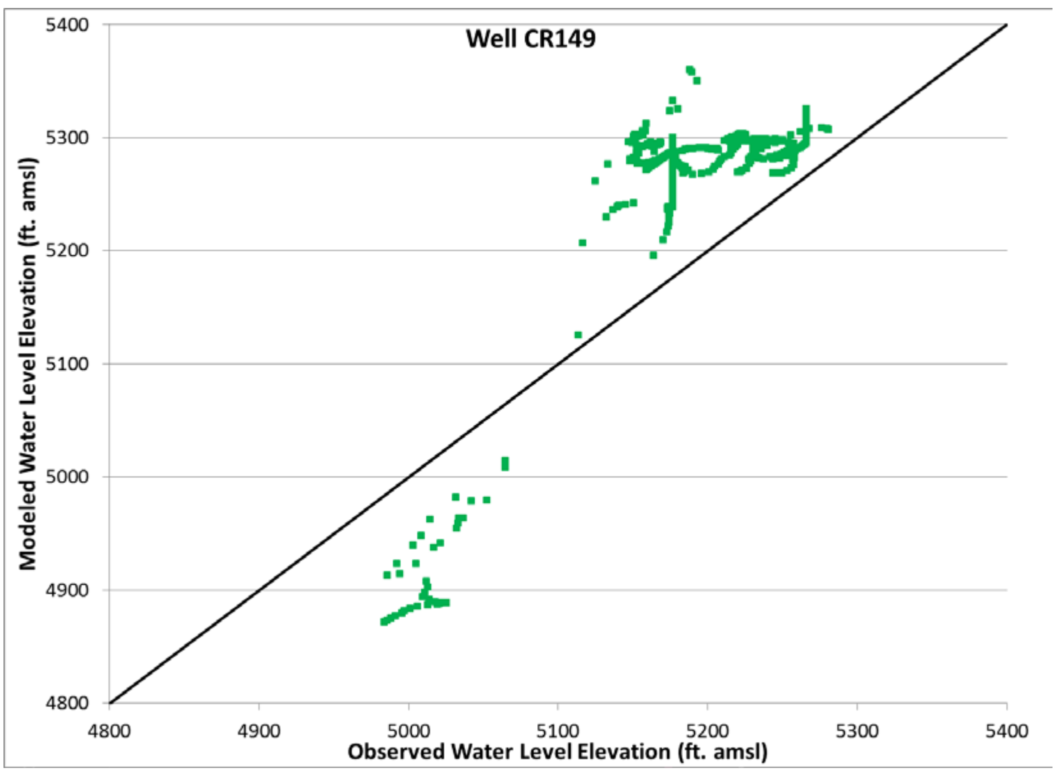

Well CR149
Modeled Water Level Elevation (ft. amsl)
Observed Water Level Elevation (ft. amsl)
5400
5300
5200
5100
5000
4900
4800
4800
4900
5000
5100
5200
5300
5400

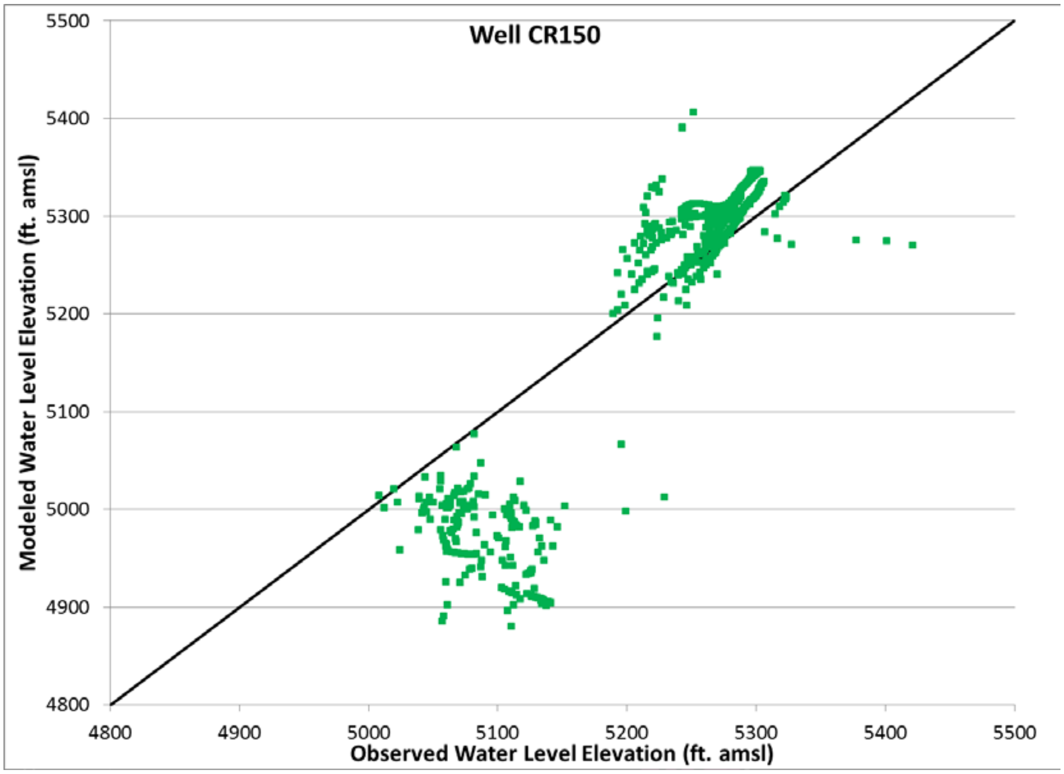
Well CR150
Modeled Water Level Elevation (ft. amsl)
Observed Water Level Elevation (ft. amsl)
5500
5400
5300
5200
5100
5000
4900
4800
4800
4900
5000
5100
5200
5300
5400
5500

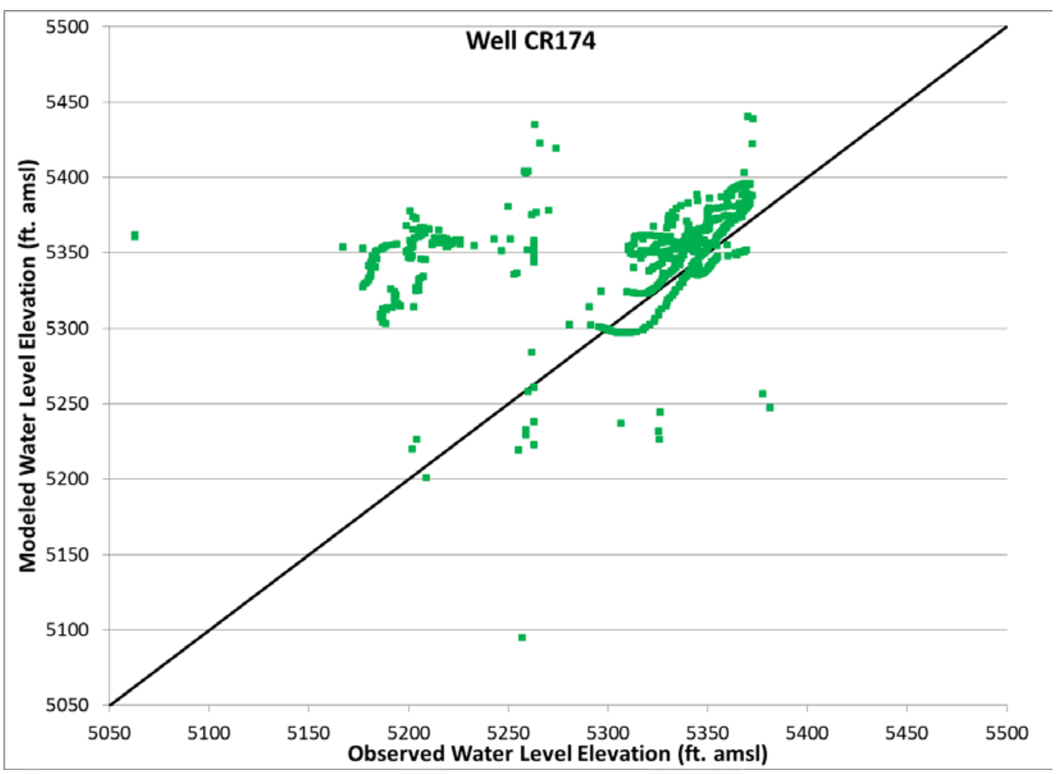
Well CR174
Modeled Water Level Elevation (ft. amsl)
Observed Water Level Elevation (ft. amsl)
5500
5450
5400
5350
5300
5250
5200
5150
5100
5050
5050
5100
5150
5200
5250
5300
5350
5400
5450
5500

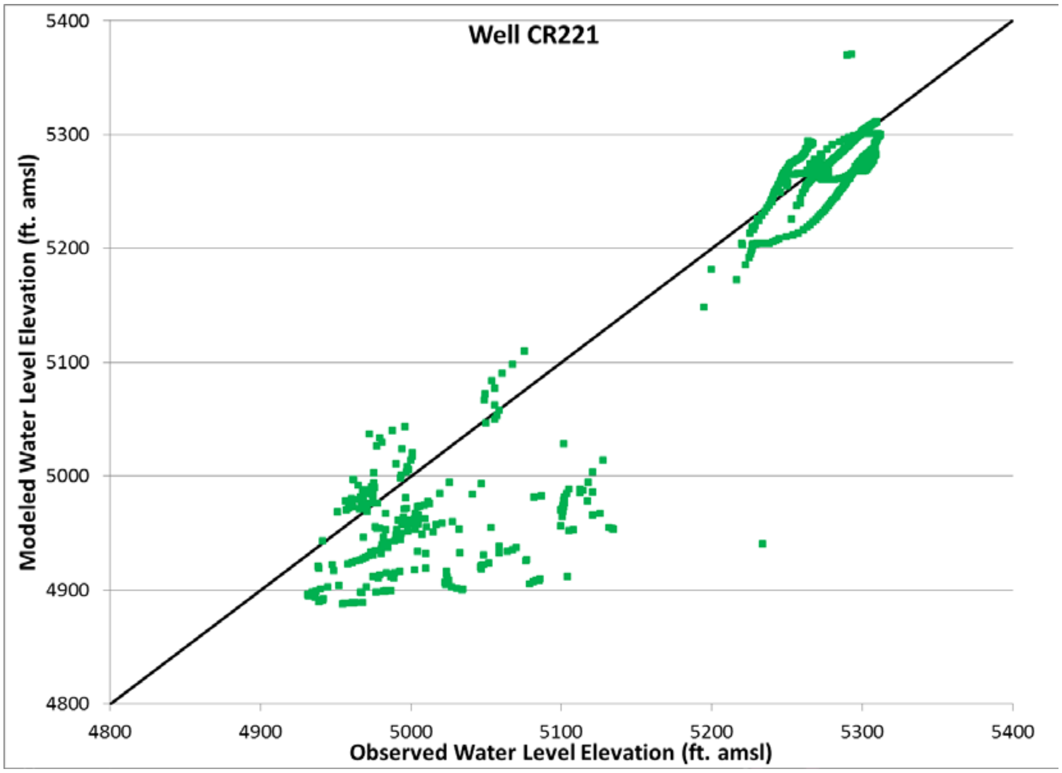
Well CR221
Modeled Water Level Elevation (ft. amsl)
Observed Water Level Elevation (ft. amsl)
5400
5300
5200
5100
5000
4900
4800
4800
4900
5000
5100
5200
5300
5400

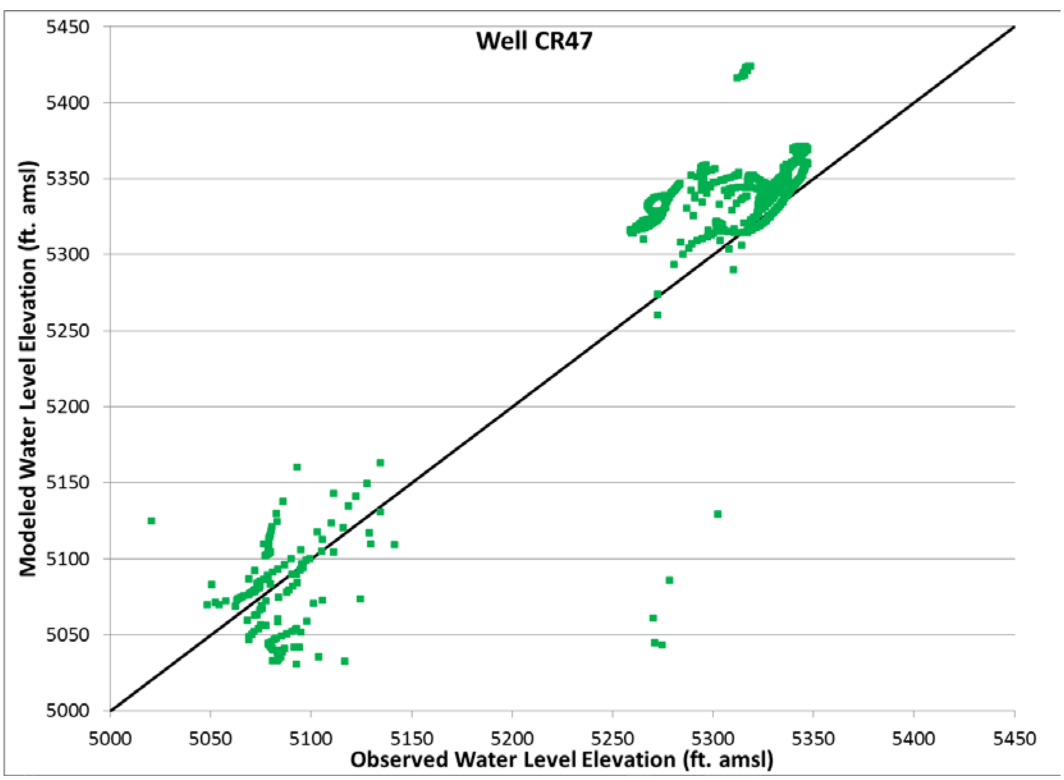
Well CR47
Modeled Water Level Elevation (ft. amsl)
Observed Water Level Elevation (ft. amsl)
5450
5400
5350
5300
5250
5200
5150
5100
5050
5000
5000
5050
5100
5150
5200
5250
5300
5350
5400
5450

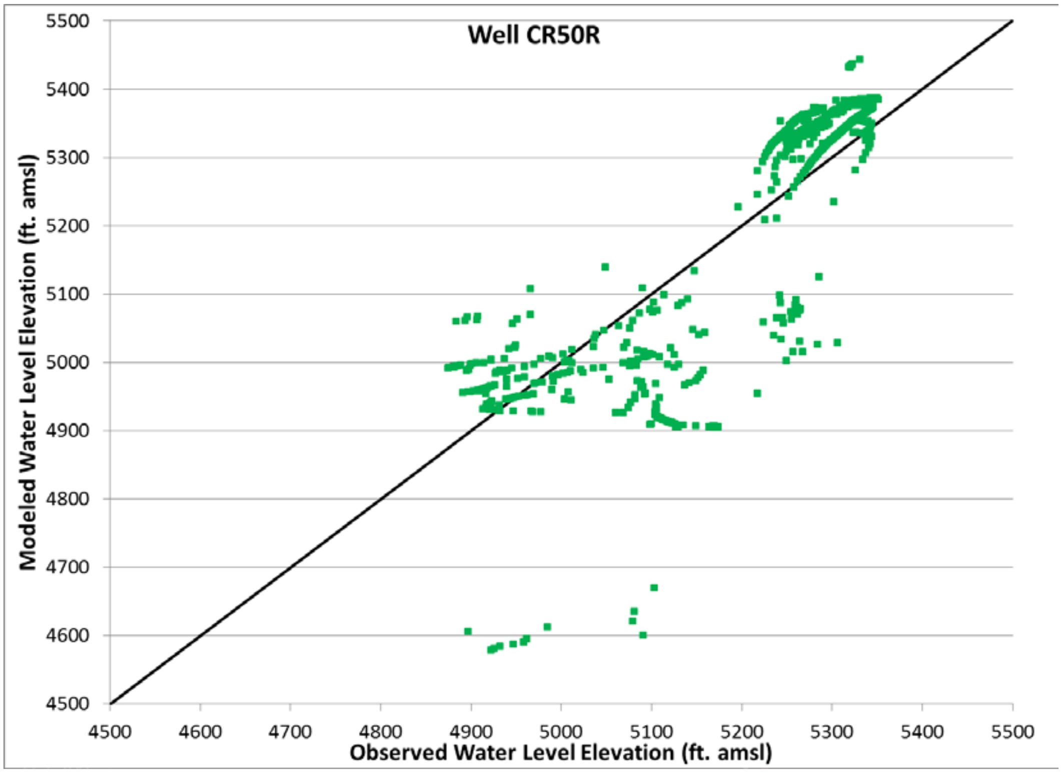
Well CR50R
Modeled Water Level Elevation (ft. amsl)
Observed Water Level Elevation (ft. amsl)
5500
5400
5300
5200
5100
5000
4900
4800
4700
4600
4500
4500
4600
4700
4800
4900
5000
5100
5200
5300
5400
5500

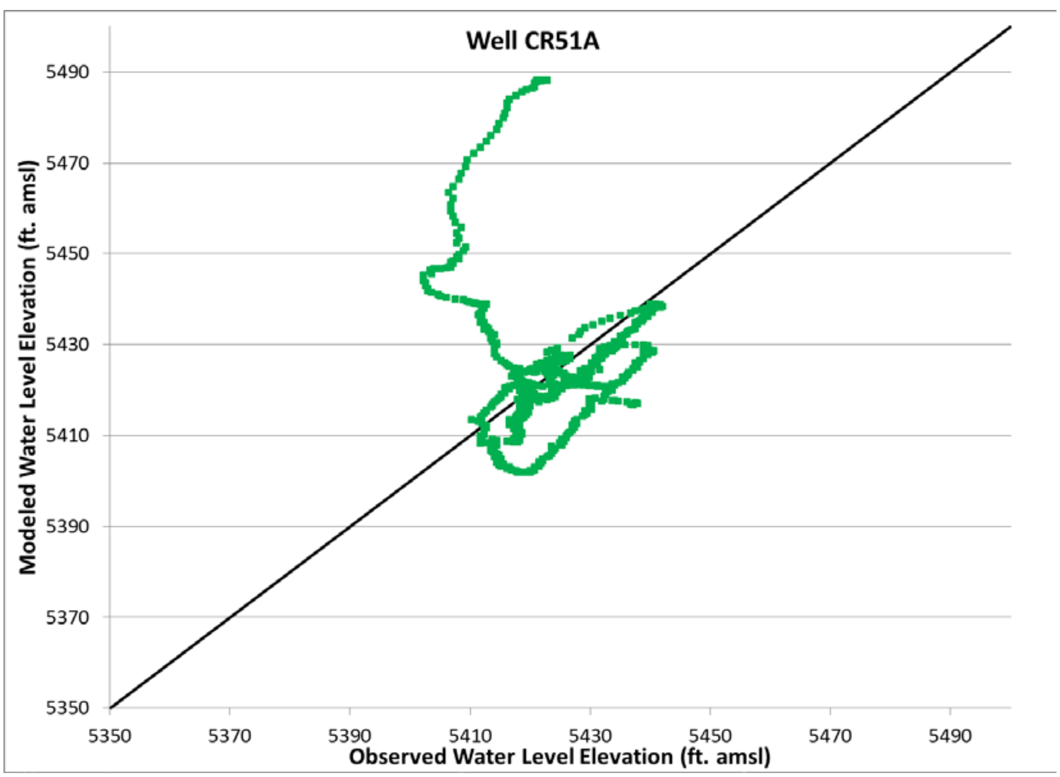
Well CR51A
Modeled Water Level Elevation (ft. amsl)
Observed Water Level Elevation (ft. amsl)
5490
5470
5450
5430
5410
5390
5370
5350
5350
5370
5390
5410
5430
5450
5470
5490

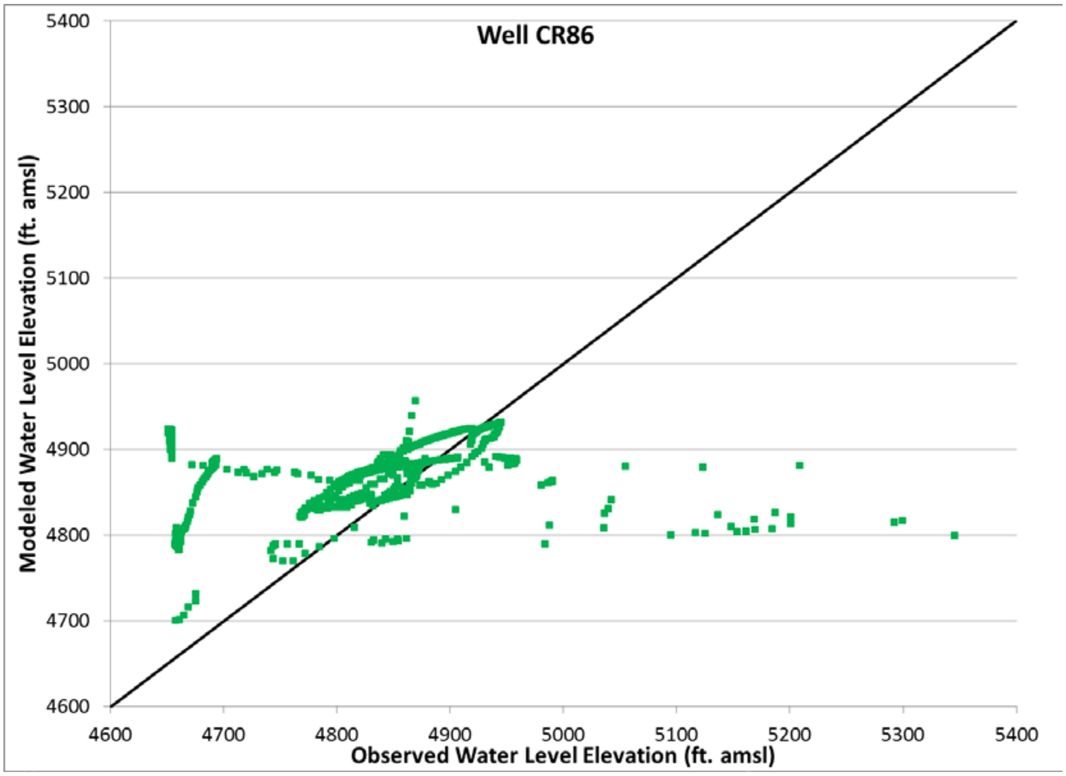
Well CR86
Modeled Water Level Elevation (ft. amsl)
Observed Water Level Elevation (ft. amsl)
5400
5300
5200
5100
5000
4900
4800
4700
4600
4600
4700
4800
4900
5000
5100
5200
5300
5400

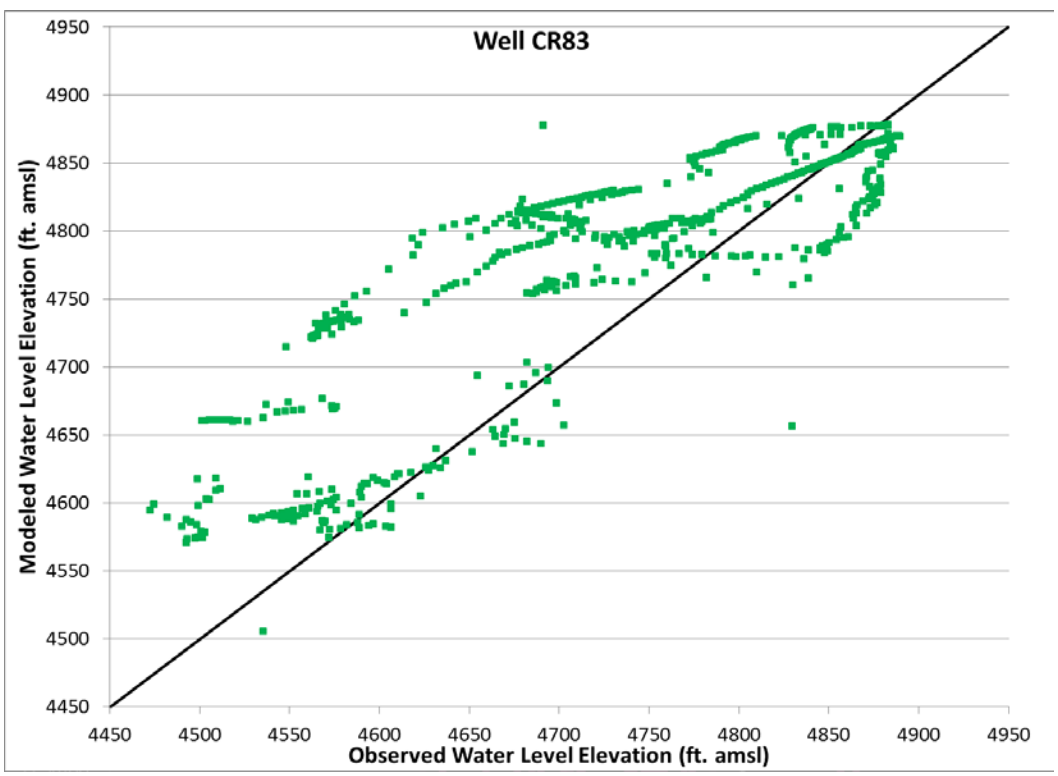
Well CR83
Modeled Water Level Elevation (ft. amsl)
Observed Water Level Elevation (ft. amsl)
4950
4900
4850
4800
4750
4700
4650
4600
4550
4500
4450
4450
4500
4550
4600
4650
4700
4750
4800
4850
4900
4950

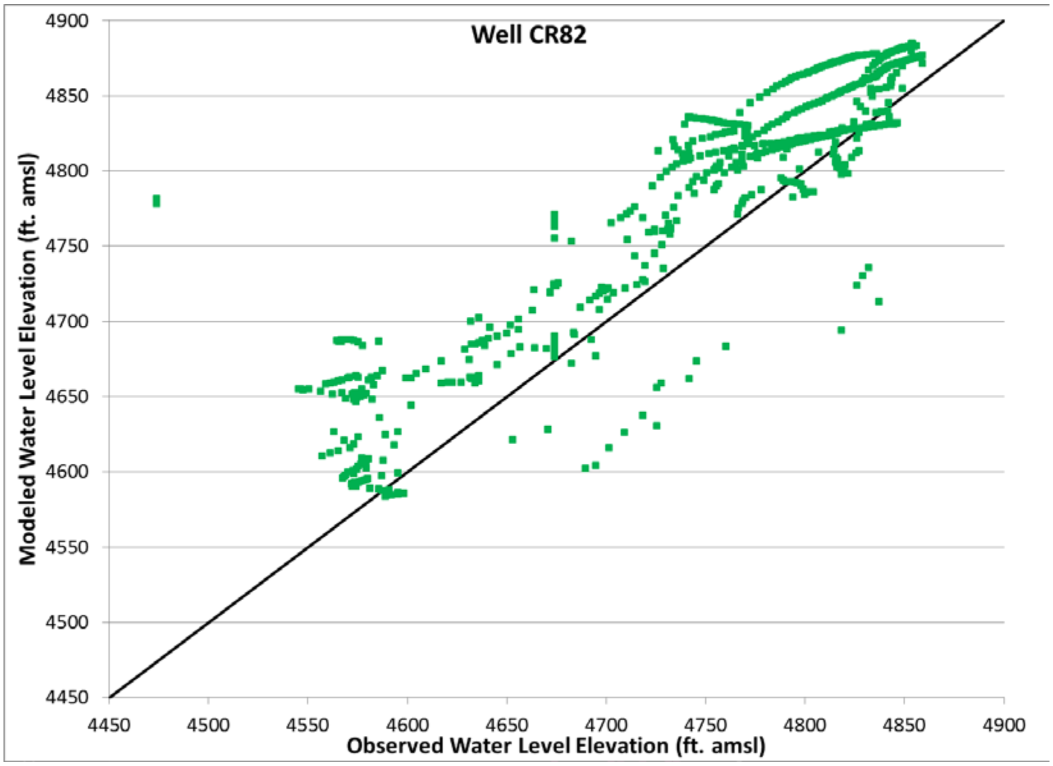
Well CR82
Modeled Water Level Elevation (ft. amsl)
Observed Water Level Elevation (ft. amsl)
4450
4500
4550
4600
4650
4700
4750
4800
4850
4900

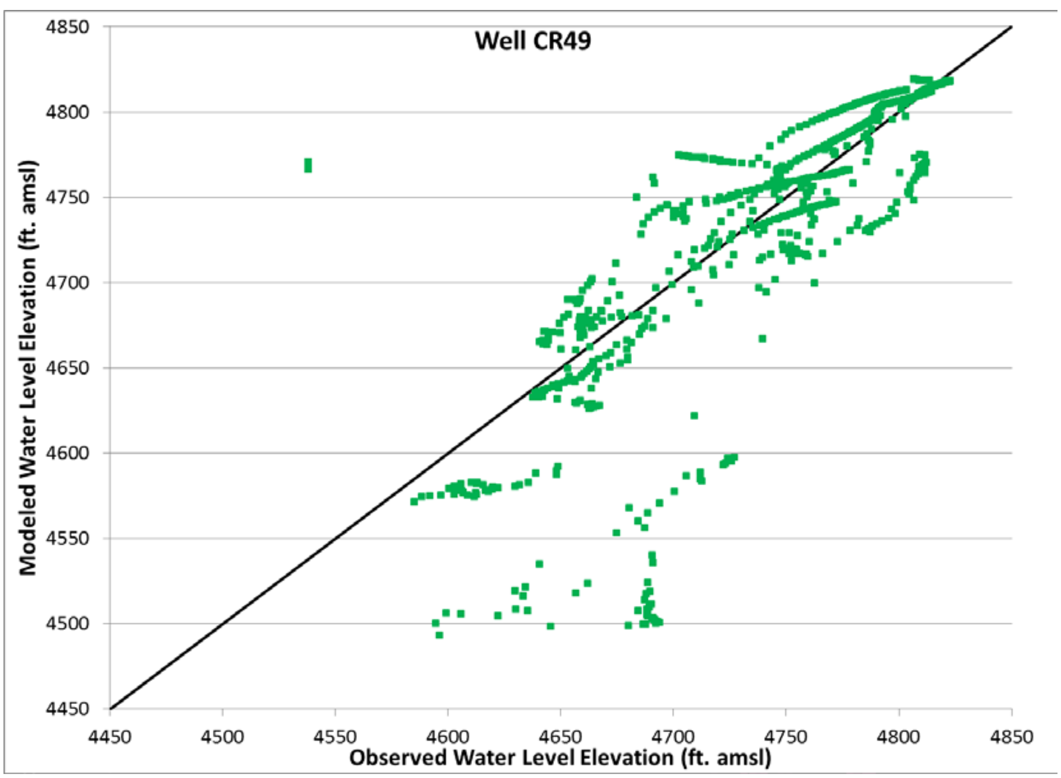
Well CR49
Modeled Water Level Elevation (ft. amsl)
Observed Water Level Elevation (ft. amsl)
4450
4500
4550
4600
4650
4700
4750
4800
4850

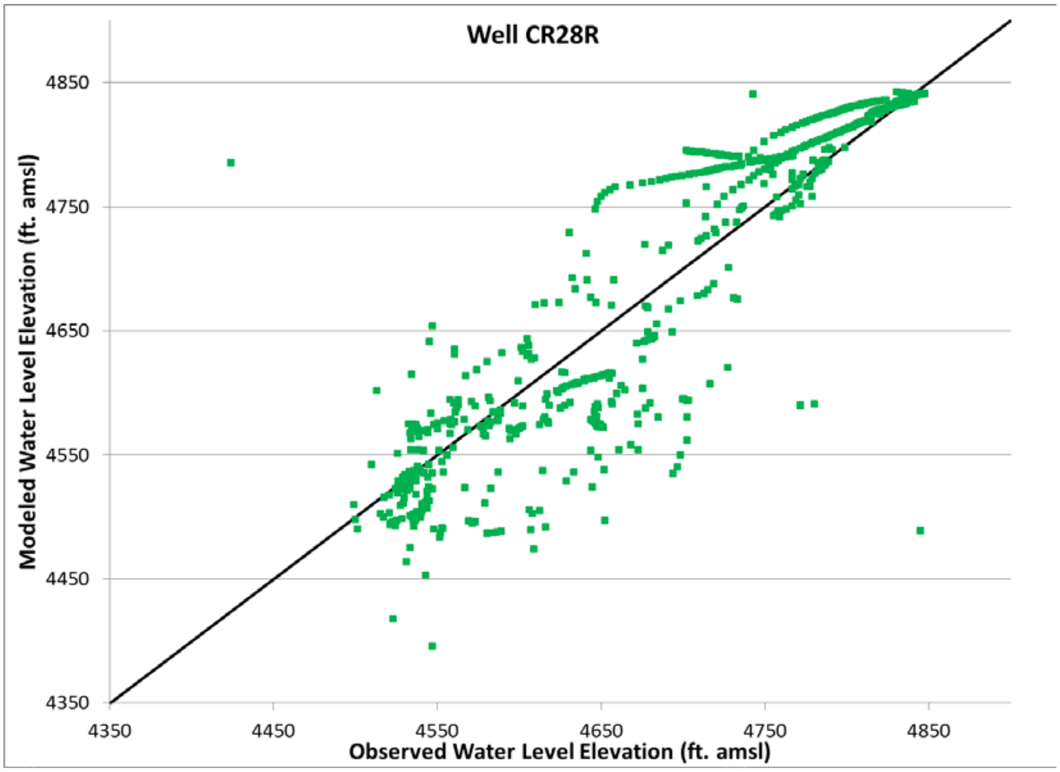
Well CR28R
Modeled Water Level Elevation (ft. amsl)
Observed Water Level Elevation (ft. amsl)
4350
4450
4550
4650
4750
4850

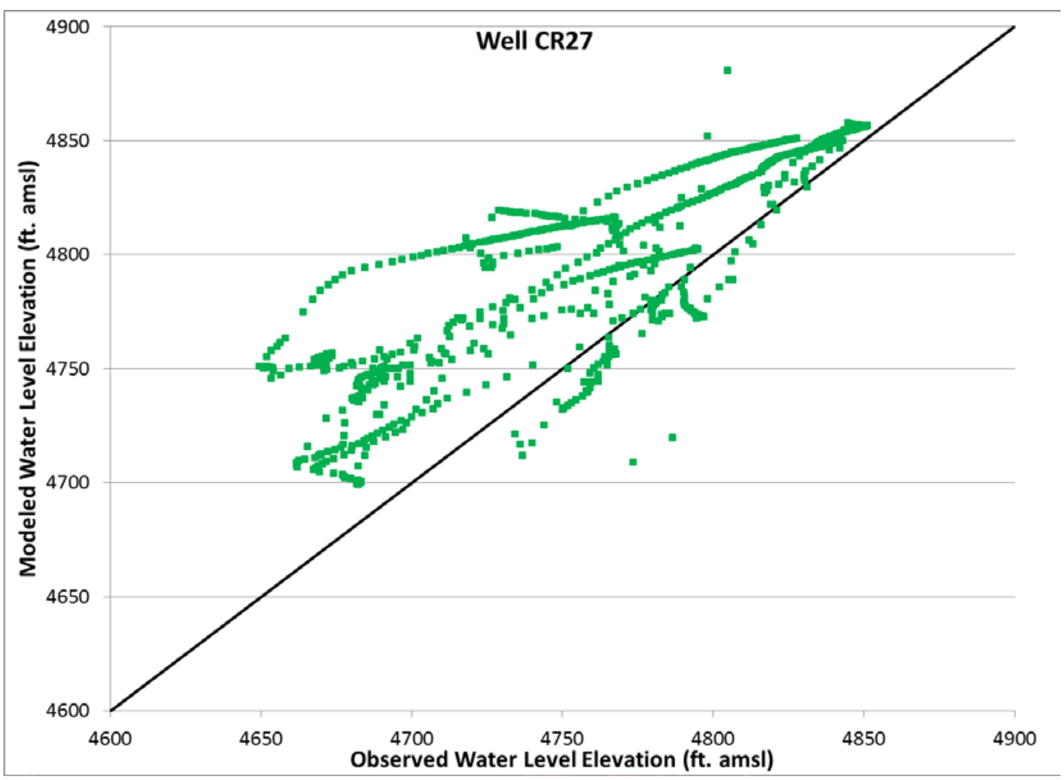
Well CR27
Modeled Water Level Elevation (ft. amsl)
Observed Water Level Elevation (ft. amsl)
4600
4650
4700
4750
4800
4850
4900

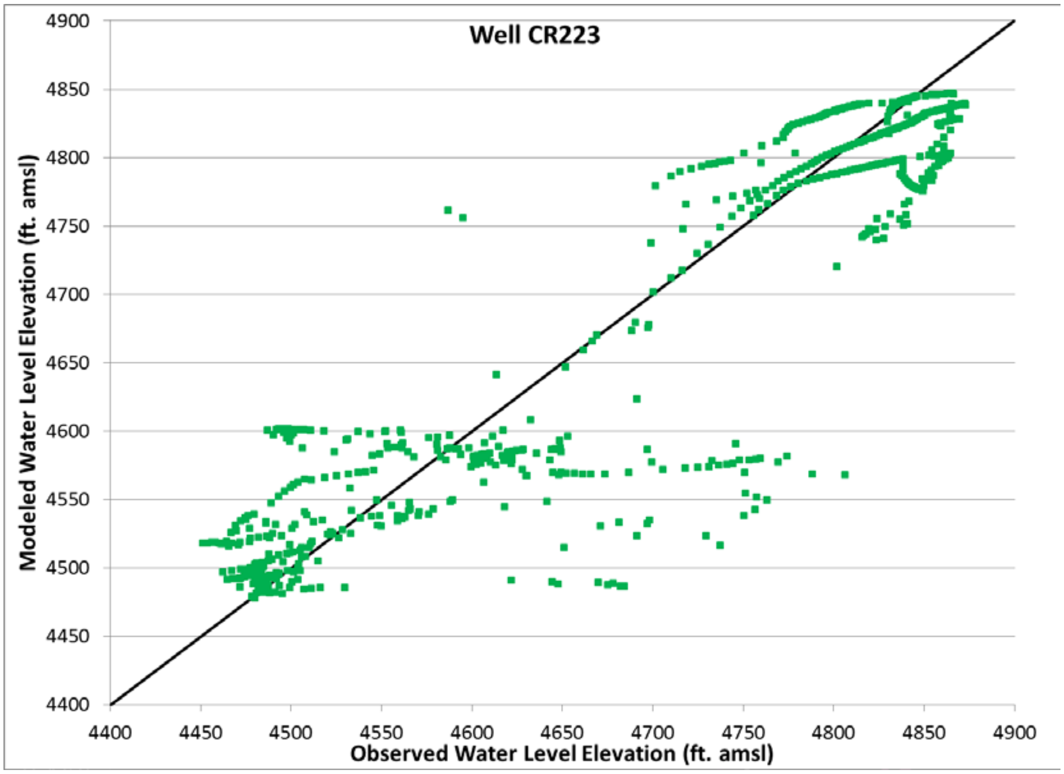
Well CR223
Modeled Water Level Elevation (ft. amsl)
Observed Water Level Elevation (ft. amsl)
4900
4850
4800
4750
4700
4650
4600
4550
4500
4450
4400
4400 4450 4500 4550 4600 4650 4700 4750 4800 4850 4900

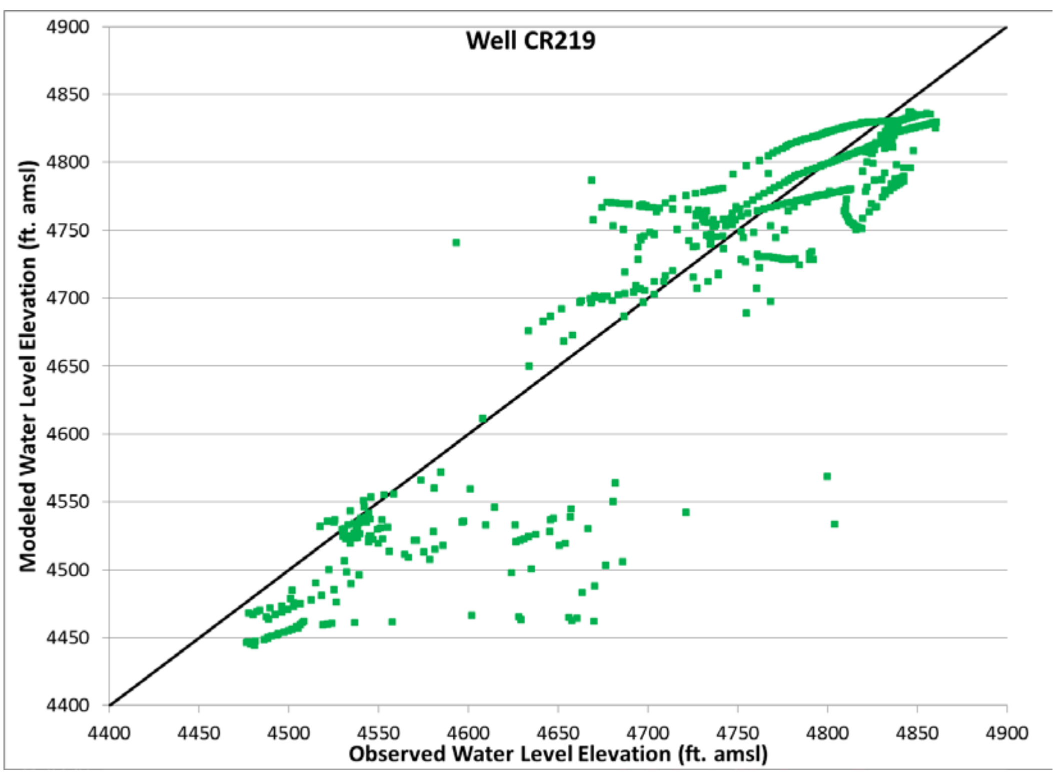
Well CR219
Modeled Water Level Elevation (ft. amsl)
Observed Water Level Elevation (ft. amsl)
4900
4850
4800
4750
4700
4650
4600
4550
4500
4450
4400
4400 4450 4500 4550 4600 4650 4700 4750 4800 4850 4900

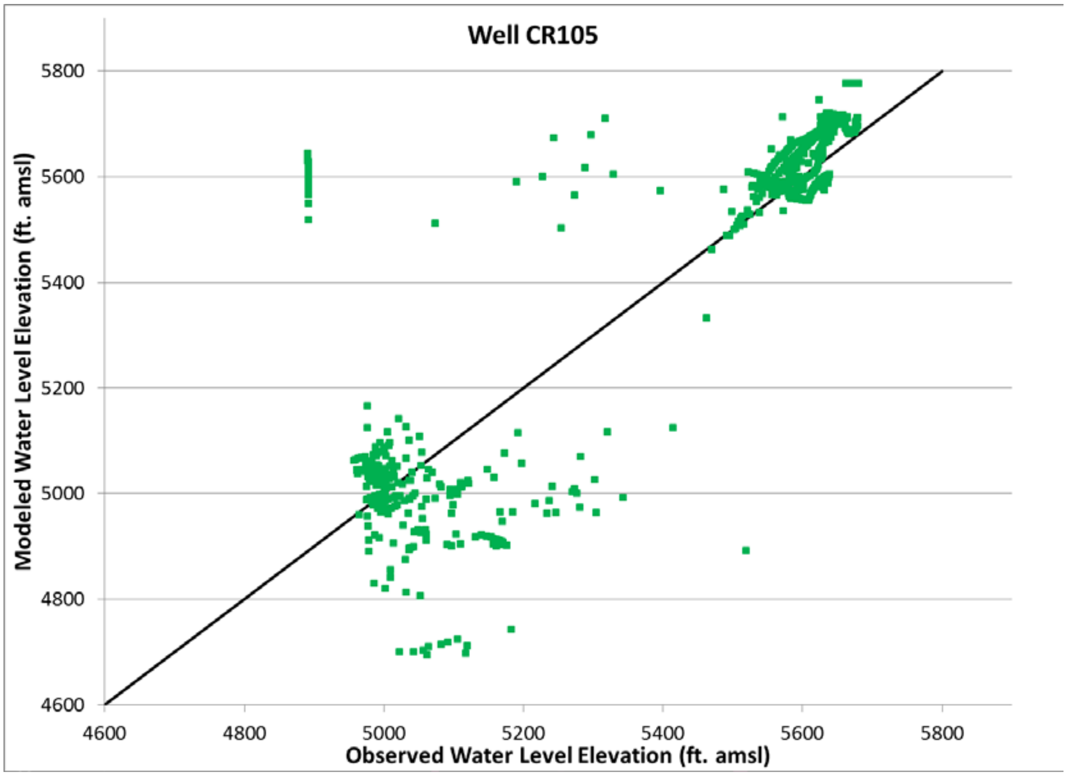
Well CR105
Modeled Water Level Elevation (ft. amsl)
Observed Water Level Elevation (ft. amsl)
5800
5600
5400
5200
5000
4800
4600
4600
4800
5000
5200
5400
5600
5800

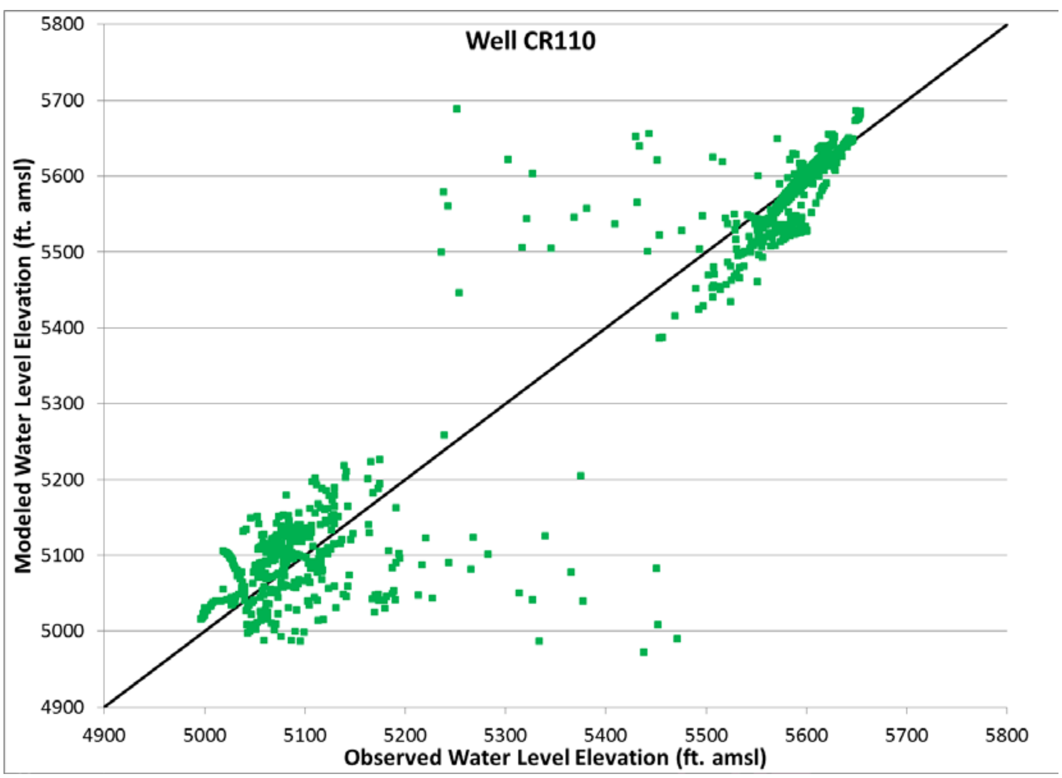
Well CR110
Modeled Water Level Elevation (ft. amsl)
Observed Water Level Elevation (ft. amsl)
5800
5700
5600
5500
5400
5300
5200
5100
5000
4900
4900
5000
5100
5200
5300
5400
5500
5600
5700
5800

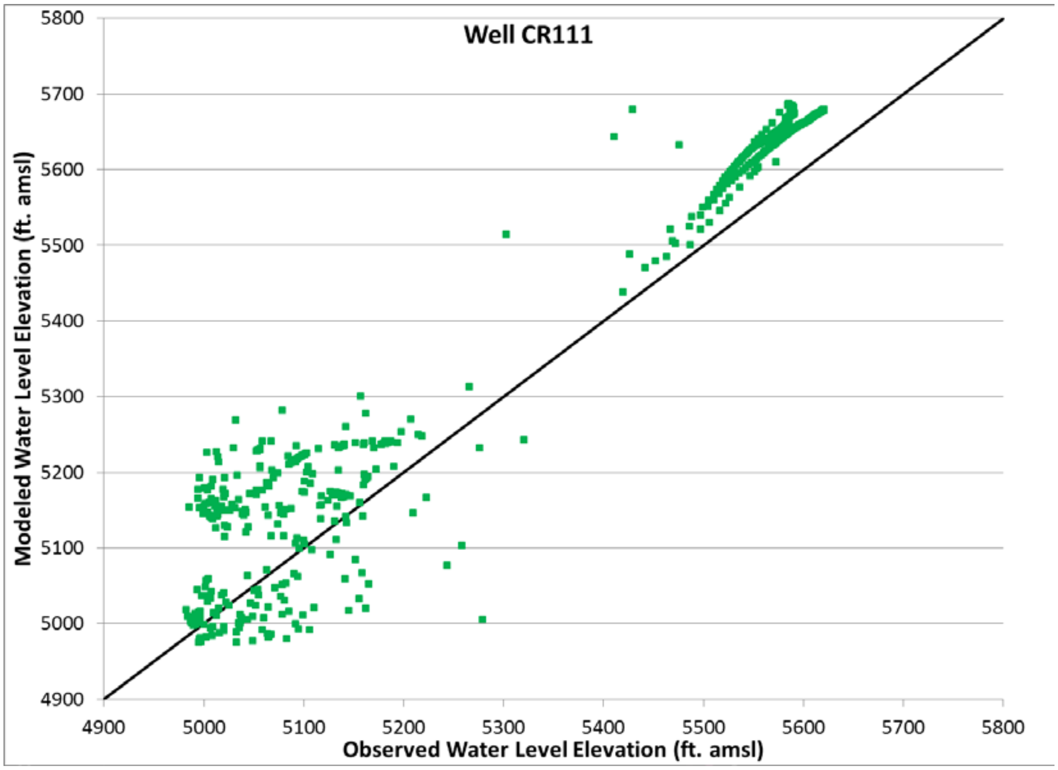
Well CR111
Modeled Water Level Elevation (ft. amsl)
Observed Water Level Elevation (ft. amsl)
5800
5700
5600
5500
5400
5300
5200
5100
5000
4900
4900
5000
5100
5200
5300
5400
5500
5600
5700
5800

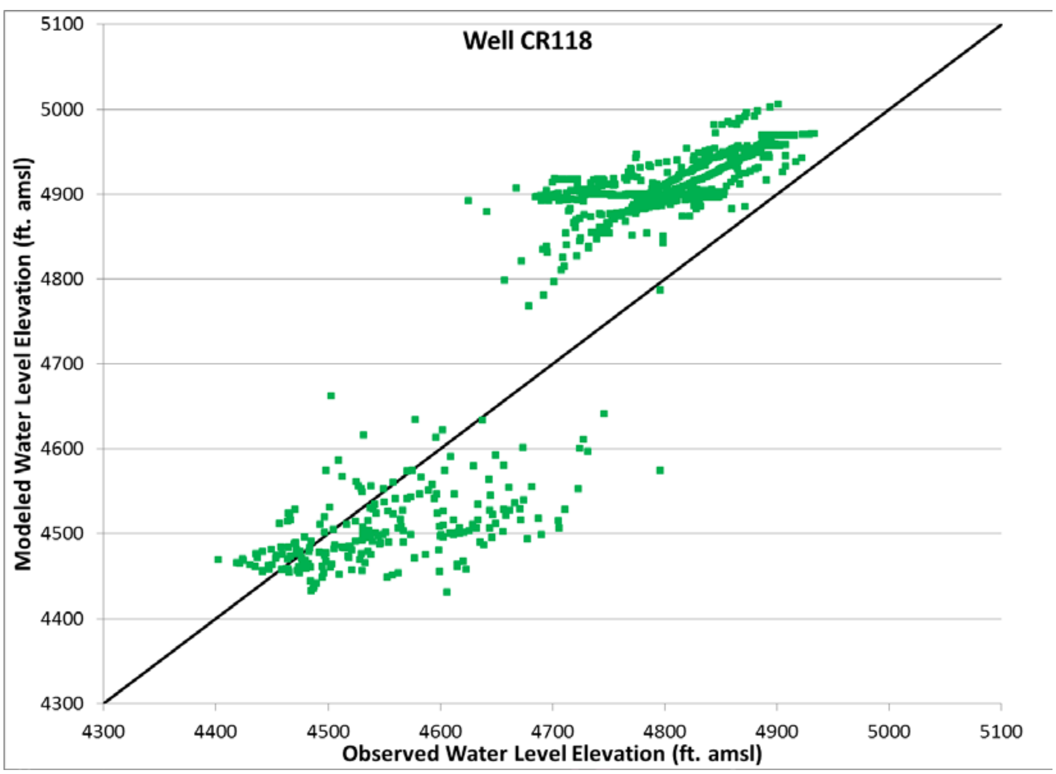
Well CR118
Modeled Water Level Elevation (ft. amsl)
Observed Water Level Elevation (ft. amsl)
5100
5000
4900
4800
4700
4600
4500
4400
4300
4300
4400
4500
4600
4700
4800
4900
5000
5100

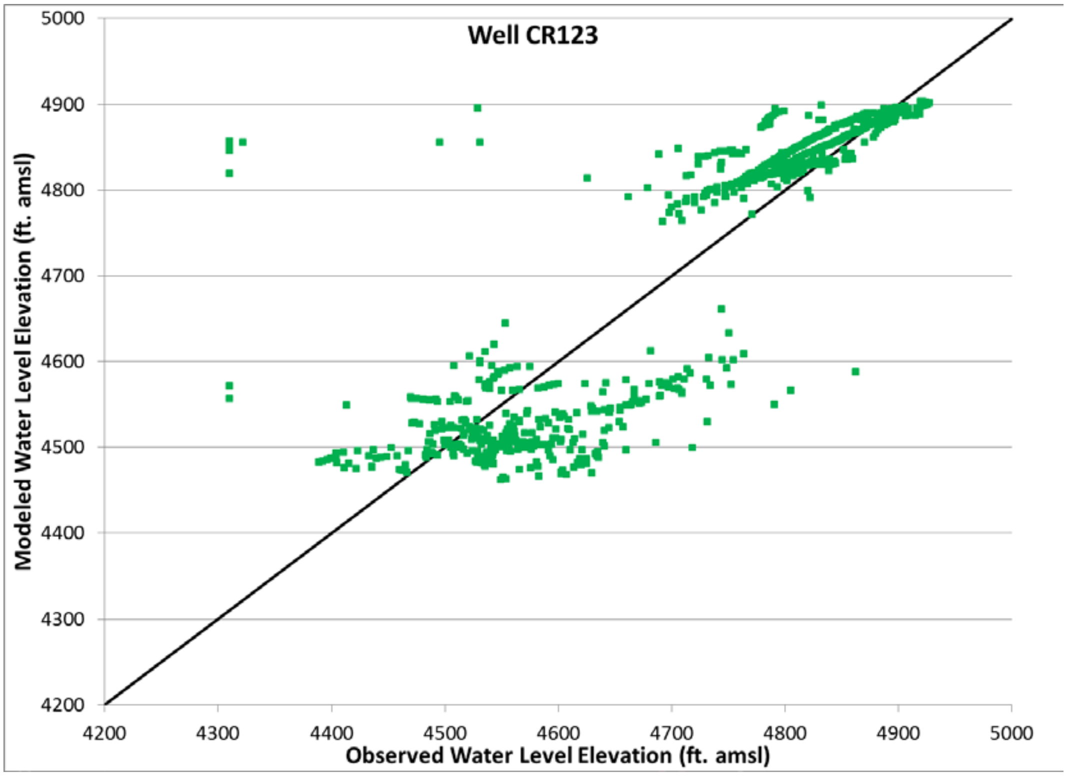
Well CR123
Modeled Water Level Elevation (ft. amsl)
Observed Water Level Elevation (ft. amsl)
5000
4900
4800
4700
4600
4500
4400
4300
4200
4200
4300
4400
4500
4600
4700
4800
4900
5000

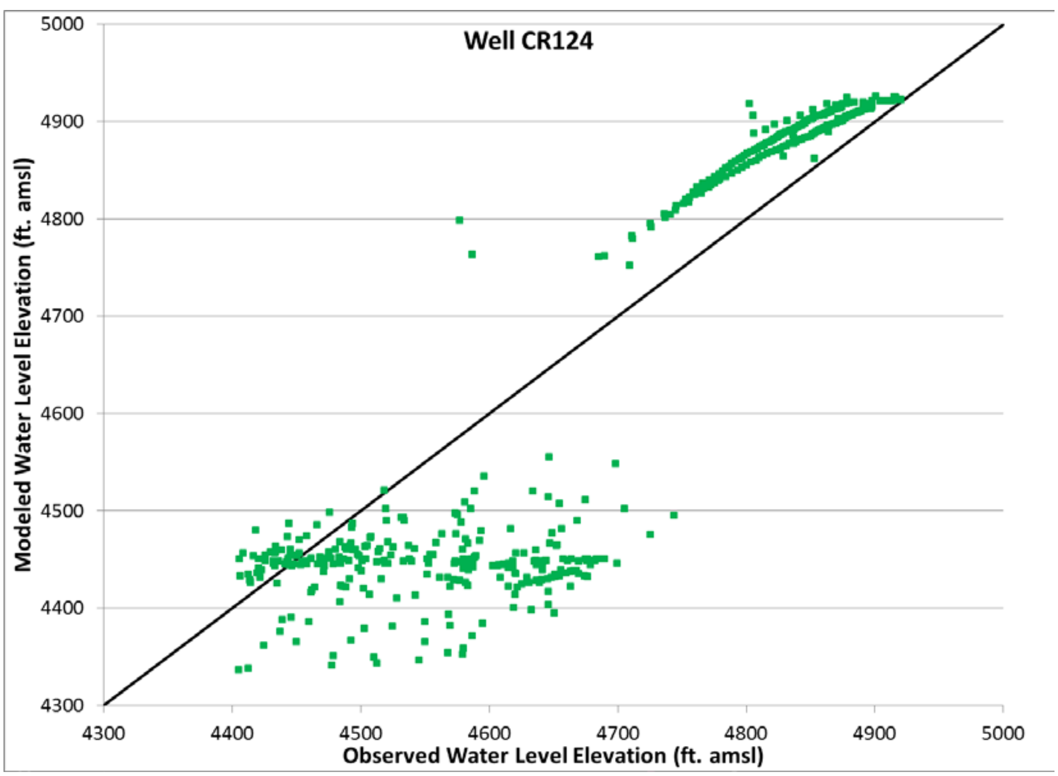
Well CR124
Modeled Water Level Elevation (ft. amsl)
Observed Water Level Elevation (ft. amsl)
5000
4900
4800
4700
4600
4500
4400
4300
4300
4400
4500
4600
4700
4800
4900
5000